Assessment of Wildfire Risk at Recreational Sites in Sri Lanna National Park, Chiang Mai, Northern Thailand, Using Remote Sensing and GIS Techniques

(リモートセンシングと GIS を用いた森林火災リスクの評価手法に関する研究 - タイ北部，スリランナ国立公園を事例として -)

Kansuma BURAPAPOL

2018

Assessment of Wildfire Risk at Recreational Sites in Sri Lanna National Park, Chiang Mai, Northern Thailand, Using Remote Sensing and GIS Techniques

A dissertation presented to

The United Graduate School of Agriculture Sciences,
Tottori University in partial fulfillment of the requirements for a degree of
Doctor of Philosophy in Agriculture (Landscape Ecology & GIS)

by

Kansuma BURAPAPOL

Approved by

Professor Dr. Ryota NAGASAWA

Faculty of Agriculture, Tottori University

The United Graduate School of Agricultural Sciences
Tottori University, Japan
March, 2018

Kansuma BURAPAPOL (2018)

Assessment of wildfire risk at recreational sites in Sri Lanna National Park, Chiang Mai, northern Thailand, Using Remote Sensing and GIS Techniques
The United Graduate School of Agricultural Sciences, Tottori University, Japan

March 2018

Ph.D Thesis

Declaration

This thesis is submitted for the degree of Doctor of Philosophy at the United Graduate School of Agricultural Sciences, Tottori University. This dissertation is the result of my own work and has not been and is not being, in part or wholly, submitted for another degree, diploma, or similar qualification.

Kansuma BURAPAPOL

Acknowledgement

This Ph.D research was made possible with the funding from Scholarship of Office of National Park, Department of National Park, Wildlife and Plant Conservation (DNP). This study was performed at the Laboratory of Landscape Ecology & GIS, Faculty of Agriculture, Tottori University, Japan.

Completing the Ph.D and writing this thesis has been a long journey, but also an amazing and enriching experience in both academic and personal terms. I have deep gratitude for many people helping me to build this dissertation over the last three years, and making this doctoral work an unforgettable experience.

First and foremost, I would like to express my sincere gratitude to my advisor Prof. Ryota NAGASAWA for the continuous support of my Ph.D study and related research, for his support, patience, motivation, and immense knowledge. His guidance helped me in all the time of research and writing of this thesis. I could not have imagined having a better advisor and mentor for my Ph.D study. And special thanks should be given to Mr. Yossawat Thiansawat (the Sri Lanna National Park superintendent) and Mr. Tanakorn Srisurak for data collection and providing informative data in terms of field survey in Sri Lanna National Park. The important supporters were my DNP colleagues; Mrs. Rewadee Panyatram and Mr. Alongkot Janbumrung. Thank you for all your helps, continuous supports, good conversations and pleasant meals.

I am also grateful to Office of National Park and DNP for the financial support of Scholarship to study in Tottori University, Japan and for providing the resources and conditions needed for the development of my Ph.D work.

In addition, friends are an essential part of surviving the Ph.D process during three years in Japan. I must thank my friends and lab colleagues (too many to list here but they know who they are!) for providing the support and friendship that I needed. A special thank you to my Indonesian friends; Miss Lissa Fajri Yayusman and Miss Prima Rizky Miralva for their company, creating a great memories and making me laugh even in the not so-good moments.

Of course no acknowledgments would be complete without giving thanks to my family (BURAPAPOL's family). All of them always gave me much of love and much of

encouragement to complete Ph.D study. I would like to express my deepest appreciation to my parents who work very hard during their entire life to provide the best for me and my sister and brother. To my sister and brother who, although the distance, always gave me the best of the advices and support. Thank you all for support, patient, unwavering belief in me and giving me the strength to finish my Ph.D dissertation. I could not have complete this long journey without family by my side. There are no words that can express my gratitude and appreciation for all you do and are for me. I love you all.

Table of Contents

List of Tables

List of Figures

List of Abbreviation

ADD : Absolute Average Difference
adj-R^2 : Adjusted R-squared
AHP : Analytic Hierarchy Process
CVI : Chlorophyll Vegetation Index
DBH : Diameter at Breast Height
DEM : Digital Elevation Model
dNBR : Differenced Normalized Burn Ratio
DNP : Department of National Parks, Wildlife and Plant Conservation of Thailand
DNs : Digital Numbers
DVI : Different Vegetation Index
EO : Earth observation
EVI2 : Two-band Enhanced Vegetation Index
FAO : Food and Agriculture Organization of the United Nations
FMC : Fuel Moisture Content
GBH : Girth at Breast Height
GIS : Geographic Information System
IUCN : International Union for Conservation of Nature and Natural Resources
Landsat OLI/ TIRS : Landsat Operational Land Imager/ Thermal Infrared Sensor
Landsat TM/ETM : Landsat Thematic Mapper /Enhanced Thermatic Mapper
LB : The Estimated Leaf Biomass
LST : Land Surface Temperature
LST_{max} : The maximum LST
LST_{min} : The minimum LST
MODIS : Moderate Resolution Imaging Spectroradiometer
NBR : Normalized Burn Ratio
NDDI : Normalized Difference Drought Index
NDVI : Normalized Difference Vegetation Index
NDWI : Normalized Difference Water Index
NIR : Near-Infrared
P-P plot : probability plot
R^2 : R-squared
RMSE : Root Mean Square Error
RS : Remote Sensing

RVI : Ratio Vegetation Index
SAVI : Soil-Adjusted Vegetation Index
SD : Standard Deviation
SWIR : Shortwave Infrared
Tb : Brightness Temperature
TVDI : Temperature Vegetation Dryness Index
USGS : United States Geological Survey
UTM : Universal Transverse Mercator
VI : Vegetation Indix
WFR : The Numerical Index of Wildfire Risk
WGS : World Geodetic System

CHAPTER 1

Introduction

1.1 Research Background

The Kingdom of Thailand is located in the tropical area of Southeast Asia between latitudes 50° 35′ and 200° 15′ north and longitudes 97° 30′ and 105° 45′ east. Its total area is 513,115 km^2 consisting of mountainous areas, highlands and lowlands. Thailand is situated in a hot and humid climatic zone which supports a variety of tropical ecosystems. According to the climate pattern and topography, Thailand has complex and varied types of forests, classified as tropical forests, which are rich in ecosystem diversity, natural communities and habitats. Moreover, forest areas are important places for the protection of ecological systems and natural resources as well as for the provision of recreational and tourism opportunities for people (Boyd, 2006). Therefore, these forest areas have been protected to prevent loss or degradation resulting from natural or man-made causes. National parks represent one type of protected forest area with special habitats, plants and wildlife. National parks are managed by the Department of National Parks, Wildlife and Plant Conservation of Thailand (DNP). A national park is a park with a large area of land that is protected because it has a wide variety of landscapes and a high diversity of native plants and animals. In addition, a national park is an open space providing outdoor recreation and camping opportunities as well as education for the public on the importance of conservation and on the natural wonders of the country in which the national park is located. Therefore, recreation and tourism play an important role in the life of a national park. Recreational areas are open sites which have a wide variety of natural features and landscapes that support tourist attractions and activities. Forests are major recreational areas in national parks, supporting nature-based activities in these areas. Thus, when forests are lost or destroyed, their destruction necessarily has a significant effect on recreational areas.

In present times, many forests in Thailand have been completely lost and destroyed, mainly as a result of human activities or natural forces. In the past, Thailand was a country with a high percentage of forest cover: around 27,360,000 hectares (ha) accounting for half of the land area (53.33%). This area is now considerably reduced, and only 31.60% of forest area remains compared to the situation 50 years ago (Figure

1.1). This indicates that Thailand's forests have followed a continuously decreasing trend.

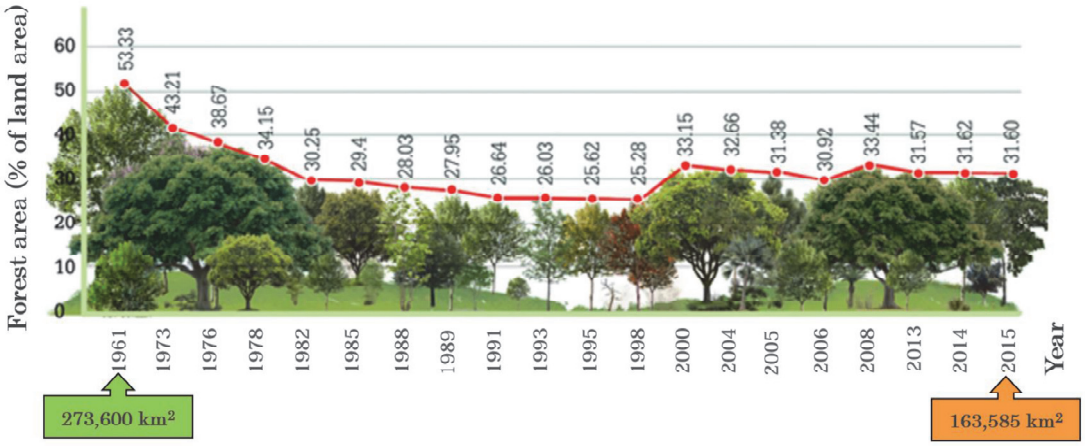

Figure 1.1 Thailand's forest situation (The Seub Nakhasathien foundation, 2017)

As previously mentioned, human activities and natural occurrences are the main causes of forest area degradation. In a developing country like Thailand, people interact with nature and forests for their livelihoods, contributing to problems caused by human actions. Plantation agriculture and illegal logging especially are major threats in forest areas. In addition, the damage caused by natural occurrences such as flood, drought and wildfire endanger tropical forest areas to an extreme degree. Interestingly, wildfire can be caused both naturally and by humans. It has become a serious problem in Thailand.

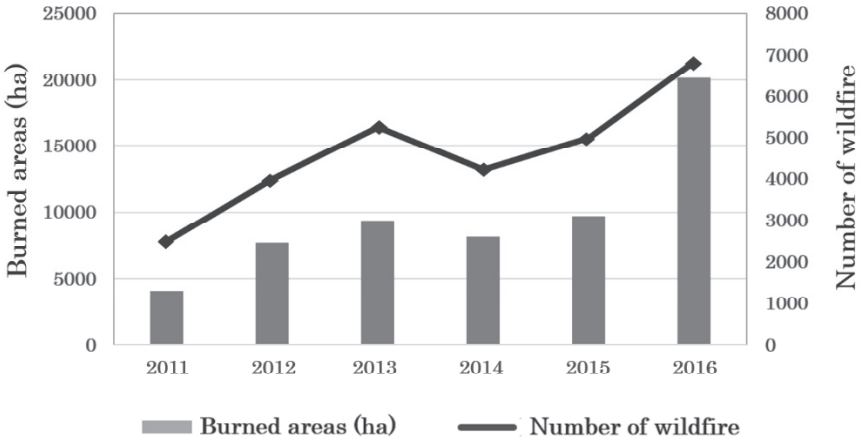

Figure 1.2 Wildfire frequency and area burned over a number of years within Thai protected forest areas (Forest Fire Control Division, 2016)

Wildfire is one of the important causes of devastating impacts on soil nutrient loss, disturbance of wildlife habitat and air pollution, as well as resulting in large burned forest areas. Moreover, wildfire in forest landscapes can also damage the natural resources, biophysical scenery and landscapes which are the bases of tourism and recreation. Since Thailand is located in a hot-humid climate, it can result in a drought. The dry season runs from November to April. In the dry season, the forest faces a dry and hot climate, resulting in drought conditions, and the forest is therefore vulnerable to fire, which is a major cause of forest degradation. Human activity is also a major cause of fire ignition, especially burning to clear agricultural areas for large plantations and the small fires used in livelihood activities. As a result, fires can burn out of control in degraded landscapes and encroach upon forest areas. Protected forest areas in Thailand have experienced a large number of wildfires over the past few decades. The statistical evidence in Figure 1.2 shows that wildfires occurring in Thai protected forest areas have been increasing in frequency and severity since 2011. This implies that the number of wildfires has been increasing, but that there is also a trend toward larger burned areas. Therefore wildfire has become a problematic phenomenon and wildfire management takes a high priority in protected forest areas, as an integral part of forest management.

FAO (2006) gives a definition of wildfire management as an approach that requires many activities for the protection of burnable forest and other valuable vegetation from fire. It involves the strategic integration of such factors as knowledge of fire regimes, probable fire effects, values at risk, level of forest protection required, cost of fire-related activities and prescribed fire technology into multiple-use planning, decision-making and day-to-day activities to accomplish stated resource management objectives. Therefore, wildfire management is the process of planning for, preventing and fighting fires in order to protect forest resource including landscape and wildlife. Moreover, the principles of wildfire management state that these processes should be considered before making decisions about what actions to take on wildfires. Wildfire prevention is the most important part of wildfire management. It is directly related to both processes of wildfire, as firstly, it can help to stop wildfires before they start and secondly, it can also reduce the spread and intensity of wildfires after they have started. Therefore, wildfire prevention plays a significant role in wildfire management. There are several strategies for wildfire prevention, such as local community-based approaches, fire detection, fuel reduction, firebreak creation and fire risk assessment. With regard to

wildfire risk assessment, the key approach is to prevent a wildfire from starting and to reduce the intensity of a wildfire, once started. In addition, it can be used for planning and preparation for wildfire suppression activities.

Risk assessments are decision support tools that integrate information regarding the likelihood and magnitude of resource responses to risk factors, in order to synthesize a conclusion about risk that can inform decision-making (Sikder et al., 2006). Assessing wildfire risk essentially requires an understanding of the likelihood of wildfires by intensity level, and the magnitude of the potential beneficial and harmful effects on valued resources from fires at different intensity levels (Finney, 2005). Therefore, wildfire risk assessment is a holistic approach that integrates the likelihood of wildfire and the critical factors responsible for igniting and driving wildfire, in order to evaluate exposure to fire risk and to identify levels of risk. In other words, assessment of wildfire risk must include consideration of the factors responsible for driving wildfire occurrence, based on understanding wildfire behavior and the factors catalyzing wildfire ignition. Wildfire behavior is a product of the environment in which the fire is burning. The fire environment includes the surrounding conditions, influences and modifying forces that determine the behavior of the fire. Fuel, weather and topography are the main interacting influences that make up the fire environment (Pyne et al., 1996). Wildfire risk assessment should also consider other factors contributing to wildfire ignition, particularly human activity, which is a major factor in the occurrence of wildfires. Essentially, through wildfire risk assessment, a combination of many factors (based firstly on fire environment, i.e., fuel, weather and topography and secondly on human activity or anthropogenic factors, i.e., distance from roads and proximity to settlements) should be considered for modeling wildfire risk.

Many tools and techniques are used for assessing wildfire risk, especially Earth observation (EO) and geographic information system (GIS) techniques. The use of EO data enables the detection and classification of objects on the Earth, including on its surface. EO data are normally acquired from remote sensing platforms such as satellites. The use of satellite remote sensing data is traditionally based on the use of various spectral indices. Vegetation indices (VIs) are a mathematical combination of different spectral bands. VIs are widely used and have benefited numerous disciplines concerned with the assessment of biomass, forest detection, plant stress, plant health, crop production and wildfire. Regarding wildfire assessment, VI has been applied in the analysis of wildfires including the effects of fire severity, pre- and post-fire events,

wildfire factors and wildfire risk zones. The use of satellite remote sensing data for the analysis of wildfire risk is traditionally based on the use of various spectral indices. Hence, the application of VI derived from remote sensing data for the extraction of wildfire factors is an interesting approach to assessing and modeling wildfire risk. GIS is an information system designed to work with data referenced by spatial or geographic coordinates. In other words, a GIS is both a database system with specific capabilities for spatially-referenced data, and also a set of operations for working with the data (Star and Estes, 1990). Therefore, GIS techniques have opened up opportunities for analyzing and integrating a great variety of wildfire factors at all geographic and spatial scales as well as for establishing a GIS-based wildfire risk model. To move forward, both techniques should be combined for the application of wildfire management at large scales and in remote areas. These techniques are suitable for identifying the spatial distribution of wildfire risk at recreation sites located in forest areas, especially in national parks. Using remote sensing and GIS techniques for wildfire risk assessment means that it is typically easier and cheaper to prevent a wildfire from starting than to put it out. In addition, remote sensing and GIS can increase the efficiency of wildfire risk reduction in forest areas and assist in the development of guidelines regarding the prevention of wildfires at recreation sites.

1.2 Objectives and Research Hypotheses

The purpose of this dissertation is firstly to assess wildfire risk and its corresponding risk levels by integrating the techniques of remote sensing and GIS, based on several factors associated with wildfire, and then to exploit the assessed wildfire risk to evaluate the wildfire risk at recreational sites. The factors selected for modeling and mapping wildfire risk are commonly recognized as factors in wildfire occurrence, namely, leaf fuel loads, soil moisture, slope, aspect, elevation, distance from roads and proximity to settlements. The capabilities of remote sensing and GIS techniques are utilized for analyzing wildfire risk at recreational sites. Therefore, the objectives of the research were formulated as follows:

(1) To estimate the spatial distribution of the leaf fuel load, as one of the selected factors influencing wildfire, by generating a predictive model of leaf fuel load using remotely sensed data based on VIs derived from a Landsat 8 Operational Land Imager (OLI).

(2) To predict the spatial distribution of soil moisture, as one of the selected factors responsible for wildfire occurrence, by establishing a predictive model of soil moisture using remote sensing based on VIs computed from Landsat 8 OLI/thermal infrared sensor (TIRS) and moderate-resolution imaging spectroradiometer (MODIS) data.

(3) To evaluate the use of soil moisture data for wildfire risk assessment.

(4) To map wildfire risk zones based on the integration of several factors contributing to wildfire, including leaf fuel loads, soil moisture, slope, aspect, elevation, distance from roads and proximity to settlements.

(5) To assess wildfire risk at recreational sites using GIS.

In addressing these objectives, the research concentrated particularly on the following hypotheses:

Regarding the first objective, to study the leaf fuel load estimation based on VIs, we hypothesized that:

(i) The difference in estimated leaf biomass between normal and dry seasons (estimated by a seasonal VI) can express the quantity of the missing leaf biomass, (i.e., the surface leaf fuel load), and that this can be used as a substitute for the actual leaf fuel load in the forest.

Regarding the second objective, to estimate the soil moisture based on VIs, we hypothesized that:

(ii) The relationship between the normalized difference water index (NDWI) and the land surface temperature (LST) performs as well as, or better than, the relationship between the normalized difference vegetation index (NDVI) and the LST, and can be applied for calculating the temperature vegetation dryness index (TVDI).

(iii) The estimated soil moisture derived from the developed model is directly related to the fuel moisture influencing wildfire occurrence.

1.3 Dissertation Outline

This dissertation is divided into seven chapters. This first chapter is intended to provide an introduction to the research, and consists of three main elements: the background, the objectives and an outline of the whole thesis. Chapter 2 reviews theoretical definitions of important terms drawn from the literature on national parks and recreational areas, wildfire, wildfire risk assessment and the applications of remote

sensing and GIS techniques in evaluating wildfire risk. This chapter also provides a conceptual framework for the methodology used in the study. Chapter 3 gives the characteristics and details of the study area.

Chapter 4 describes the leaf fuel load estimation required to achieve the first objective. Many potential VIs extracted from remote sensing data are compared for their ability to estimate leaf biomass, and are then used to estimate leaf biomass in normal and dry seasons (a seasonal VI). The leaf fuel load is estimated based on the difference in the estimated leaf biomass in normal and dry seasons. The difference in the estimated leaf biomass can determine the quantity of the missing leaf biomass which is regarded as the leaf fuel load on the ground surface.

To accomplish the second and third objectives, chapter 4 investigates the relationship between VIs (NDVI and NDWI) and the LST before calculating the TVDI. The spatial distribution of soil moisture is estimated based on the TVDI (modified from NDWI and LST) and the normalized difference drought index (NDDI). Based on the results for the estimated soil moisture, the correlation with leaf fuel moisture for wildfire risk assessment is evaluated.

To fulfill the fourth and fifth objectives, chapter 5 integrates crucial factors influencing wildfire computed from remote sensing data, (i.e., leaf fuel load and soil moisture) and GIS data, (i.e., slope, aspect, elevation, distance from roads and proximity to settlements), to establish a wildfire risk model using pairwise comparison and GIS approaches. A map of wildfire risk zones generated from the model is later used to assess the risks of wildfire at recreational sites.

Finally, in chapter 6, overall conclusions are given.

CHAPTER 2

Theoretical and Conceptual Framework

2.1 National Parks and Recreational Areas

Thailand is one of the tropical countries located in Southeast Asia in which forests are valued for their high biodiversity, ecosystems and commercial importance (Kummer and Turner, 1994). Forests in Thailand are rich in biological diversity, containing approximately 6-10% of the total number of species known thus far (Baimai, 2010). There are various kinds of tropical forest in Thailand including evergreen forest, pine forest, dry dipterocarp forest, mixed deciduous forest, mangrove forest and peat swamp forest (Figure 2.1). These variations in forest type provide a multitude of benefits in terms of goods (timber, food, fuel and bioproducts), ecological functions (habitat for a vast array of plants and wildlife) and places for recreation. Thailand's forests have been managed according to conservation and protection objectives. Forest conservation refers to a range of activities, tools and approaches to maintain forest health and biodiversity. Forest protection refers to the creation of parks and other areas to legally protect them from industrial activity and to help preserve healthy ecosystems. Forests in Thailand representing around 20% of total land area have been placed in protected areas managed by DNP. These protected areas have been divided into four main types and include 130 national parks, 59 wildlife sanctuaries, 79 non-hunting areas, and 120 forests (Office of National Park, 2017). Clearly, national parks make up the largest number of these protected areas and play an important role in sustainable forest management.

National parks are usually large areas of protected land, primarily established for the purpose of conservation and enhancement of the natural scenery, wildlife and cultural heritage (Mallarach, 2008). IUCN defines a national park as a natural area of land or sea which provides a foundation for spiritual, scientific, educational, recreational and visitor opportunities (IUCN, 1994). Hence, national parks encompass a wide range of native plants and animals as well as unspoilt landscapes, and they allow and encourage access for educational, recreational and tourism purposes. Nowadays, national parks are always open to visitors (Gissibl et al., 2012) and are important tourist destinations. According to Fennel and Smale (1992), national parks are attracting increasing numbers of nature-oriented ecotourists.

Figure 2.1 Different types of forest in Thailand

This means that most national parks provide tourism facilities based on natural outdoor recreation and camping opportunities, as well as classes designed to educate the public on the importance of conservation and on the natural features of the country in which the national park is located. Tourism and conservation objectives are complementary and jointly achievable in both national parks and game reserves, although tourism should be secondary to conservation, as asserted by the proponents of ecological tourism (Yunis, 2003). Therefore, recreational activities and areas play an important role in the life of a national park since they contribute to tourism opportunities and even have the potential to actively promote the sustainable management of the national park.

There are many different kinds of tourism and recreation based on the unique landscape and special scenery of a particular national park, including recreation, outdoor recreation, adventure tourism and nature-based tourism. Recreation can be defined as the pursuit of leisure activities during one's spare time (Tribe, 2011) and can include many different activities such as hiking, climbing and fishing. This definition of recreation therefore pertains to tourism. A recreational area is an area used by the public for recreation and provides satisfaction and pleasure for people. Recreational areas in national parks which are associated with forests and other natural resources (such as mountains, waterfalls, caves, hot springs and beaches), offer nature-based recreational activities (Figure 2.2).

Figure 2.2 Natural resources and nature-based recreation activities in Thai national parks

Hence, forests, natural resources and wildlife in national parks provide recreation opportunities and settings, and support a wide range of activities, (e.g., walking and hiking on trails, nature observation, camping and picnicking, biking, watching birds and wildlife, boating and canoeing). Recently, these recreation activities have become the fastest-growing tourism sector in national parks while the areas supporting these activities have been increasingly threatened in many ways. One of the causes of damage to recreational areas is wildfires. Wildfires have a negative impact on recreational areas due to landscape-scale damage and result in a decline in tourism activities. Hence, it is necessary to recognize the need for professionalism in the management of tourism and recreation in protected areas (Weaver, 2001; Worboys et al., 2001; Eagles et al., 2002; Newsome, 2002). This therefore implies that providing recreational areas for tourism while also protecting the national park resources from wildfire is an important component of national park management.

2.2 Wildfire

2.2.1 Characteristics of Wildfire

Wildfire is fire in a wild area, especially in a forest, that is not controlled and that can burn a large area of the forest landscape. The pattern of fire effects on forests

depends on the temporal and spatial scale of fires. Wildfire is one of the most important causes of impacts on landscapes and ecosystems (Brown and Kapler, 2000; Bond and Keeley, 2005; Santi et al., 2013). A concept of three fire triangles can describe the characteristics of wildfire and its role in a forest landscape and ecology (Figure 2.3). This concept indicates the relative importance of the major factors of climate, fuel and landscape variables at different scales (Timothy, 2014). At the smallest scale (Figure 2.3 – lower left), fire begins with combustion as described in the fire triangle. There are three basic components that are required for a fire to ignite, burn and continue to burn. These are oxygen, heat and fuel. Fuel is any material that can ignite and be burned, oxygen is an essential part of the chemical reaction needed to create fire and heat is needed for ignition.

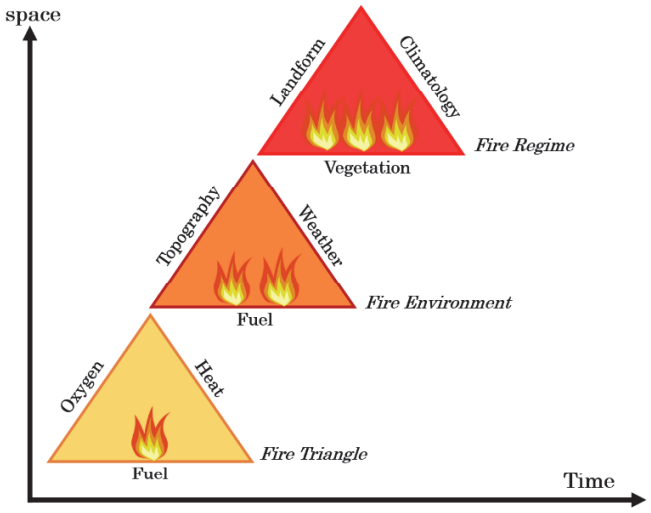

Figure 2.3 Concepts of fire change across spatial and temporal scales, modified from Mark and Kevin (2009)

At the next temporal and spatial scale (Figure 2.3 – middle), there are three factors that make up the fire environment, namely fuel, weather and topography. These factors influence fire behavior including ignition probability, rate of fire spreading, and fire intensity at seasonal to annual time scales (Rothermel, 1972; Pyne et al., 1996). Fire behavior is a product of the environment in which the fire is burning (Pyne et al., 1996). It refers to the manner in which fuel ignites and flame develops, how fast a fire spreads and how intensely a fire burns. In wildfires, this behavior is primarily related to the fire environment, i.e., the weather, topography, and fuel characteristics. Many researchers have studied fire behavior and found that it is affected by many factors, such as weather conditions (Bailing et al., 1992), fuel characteristics (Mouillot et al.,

2002; Schoenberg, 2003), human activities (Velez, 1992), fire management activities (Fried et al., 2008) and changes in land uses (Rego, 1992) and climate (Flannigan et al., 2000; Fried et al., 2004).

On timescales of decades to millennia (Figure 2.3 – upper right), the fire regime triangle describes variables that determine the characteristic pattern, frequency, and intensity of fire at landscape and broader scales, reflecting the linkages between vegetation as a determinant of fuel, climate conditions as a creator of weather and ignition sources, whether human or natural (Parisien and Moritz, 2009; Krawchuk and Moritz, 2011). Therefore, in understanding the characteristics of fire, it is helpful to define linkages between the factors responsible for wildfire and the surrounding conditions, influences and modifying forces that determine fire behavior, and which can affect fire spreading and fire severity across landscape-scale forest areas.

There are three types of wildfire: ground fire, surface fire and crown fire (Figure 2.4). A ground fire burns organic material in the soil or peat, and other materials which can ignite and burn under the ground. This is a persistent slow-burning fire because the combustible materials (ground fuels) are compacted, have a limited oxygen supply and are protected from wind. A surface fire burns in the surface fuel layer which lies immediately above the ground fuels but below the canopy or aerial fuels. Surface fuels consist of needles, leaves, grass, dead and fallen branches and logs, shrubs, low brush, and short trees (Brown et al., 1982). The rate of surface fire spreading depends on the density of these fuels, the continuity and size of trees and

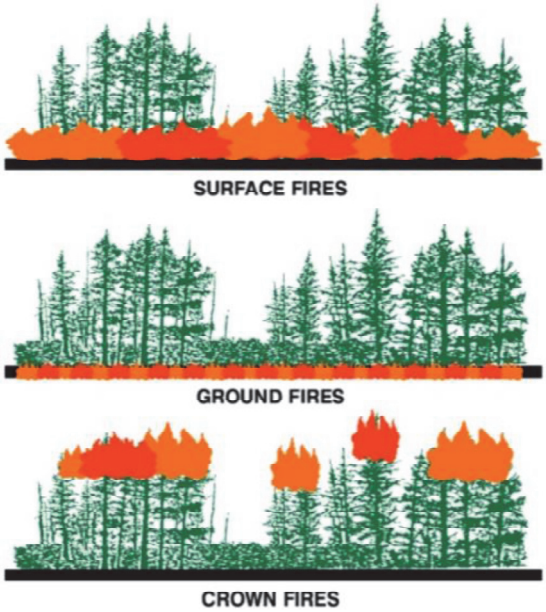

Figure 2.4 Types of wildfire (source: Slideshare.net)

underbrush, the slope of the terrain and the weather. A crown fire burns and spreads through the crown or canopy of trees. Canopy fuels normally consumed in crown fires consist of live and dead foliage, lichen, and fine live and dead branch wood found in a forest canopy (Scott and Reinhardt, 2001). The influence of wind is greater in the tree canopy and where this canopy is interconnected or continuous, fires can spread quickly and extremely. In general, wildfire in Thailand is classified as surface fire (Figure 2.5). It occurs annually during the dry season from November to April with the peak period in February and March. The most common surface fires take place mainly in dry dipterocarp forests and in mixed deciduous forests. This is because during the dry season, under certain drought conditions, dipterocarp and deciduous trees shed their leaves in a cycle which helps them to survive in drought conditions. The dead leaves fall to the ground surface and form the largest part of the fuel load. This results in fuel accumulation on the ground surface, which can ignite and burn down to the surface to become a surface fire. Therefore, dipterocarp and deciduous forests are the main areas prone to wildfire in Thailand, and their dead leaves can result in the development of extreme fire behavior, contributing to intense and uncontrolled fires.

Figure 2.5 A surface wildfire in Thailand

2.2.2 Factors Influencing Wildfire

There are several factors that must be considered with regard to wildfire occurrence. Not only factors based on the fire environment, but also factors derived from human activities influence the stages of wildfire occurrence. At the initial stage of wildfires, human activities are the most important factor contributing to wildfire ignition. After combustion occurs and a fire begins to burn, there are several factors that determine

how the fire behaves and spreads. These factors are based on the fire environment including fuel, weather and topography. Hence, determining these factors can reduce fire likelihood and the occurrence of conditions that contribute to wildfire. The factors affecting wildfire occurrence which are considered in this research for analyzing wildfire risk, are listed below;

Fuel Load

Fuel is any organic material, living or dead, that can ignite and burn. In the case of wildfire, fuels are primarily carbohydrates (cellulose and hemicellulose) derived from vegetative biomass that can be burned (Mark and Kevin, 2009). Bracmort (2013) states that fuel loads typically exclude biomass in live, commercially valuable trees. Thus, fuel loads consist of dead biomass (needles or leaves, branches that have fallen, and older dead cellulose). Therefore, the leaf biomass of trees in forests, especially dipterocarp and deciduous forests, can provide annually available surface fuel, because these leaves are typically shed in the dry season. Consequently, this dead-leaf biomass becomes an important fuel lying on the ground (Figure 2.6).

Figure 2.6 Most of the surface fuel in dipterocarp (left) and deciduous (right) forests derives from dead leaves

As reviewed above, fuel is one of the components of combustion and fire environment; the amount of fuel has therefore a considerable effect on fire behavior. Thus, analysis of the fuel characteristics is a strategy in the evaluation of fire behavior. Several researchers have devised fuel models to provide estimated values of fuel loadings, surface area to volume ratios, fuel depths, fuel particle density, heat content and moisture of extinction for fire behavior modeling (Rothermel, 1983; Scott and Burgan,

2005). Three sets of fuel models are commonly used in large landscape-scale contexts to describe predicted fire behaviors (Anderson, 1982; Noonan-Wright et al., 2013), fire danger (Deeming and Brown, 1975; Deeming and Burgan, 1977) and fire risk and potential (Burgan et al., 1998). Anderson (1982) states that fuel load and fuel depth are significant fuel properties for predicting whether a fire will be ignited, its rate of spreading and its intensity. Very low volumes of surface fuel can result in a low fire intensity, whereas larger volumes of surface fuel define a risk of high-intensity fires and an extreme overall fuel hazard. Thus, total fuel accumulations (fuel loads) contribute to fire intensity and damage and should be considered when assessing wildfire risk.

Soil Moisture

The climate in Thailand is controlled by tropical monsoons and the weather is generally hot and humid. Thus, Thailand's seasons are generally divided into two: the hot or dry season and the rainy season. In reality, however, the weather is relatively hot for most of the year. Dry weather is one of the most important parameters influencing wildfire occurrence (Yongqiang et al., 2010). Drier conditions increase the chances of a fire starting, and help a burning fire spread, resulting in a more intense and long-burning fire. One of the indicators commonly used for detecting drought conditions is the level of soil moisture. Drier conditions cause soils to be drier for longer, increasing the likelihood of drought and a longer wildfire season. Moreover, the level of fire severity depends upon heat transfer in the soil during the combustion of above-ground fuels and surface organic layers (Neary et al., 2005). During the burning process in a wildfire, heat can rapidly transfer from the fire to the dry soil. Consequently, the wildfire spreads quickly and soon becomes intense. Krueger et al. (2015) studied the influence of soil moisture on wildfire size and found that large growing-season wildfires occurred exclusively under conditions of low soil moisture. In addition, soil moisture is positively correlated with fuel moisture, because fuel moisture is fundamentally controlled by plant physiology and soil water availability. Dead-fuel moisture especially is affected by soil moisture (which is also affected by weather) near the dead-fuel surface (Dimitrakopoulos et al., 2011). Therefore, considering soil moisture as a factor linked to wildfire is likely to be effective for evaluating wildfire risk.

Topography

Topography refers to the surface features of the land, and this is the most constant of the three fire environment components. Topographic features can cause dramatic changes in wildfire behavior and can affect how prone the area is to fire. All topographic features, including slope, aspect and elevation, influence fire behavior (Rothermel, 1991; Anderson, 1982) and particularly fire spread (how fast a fire moves in feet per hour), therefore affecting the distribution of burned areas across landscapes.

Slope is the angle of incline on a hillside. Slope can be a primary influence on wildfire behavior because the slope increases the radiation and convection heat transfer up the slope. The steeper the slope the greater the up-slope heat transfer and thus, the higher the fire spreading rate and intensity. Curry and Fons (1938; 1940) suggested that slope resulted in increased heat transfer between the flames and the fuel ahead of them. McArthur (1968) suggests that slope can significantly affect the rate of spread of fire, especially immediately following ignition. He suggests that when compared to flat terrain, directional fire spreading rates will double on 10-degree slopes and increase fourfold on 20-degree slopes. Therefore, as the steepness of the slope increases, the fire spreads more quickly. On the other hand, fires tend to move more slowly as the slope decreases.

Aspect is the direction in which a slope faces. Aspect affects fire behavior through the degree of solar exposure and the wind that different aspects receive. Normally, in the northern hemisphere, a north-facing slope faces away from the sun and thus is generally cooler and moister than south-facing slopes. Conversely, south and southwest aspects receive more sunshine leading to lower humidities and higher fuel temperatures (Pyne et al., 1996) and therefore have the most favorable conditions for starting and spreading fires.

Elevation is the height of the given terrain above mean sea level. Elevation influences fire spread by impacting the wind behavior and precipitation patterns (Bennett et al., 2010) and thereby plays a large role in determining the conditions and amount of fuel. Fuels at lower elevations will dry out earlier than fuels at a higher elevation due to higher temperature. In extremely high elevations there may be no fuel. Therefore, low elevation areas are more prone to fire due to higher temperature and less precipitation (Veblen et al., 2000; Harmon, 1982).

Human Activities

Human activity is the primary cause of wildfires in terms of the probability of ignition and combustion, though it does not influence the behavior of wildfire. Most fires caused by humans are accidental. Accidental fires in forests are usually caused by carelessness or inattention. Some are intentionally set by arsonists. An important cause of wildfire ignition in Thailand is human activity on the part of people living in areas surrounding the forests and visitors traveling through national parks (Table 2.1). The most frequent cause of wildfire ignition, accounting for 43.01% of fires, is the collection of non-timber forest products from forest areas by local people in pursuit of their livelihoods. The second most frequent is unidentified causes associated with campers, hikers or others traveling through the forest, followed by illegal hunting (15.98 %). Even if hunting wildlife is prohibited in forest protected areas, there are still some people, especially local people living in or near the forests, who hunt wildlife for their livelihood. These people use fire to flush out wildlife. Another important cause is the burning of agricultural debris by farmers (11.31%). Burning debris in agricultural lands can cause fires to spread to nearby forests accidentally. Since most wildfires are ignited as a result of human activity and behavior, these anthropogenic sources should be considered as a wildfire factor. Anthropogenic factors which are important variables influencing fire occurrences are represented by factors such as distance from roads and proximity to settlements (Avila-Flores et al., 2010).

Table 2.1 Causes of wildfire ignition in Thailand (Forest Fire Control Division, 2011)

Causes of wildfire ignition	%
1. Gathering forest non-timber products	43.01
2. Illegal wildlife hunting	15.98
3. Agricultural debris burning	11.31
4. Cattle raising	3.48
5. Incendiary fire	0.43
6. Illegal logging	1.08
7. Carelessness	0.60
8. Other causes/Unidentified causes	24.11

Distance from roads is an indicator of accessibility to the forest. Forests located near roads are more prone to disturbance than forests located in remote areas which are not easily accessible (Laurance et al., 2009; Nepstad, 2001). This is because roads provide

a transportation route leading to increased human activity and thus roads inside and surrounding the forest provide more opportunities for accidental or man-made fires. The second factor identified as an anthropogenic causative factor is proximity to settlements. Forest areas near to settlements are more prone to fire ignition because accidental fires can be caused by residents inside the forest through day-to-day or cultural practices (Jaiswal et al., 2005).

In accordance with the reviewed literature, the factors considered in this research that influence wildfire occurrence include leaf fuel load, soil moisture, slope, aspect, elevation, distance from roads and proximity to settlements. These factors are used as inputs into wildfire risk assessments for mapping the wildfire risk of recreational areas in the national park.

2.3 Wildfire Risk Assessment

A risk assessment is conducted when predicted outcomes are uncertain, but possible outcomes can be described and their likelihoods can be estimated (Haynes and Cleaves, 1999). Typically, risk analysis concerns the measurement and communication of uncertain future events with extreme consequences (Brillinger, 2010). In addition, Sikder et al. (2006) consider risk assessments as decision support tools that integrate information regarding the likelihood and magnitude of the resource response to risk factors, in order to synthesize a conclusion about risk that can inform decision-making. Thus, it can be said that risk assessment is the process of estimating the likelihood and magnitude of the occurrence of an unwanted and adverse effect. The risk assessment is also generally used to describe the potential for loss, determined from estimates of likelihood and associated outcomes. Analysis of risk can help scientists and managers better understand the issues and can serve as a decision support tool regarding the timing, location and potential effects that might occur in future events. Wildfire risk, therefore, is the chance that a fire might start in wild lands or forests, as affected by the nature and incidence of causative factors. Assessing wildfire risk therefore requires the likelihood of wildfire to be analyzed by intensity level, so that the magnitude of potential beneficial and adverse effects to valued resources from fire can be assessed at different intensity levels (Finney, 2005). Bachmann and Allgower (2000) have suggested a structured wildfire risk assessment that incorporates not only the 'risk' in terms of probability and outcome, but also considers issues of wildfire occurrence, wildfire behavior, and wildfire effects. Therefore, the concept of risk assessment is

fundamentally related to the factors influencing wildfire occurrence and behavior. These factors can be used not only to evaluate potential wildfire areas but also to identify, quantify, and prioritize the different intensity classes of the risk.

2.4 Remote Sensing Data and GIS

In the context of wildfire risk assessment at a landscape level, remote sensing and GIS are appropriate techniques for providing a large-scale geospatial assessment of the wildfire risk potential. Application of remote sensing and GIS techniques for wildfire risk mapping is increasingly recognized as a technique for sustainable management of forest resources and recreational areas in national parks. Therefore, understanding remote sensing and GIS concepts is important in order to apply them to assessing wildfire risk over wide areas.

2.4.1 General Concepts of Remote Sensing

Remote sensing, also called EO, is the technique of observing and analyzing objects or areas at the Earth's surface from a distance, without being in direct contact with them. There are numerous books devoted to remote sensing, dealing with the general background to remote sensing and its applications (Cracknell and Hayes, 2007; Gibson and Power, 2000; Barrett and Curtis, 1992; Colwell, 1983; Swain and Davis, 1979).

Remote sensing activities include recording, processing, analyzing, interpreting and finally obtaining useful information from the data in the form of images usually generated from sensors on platforms (satellites and aircraft). Remote sensing techniques allow images of the Earth's surface to be recorded using various wavelength regions of the electromagnetic spectrum. Remote sensing systems can be categorized as using active or passive sensors (Figure 2.7). Active sensors provide their own energy source for illumination. For example, a radar sensor sends out sound waves and records the reflected waves coming back from the surface. Advantages of active sensors include the ability to obtain measurements whenever they are required. Passive sensors, on the other hand, need an external energy source. These sensors measure reflected light that was emitted from the sun. They detect sunlight radiation reflected from the Earth and thermal radiation in the visible and infrared parts of the electromagnetic spectrum. These sensors do not emit their own radiation, but receive natural light and thermal radiation from the Earth's surface. Most passive sensors make use of a scanner for imaging, e.g., Landsat and moderate-resolution imaging spectroradiometer (MODIS) sensors.

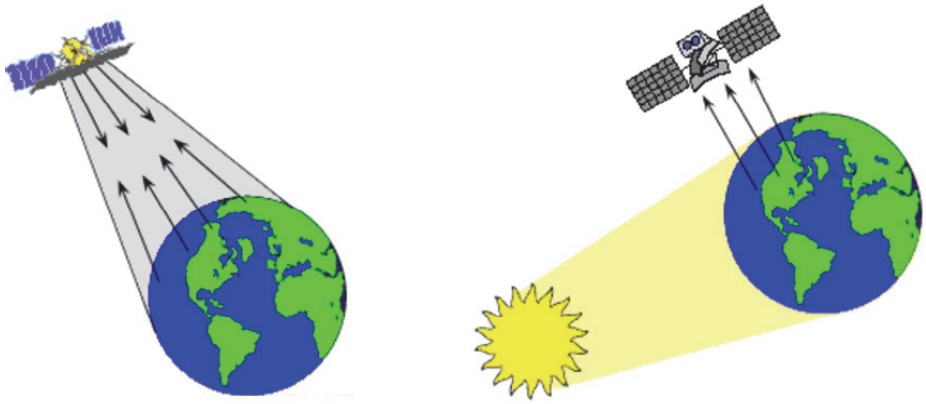

(a) Active remote sensing (b) Passive remote sensing

Figure 2.7 Types of remote sensors (a) active remote sensing and (b) passive remote sensing (source: Canada Centre for Remote Sensing-CCRS)

Equipped with spectrometers they measure signals in several spectral bands simultaneously, resulting in so-called multispectral images which allow numerous interpretations (Albertz, 2007). Passive systems are therefore much more common than active systems.

Passive systems used in remote sensing applications operate in the visible, infrared, thermal infrared, and microwave portions of the electromagnetic spectrum. These wavelength intervals in the electromagnetic spectrum (bands) are usually used to interpret remote sensing data. Of these, the red (ρRED: 0.6-0.7 μm) and near-infrared (NIR) (ρNIR: 0.75-1.35 μm) bands have been found to be the most relevant for remote sensing of vegetation (Myneni et al., 1995). Compressing spectral bands into VIs is more effective for the interpretation of remotely sensed data than using reflectance from individual spectral bands.

VIs are mathematical functions calculated from the ratio, difference, ratio difference and sum of the reflectances of two bands (Jackson and Huete, 1991). They are designed to enhance the contribution of vegetation properties and allow reliable spatial and temporal comparisons of terrestrial photosynthetic activity and canopy structural variations (Bannari et al., 1995). Such indices are not only used for vegetation analysis but can also be applied for wildfire analysis. Some VIs have been applied to wildfire assessment. For instance, Escuin et al. (2008) studied the capacity of the NDVI and the normalized burn ratio (NBR) derived from Landsat TM/ETM to enable fire severity assessment. They found that both indices were suitable for discriminating between fire severity levels. Chuvieco et al. (2004) combined NDVI and surface temperature to

obtain an estimate of live fuel moisture content for forest fire danger ratings. The results showed that using NDVI and surface temperature together with data on the seasonal trends of fuel moisture content and vegetation types can provide an empirical model which enables the spatial estimation of fuel moisture content to be derived. Moreover, Chafer et al. (2004) used different images of NDVI to define six fire severity classes and found that NDVI values produced a high-accuracy classification. Therefore, applying VIs for wildfire risk assessment is likely to be an effective technique in spatial mapping of wildfire factors computed from VIs, (i.e., leaf fuel load and soil moisture).

2.4.2 General Concepts of GIS

2.4.2.1 Definitions of GIS

A GIS is a set of tools for collecting, storing, retrieving, transforming and displaying spatial data from the real world for a particular set of purposes (Burrough, 1986). In addition, a GIS is an organized collection of computer hardware, software, geographic data and personnel, designed to efficiently capture, store, update, manipulate, analyze, and display all forms of geographically referenced information (ESRI, 1990). A GIS is defined by Young (1986) as a method of storing and retrieving data which are held in a structured form, have a location identifier and can therefore be manipulated and mapped in variety of ways. In essence, a GIS is a computer system for capturing, storing, querying, analyzing, and displaying geospatial data (Chang, 2014).

2.4.2.2 Data and Spatial Data Model

Data types in GIS can be classified into two main categories: 1) spatial data used for describing the absolute and relative location of geographic features and 2) attribute data or non-spatial data used for describing the characteristics of the spatial features. The spatial data, also known as geospatial data, describe both the location and the attributes of spatial features. This means that spatial data in a GIS give information about a physical object that is identified as features and boundaries with a geographic location and represented by numerical values in a geographic coordinate system.

A model is simply a means of representing reality, and spatial data models provide abstractions of spatially referenced features in the real world (Lloyd, 2010). A model of spatial features explains how spatial objects and spatial phenomena are related. The most common form of model, used for representation of real-world objects or phenomena associated with a location on the Earth, is the map. Spatial data can represent real-

world features with discrete boundaries as well as real-world phenomena with non-discrete boundaries. In general, spatial data can be stored and analyzed in vector and raster models. A vector data model uses the geometric objects points, lines and polygons to represent spatial features with a clarified spatial location and boundary. Each feature is assigned an ID so that it can be associated with its attributes. Furthermore, the vector data model uses a two-dimensional Cartesian (x, y) coordinate system to store the shape of a spatial feature.

The raster data model, on the other hand, uses a grid and grid cells to represent spatial features. A matrix of cells (or pixels) is organized into rows and columns (or a grid) where each cell contains a value representing information. Thus, points can be represented by single cells, lines by sequences of neighboring cells, and polygons by collections of contiguous cells. Data stored in a raster format representing real-world phenomena consist of: 1) thematic data representing discrete objects that have known and definable boundaries and 2) continuous data, representing phenomena in which the value at each cell location is measured from a fixed registration point. The main difference between vector and raster data is that raster data have spatial resolution. The spatial resolution of the raster data set is determined by the size or resolution of individual grid cells. For instance, Landsat satellite image data are raster data with cell sizes of 30m x 30m.

Thus, a GIS data model is a conceptual description of how spatial data are organized for use by the GIS. Combining vector and raster data, i.e., the two different ways of representing spatial data, can create a rich set of informative maps.

2.5 Integrating Remote Sensing and GIS for Wildfire Risk Assessment

Remote sensing and GIS are complementary technologies that, when combined, enable improved monitoring, mapping, and management of forest resources (Franklin, 2001). The integration of the two technologies can efficiently manipulate, spatially analyze and display landscape variables which can support the management of wildfires, (e.g., Chuvieco and Congalton, 1989; Ambrosi et al., 1998; Kuntz and Karteris, 1995). Likewise, these technologies can be used as an effective and powerful method for developing decision support systems for planners or decision makers concerned with wildfire.

With respect to wildfire risk assessment, the combination of remote sensing and GIS techniques has been applied to enhance and develop wildfire risk models and wildfire risk classification maps. Typically, both techniques have been used to analyze wildfire

risk through mathematical modeling for generating wildfire risk classification maps. Firstly, remote sensing imagery needs to be converted into tangible information which can be utilized in conjunction with other data sets, often within a widely used GIS (Blaschke, 2010). For inputting spatial data in GIS, the resource information must be in the form of a map, hence the mapping of the thematic layers is one of the primary requirements. This means that remote sensing is the primary source for many kinds of thematic data critical to GIS analyses for generating resource maps. In a GIS database, all features must be accurately positioned. Later, all data layers from remotely sensed and GIS data should be correctly georeferenced to a map projection and coordinate system. Finally, these layers are considered as different layers of information in an integrated analysis, using mathematical functions in order to create a specific and useful model and map.

A large number of studies have been carried out using remote sensing and GIS techniques for wildfire risk assessment, as shown in Table 2.2. Based on this table, factors influencing wildfire are produced from remote sensing and GIS data, and are created in different layers and overlaid using many mathematical methods to classify wildfire risk. Therefore, in this research, remote sensing is used as a source of information on leaf fuel load and soil moisture factors, and GIS is used to provide information on other factors such as slope, aspect, elevation, distance from roads and proximity to settlements. Subsequently, GIS processing makes it possible to create wildfire risk models using mathematical functions. For the remote sensing and GIS analysis in this research, ERDAS IMAGINE 9.1 software is used for remote sensing processing and ArcGIS 10.4 software is used for GIS processing.

2.6 Overall Conceptual Framework of the Research

This research sets out to assess and classify wildfire risk in Sri Lanna national park and thereby evaluate the risk at recreation sites in this park. The conceptual definition of a wildfire risk assessment should include the most relevant factors associated with wildfire. Factors chosen for the study are widely recognized as crucial for wildfire occurrences. These factors, especially leaf fuel load and soil moisture, are analyzed using remote sensing data, and subsequently all factors are overlaid using a pairwise comparison matrix to model the wildfire risk classification. Finally, a map produced from this model is used to evaluate recreation sites with respect to wildfire. Figure 2.8 shows the structured methodology applied in the various chapters of the research.

Table 2.2 Previous studies that have used remote sensing (RS) and GIS for assessing wildfire risk

Factors and theirs sources	Country	Methods	Authors	Results
RS: Vegetation species GIS: Elevation, slope, aspect, and proximity to roads	Spain	An integrated analysis of spatial factors by weighting factors (structural fire index) to create fire hazard models	Chuvieco and Congalton (1989)	The proposed model performed properly in identifying the areas subjected to a higher fire hazard
RS: Vegetation type GIS: Slope, proximity to settlements, and distance from roads	India	The utilization of spatial factors by weighting factors to establish a fire risk model	Jaiswal et al. (2002)	The model was found to be in strong agreement with actual fire-affected sites.
RS: Fuel GIS: Solar radiation, topographic wetness, and population density and distance from roads	US	The five factors were modeled and ranked for each factor to create a weighted overlay model	Lein and Stump (2009)	The results of a parsimonious GIS-based model were reasonable when compared to the historic pattern.
RS: Vegetation moisture GIS: Slope, aspect, and distance from roads and settlements	Greece	The combination of five influential factors by using risk indices for weighting factors to map forest fire risk	Siachalou et al. (2009)	Overlaying the fire risk zones to the classified burned areas provided a good reliability for the approach
RS: Vegetation moisture, GIS: Elevation, slope, aspect, distance from roads and proximity to settlement areas	Iran	The six factors were assembled into a model by weighting factors to produce forest fire risk maps	Adab et al., (2013)	The effective combination of different forest fire-causing variables with remote sensing data in a GIS environment can identify and map forest fire risk.
RS: Normalized difference water index (NDWI) GIS: Slope, aspect, elevation and distance from roads and settlements	India	The utilization of geospatial data by GIS and use of an analytic hierarchy process (AHP)	Thakur and Singh (2014)	The GIS along with AHP can be successfully employed in identifying fire-prone areas. Moreover, using AHP helps to understand the nature of the problem and the results thus obtained can be used for planning and management of forest resources.

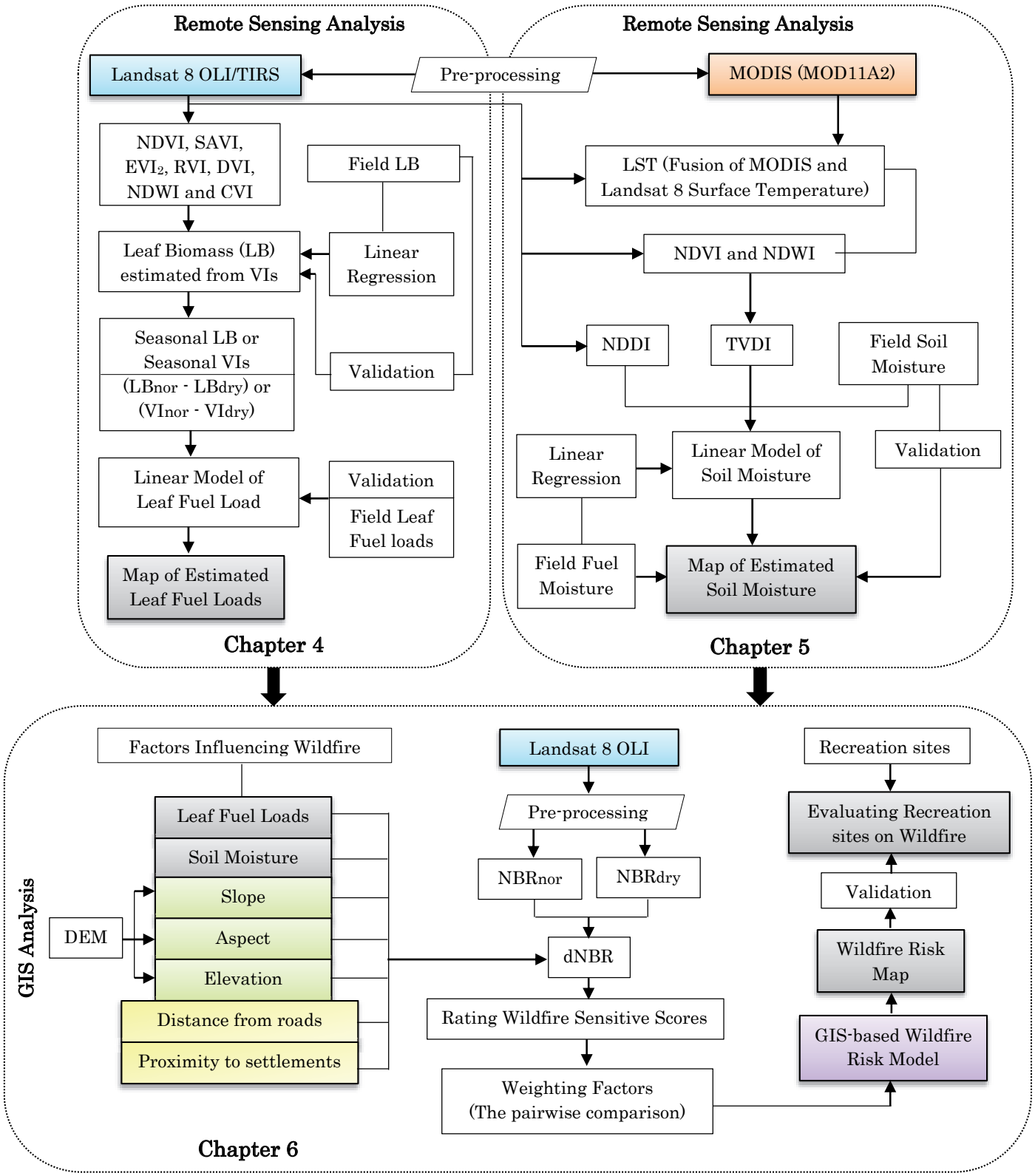

Figure 2.8 Overall conceptual framework of wildfire risk assessment at recreational areas

CHAPTER 3

Study Area Characteristics - Sri Lanna National Park

3.1 Physical Conditions

3.1.1 Geographic Location

Sri Lanna national park is situated in Chiang Mai province in northern Thailand. The area is at a latitude of 19° 16′ 56″ north and a longitude of 99° 5′ 28″ east (Figure 3.1). The national park is the eighth largest national park in Thailand with an area of 140,600 ha of forested and mountainous terrain occupying three districts of Chiang Mai: Chiang Dao, Prao and Mae Tang. Sri Lanna national park is geographically characterized by several mountain ranges, which are aligned north to south with differences in altitude, and the area has generally a slope of more than 35%. The park therefore includes rich and fertile forest which provides habitats for many plants and wildlife species.

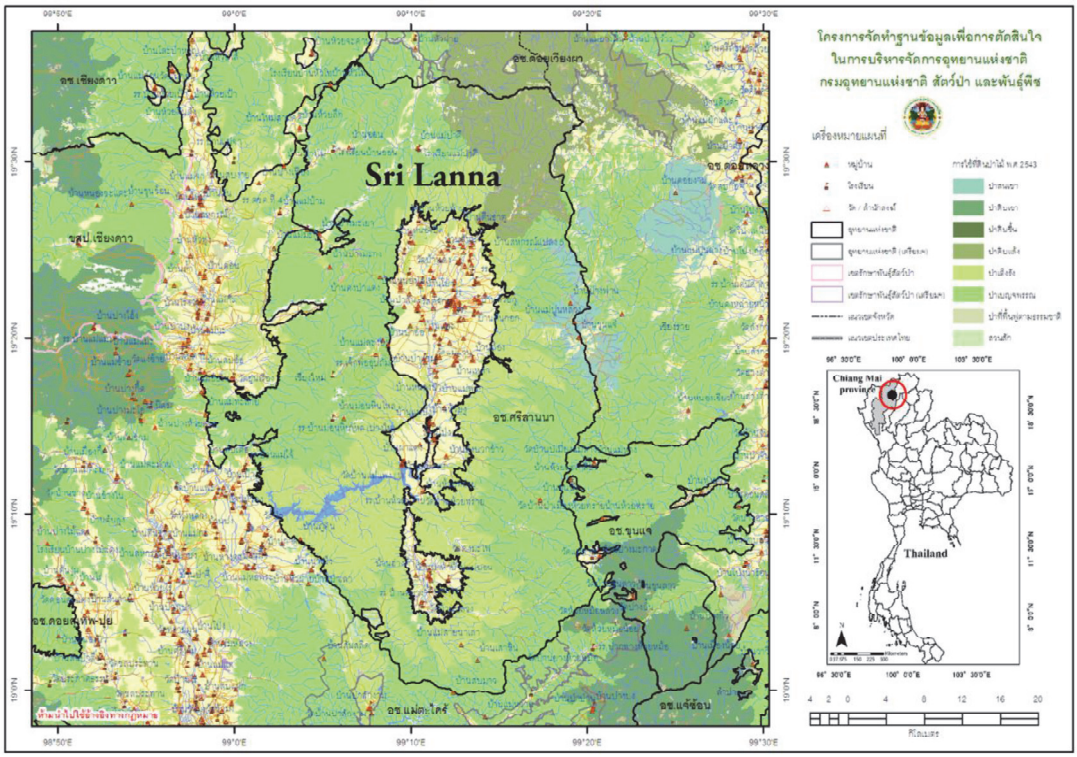

Figure 3.1 Geographic location of Sri Lanna national park (Office of National Park, 2017)

3.1.2 Topographical Characteristics

Most of the area of Sri Lanna national park consists of a mountain chain, running north to south, with elevations varying from 400 to 1,718 m above sea level (Figure 3.2). The highest point is Doi Chom Hot peak at 1,718 m. The park is part of a great watershed area on the upper Ping River basin, which is one of the largest drainage basins of the Chao Phraya watershed. Hence, this park is the source of various tributaries of the Ping River and the Mae Ngat River. In 1973, there was a severe flood in Inthakhin and Chorlae subdistricts of Chiang Mai province. To provide the desired flood protection, the Mae Ngat Somboon Chol reservoir was constructed in 1997 on the Ping River. The reservoir is located in the mountains in the western part of Sri Lanna national park, and is approximately 20 km^2 in size. This reservoir has provided multiple benefits for the people, such as mitigation of severe floods, irrigation and distribution of water resources, hydroelectric power generation, fishing and outdoor recreation in Sri Lanna national park.

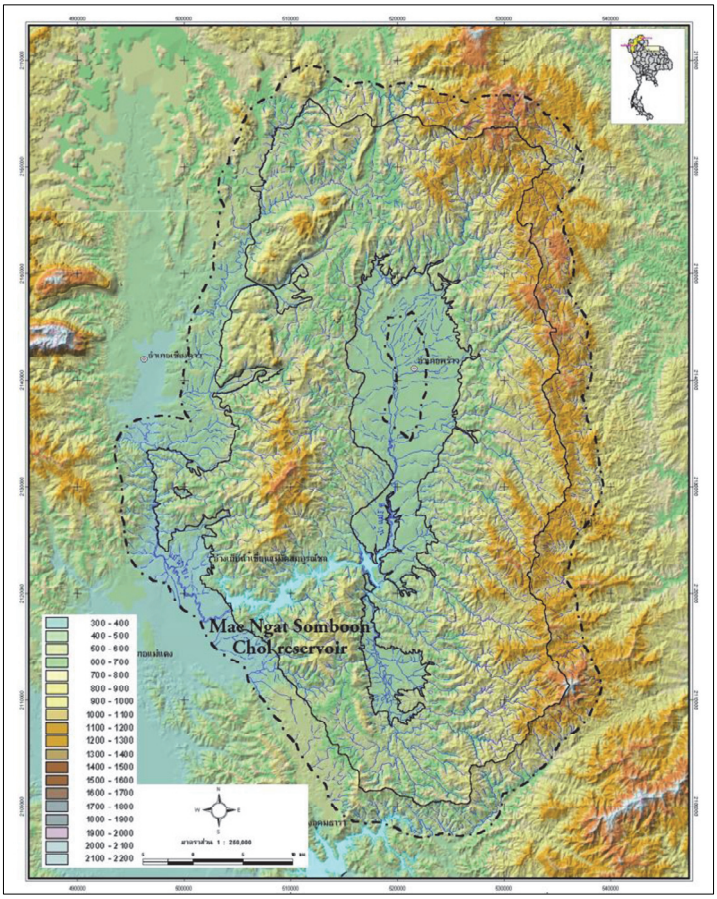

Figure 3.2 Topographical characteristic of Sri Lanna national park (DNP, 2003)

3.1.3 Geological and Soil Characteristics

The park generally features a rugged mountain range with steep slopes. The western area is covered by limestone mountains with a height of 300-400 m above sea level. The limestone formations have been covered by sandstone, limestone and shale. The geological characteristics consist mainly of sedimentary rock, igneous rock and alluvial and flood plain deposits (DNP, 2003). The strata were formed between the Ordovician period and the Quaternary period. Soil properties in the park are closely related to slope; 92.2% of the park area is classified as a soil slope complex series, which is found in areas with slopes that exceed 35%. Sandy and sandy loam soils are dominant. The soil surface in places covered with forest is still deep and fertile but the cleared areas are shallow as a result of soil erosion, with some gravels at the surface. Large and small gullies run mainly from east to west (DNP, 2003).

3.2 Meteorological Conditions

Sri Lanna national park is located in the tropical area where the climate is controlled by tropical monsoons. The climate can be described as a tropical monsoon climate with a rainy and a dry season, due to strong monsoon influences. The weather is generally hot and humid with high temperatures across most of the park throughout most of the year. The average humidity is 72%, with a maximum value of 89% from June to October and a minimum value of 49% in March. The seasons are generally divided into the rainy season (June to October), cool season (November to February), and hot or dry season (March to May). In reality, it is, however, relatively hot for most of the year, and between November and April the weather is mostly dry.

Temperature: the mean annual temperature in the area is 26.7°C, while the minimum and maximum temperatures of the coldest (January) and hottest (April) months are 11.0°C and 39.5°C, respectively. However, over 30 years, the minimum and maximum temperatures have been 3.7°C and 41.4°C respectively.

Precipitation: this area has mean annual precipitation of 1,156.26 mm, which is rather lower than other areas in the northern part of Thailand. The rainy season lasts from May to October and reaches its peak in August with a maximum precipitation of 256.76 mm. The lowest average precipitation of 4.10 mm occurs in February.

According to the facts, the dry season extends for five months, from November to April, when maximum temperatures usually reach 40°C. The total rainfall is very low

and represents just 6.8% of the total for the year (Figure 3.3). During the long dry period, rain is rare, leading to drought conditions. This is when wildfire typically occurs.

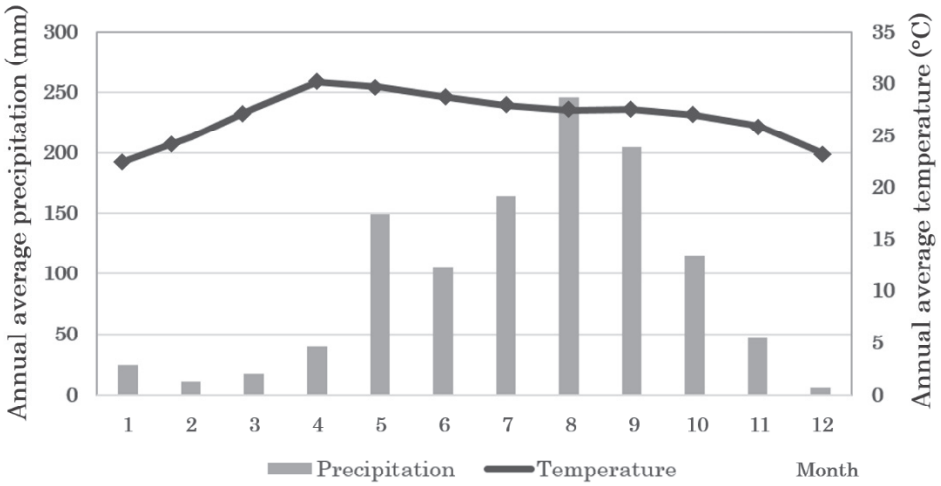

Figure 3.3 Average temperature and precipitation in the years 2010 to 2016

3.3 Resources Base in Sri Lanna National Park

3.3.1 Forest Resources

Sri Lanna national park is located in a hot, humid climatic zone and has valleys and mountain ranges with altitude differences that support a variety of tropical ecosystems and a diversity of plants and animals. The forest in Sri Lanna national park is composed of numerous forest types (Table 3.1). Dipterocarp and deciduous forests are the main types, covering over half of the park's area (63.39% of the total area). This research focused only on dipterocarp and deciduous forests because wildfire occurs mostly in these forest types.

Dipterocarp forest is distributed at an elevation of 200-1,200 m and 800-1,200 m above sea level. Trees in dipterocarp forest consist of more than 45 species with *Dipterocarpus obtusifolius Teijsm, Sharea obtuse, Dipterocarpus tuberculatus Roxb., Shorea siamensis and Gluta usitata (Wall.) Ding Hou* as the five most common species. The distribution of deciduous forest is found at an elevation of 50-800 m above sea level, with approximately 98 tree species. Common trees found in this type of forest are *Tectona grandis, Plerocarpus Indicus, Xylia xylocarpa, Lagerstroemia floribunda Jack and Terminalia alata Heyne ex Roth*. In addition, various bamboos, ferns and palms can be found in the low areas of the national park. However, because of human disturbances, logging concessions in the past and areas annually burned by forest fire,

almost all of the natural forests in dipterocarp and deciduous forests have been damaged and have become secondary forests. The forests re-emerged after the land was converted to farms and then abandoned, and much of the forest has recovered from fires. Therefore, trees in dipterocarp and deciduous forests are usually small trees. Dipterocarp and deciduous forests have semi-open canopies and tall and straight-stemmed trees. According to our field survey, these forests have a structure of up to four different layers: 1) a top layer of trees with heights of 12–15 m or more and stem diameters exceeding 30–35 cm, 2) a main layer of trees with heights of 5–12 m or more and stem diameters exceeding 10–20 cm, 3) a layer of weeds and saplings and 4) a ground layer of generally sparse grass cover. Layers 3 and 4 are generally clear and sparse because of annual burning by wildfires.

Table 3.1 Variety of forest types in Sri Lanna national park (DNP, 2003)

Forest types	Area (ha)	%
1. Dipterocarp forest	51,450.73	36.60
2. Deciduous forest	37,665.68	26.79
3. Hill evergreen forest	28,799.87	20.48
4. Pine forest	12,280.69	8.73
5. Dry evergreen forest	6,805.38	4.84
6. Other (Mixed forest plantation, water sources)	6,805.38	2.56
Total	140,600.00	100.00

3.3.2 Wildlife Resources

This park is a habitat for wildlife, especially mammals including tiger, barking deer, serow, black bear, wild boar, chiroptera, siamese hare and northern red muntjac, and also various species of birds such as ducks, coucals, bulbuls, egrets and barbets. Based on a survey report from DNP (2003) as shown in Table 3.2, a large number of bird species are found in this area, and Sri Lanna national park is therefore one of the best places for birdwatching. Bats are the most mammals and one of the protected wildlife is goral. Most reptiles are of the snake family, most amphibians are of the ranidae family, and most fish are of the cyprinidae family.

Table 3.2 Wildlife resources in Sri Lanna national park

Types	Order	Family	Species
1. Mammals	9	26	64
2. Birds	11	33	117
3. Reptiles	2	12	38
4. Amphibians	2	6	33
5. Fish	6	15	40
Total	30	92	292

3.4 Human Resources

There are 3,499 and 14,848 households inside and near Sri Lanna national park, respectively (DNP, 2003). Almost all community members are local people who have a similar education level within the compulsory education system (primary education). Of these, 70% work in farming and agricultural occupations and another 30% are employees and merchants. Agricultural land surrounding the park extends to around 42,500 ha. The main agricultural crop is rice, followed by longan, mango, soybean and tobacco. Almost all the people are Buddhist, and they therefore share similar lifestyles, beliefs and traditional culture. Some of the local people rely on the forest in Sri Lanna national park for their livelihood, especially for gathering forest non-timber products such as firewood and food. Furthermore, some of them benefit from the water source of Mae Ngat Somboon Chol reservoir for consumption and farming.

3.5 Tourism and Recreation in Sri Lanna National Park

Due to its geographical location and its variety of tropical ecosystems, Sri Lanna national park has several large forests and much interesting scenery, and is therefore attractive to tourists. These attractions have become well-known recreational and tourism locations. Moreover, many forms of recreation are available in this park, such as campsites, natural study trails, and a reservoir. The statistical evidence presented in Figure 3.4 shows that the number of tourists who visit and travel in Sri Lanna national park has been continuously increasing for several years, resulting in a high income from the tourism sector in the park. The growing tourism in Sri Lanna national park highlights the fact that Sri Lanna national park has a unique landscape and a high diversity of plants and wildlife, and is therefore able to support a high level of

tourism and many recreational activities. Therefore, the park has become a popular tourist destination.

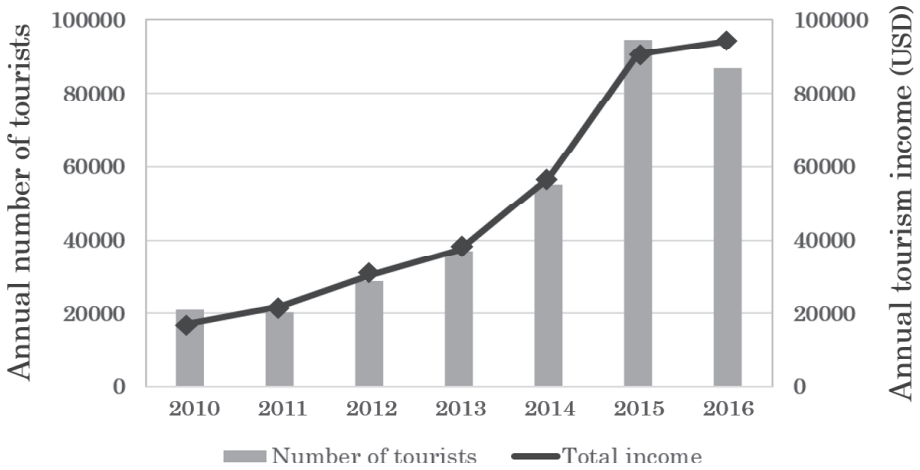

Figure 3.4 Number of tourists and total income from tourism in Sri Lanna national park in the years 2010 to 2016

There are many different kinds of tourist activities in this mountainous park including recreation, outdoor recreation, adventure tourism and nature-based tourism (Figure 3.5). Below are examples of various tourist attractions contributing to the recreational activities in the park.

Mon Hin Lai waterfall consists of nine levels of waterfall, and is full of water all year round, creating spectacular views, grandiose rivers and pristine streams.

Mae Ngat Somboon Chol reservoir is situated in a large area of forest and is therefore surrounded by beautiful natural scenery. There are many activities available on the reservoir such as boating, canoeing, fishing and staying in a floating house.

Pha Daeng cave is a large limestone cave with beautiful stalactites and stalagmites. The cave has a large room and an 800 m passage. Many bat species inhabit the cave.

Huay Kum nature trail is forest roadways providing an educational experience in a diverse forest containing both primary and native trees and flora.

(a) Attractive places of nature-based tourism

(b) Recreational activities

Figure 3.5 Attractive places for nature-based tourism and recreational activities in Sri Lanna national park

Table 3.3 gives a list of attractive places and recreational sites in Sri Lanna national park. There are several sites for each of many kinds of recreational activities such as cultivated and managed landscape for camping, mountains for hiking, climbing and biking, hot spring sources for relaxing and fertile forests for bird watching and wildlife viewing. Unfortunately, some of the recreation areas have been damaged by wildfires which occur annually during the dry season, peaking in February and March, and mainly occur in the dipterocarp and deciduous forests. Most wildfires in the park are classified as surface fires. Fires start during the dry season, when there is the greatest leaf accumulation on the ground surface from dipterocarp and deciduous trees, providing the largest proportion of fuel load. Thus, this study was limited to such areas of the national park with the highest potential for wildfires.

Table 3.3 List of attractive places and recreational sites in Sri Lanna national park

No.	Name of recreational site	Type of recreation
1	Wat Mae Pang	Temple site
2	Wat Tham Doi Kham	Temple site
3	Nam Ru Conservation Forest	Natural learning site
4	Wat Phra Chao Lan Thong	Temple site
5	Mae Wa Reservoir	Rest viewpoint
6	Ban Nong Krok Hot Spring	Hot spring
7	Wat Phrathat Doi Nang Lae	Temple site
8	Huai Pa Phlu Waterfall	Waterfall
9	Mae Kon Reservoir	Rest viewpoint
10	Wat Phrathat Jai Klang Muang	Temple site
11	Mae Pang Reservoir	Rest viewpoint
12	Huay Kum Nature Trail and Camping site	Nature trail and campsite
13	Pha Daeng Cave	Cave
14	Pla Prung Reservoir	Rest viewpoint
15	The Elephant Training Center, Chiang Dao	Elephant Training Center
16	The Elephant Training Center, Mae Ping	Elephant Training Center
17	Wat Phrathat Muang Noeng	Temple site
18	Nang Lae Waterfall	Waterfall
19	Mon Hin Lai Waterfall	Waterfall
20	Mon Hin Lai Viewpoint	Rest viewpoint
21	Sri Lanna office area, Mae Ngad Reservoir	Rest viewpoint and campsite
22	Doi Jom Hod	Rest viewpoint

CHAPTER 4

Mapping wildfire fuel load distribution using Landsat 8 Operational Land Imager (OLI) data in Sri Lanna National Park, northern Thailand

4.1 Introduction

Wildfires, which occur in many countries during the dry season, can be said to have both advantages and disadvantages. If managed properly, a wildfire could be advantageous as a vital component of the normal functioning of a forest ecosystem. Conversely, when uncontrolled, a wildfire represents a major threat because it could devastate huge areas of forest, degrade the environment, and diminish natural resources (Landsberg, 1997). Wildfires, especially in northern Thailand, have become an increasingly frequent and problematic phenomenon. Wildfires, especially in northern Thailand, have become an increasingly frequent and problematic phenomenon. For example, an area of 22,995 ha of forest that recently burned down accounted for 1.2% of the entire area of national protected forest (DNP, 2014; Forest Fire Control Division, 2015). This resulted in soil nutrient loss, disturbance of wildlife habitat, air pollution, and a decline in tourism. Wildfires in Thailand are mostly classified as surface fires in dipterocarp and deciduous forests, and they occur annually during the dry season, with peak activity in February and March. A surface fire occurs via ignition of the surface fuel layer, which consists of combustible materials lying on the ground, i.e., mainly fallen dead leaves, twigs, grasses, forbs, boles, stumps, shrubs, and short trees (Brown and Davis, 1973).

Fire behavior, defined as the manner in which fuel ignites, flame develops, and fire spreads, is affected by many factors, such as the fuel load and its characteristics, weather conditions, human activities, and land use changes. Among these, fuel is considered one of the most important factors leading to wildfire occurrence. The control of fuel (combustible material) levels can result in the avoidance of catastrophic wildfires (Wagle and Eakle, 1979). Thus, management of fuel on the forest floor is a feasible and effective approach for controlling and reducing the risk of wildfires (Rothermel, 1972). Fuel load refers to the weight of all fuels present per unit area, and it represents the proportion of the total biomass that could burn during a worst-case scenario (DeBano et al., 1998). Therefore, the biomass found within a particular area can be truly representative when estimating fuel load.

Remote sensing techniques are capable of quantitative estimation and monitoring of biomass (Tucker, 1979). A combination of two or more wavelength characteristics can be used to construct VIs, which have been shown correlated with vegetation biomass, such as the soil-adjusted vegetation index (SAVI) (Huete 1988, Richardson and Everitt 1992), two-band enhanced vegetation index (EVI2) (Pfeifer et al., 2012), and ratio vegetation index (RVI) (Anderson and Hanson 1992). In particular, the NDVI has been used widely as a predictor of ground vegetation biomass. Curran et al. (1992) applied Landsat TM data to a study of the linear relationship that exists between the NDVI and the leaf area index, demonstrating the potential use of Landsat TM data in studying seasonal dynamics of a forest canopy. In addition, many studies have applied the NDVI for wildfire and fuel assessments. For example, an investigation by Wagtendonk and Root (2003) showed that a temporal NDVI, derived from Landsat TM data, could be used for fuel classification. Similarly, Darmaran et al. (2001) presented an NDVI analysis of Landsat TM data to derive fuel types for mapping forest fire hazard in East Kalimantan, Indonesia. However, these studies focused on classification of fuel type, which is insufficient for understanding fire behavior and minimizing wildfire intensity and spread. The amount of fuel load should also be considered and addressed as one of the primary factors influencing fire behavior because fuel load can determine the hazard classification of wildfires.

The aim of the present study was to identify techniques for generating a predictive model of leaf fuel load using VIs derived from a Landsat 8 OLI, based on regression analysis and ground data, and to apply the model to map the spatial distribution of leaf fuel load. To achieve this goal, we investigated the relationships between the calculated standard leaf biomass in sample plots and each potential VI, i.e., NDVI, SAVI, EVI2, RVI, different vegetation index (DVI), NDWI, and chlorophyll vegetation index (CVI), to compare the strength of correlation of each index with the calculated standard leaf biomass, in order to establish a linear equation for leaf biomass estimation. Furthermore, we explored the seasonal difference of estimated leaf biomass to determine the leaf fuel load model. According to Shugart et al. (2006), fuel load is associated with changes in total biomass. Lastly, we hypothesized that the difference of estimated leaf biomass between normal and dry seasons (estimated by a seasonal VI) can express the quantity of the missing leaf biomass (i.e., the surface leaf fuel load), and that this can be used as a substitute for the actual leaf fuel load in the forest.

4.2 Materials and methods

4.2.1 Field data measurement

The sample plots with heterogeneous ecological conditions were selected from radiometrically and geometrically corrected Landsat 8 images and topographic maps (indicating different slopes, aspects, and forest types). The twenty-seven selected plots (14 plots of dipterocarp forest and 13 plots of deciduous forest) were surveyed in Sri Lanna national park during the dry season in March 2015 (Figure 4.1). Leaf biomass was measured from the 30 × 30 m^2 sample plots, corresponding to the spatial resolution of the Landsat 8 pixel size, for the linear regression analysis. Each sample plot was centered on the coordinates assigned to the center of the respective Landsat 8 pixel. The location of the center of the sample plot was determined and recorded using a handheld GPS (Oregon550TC, GARMIN, USA). Each plot was allocated a 1 × 1 m^2 subplot at the center of the 30 × 30 m^2 sample plot in order to collect leaf litter on the ground surface. Then, the leaf litter in the 30 × 30 m^2 sample plot was estimated based on the 1 × 1 m^2 subplot using the method of ratio and proportion.

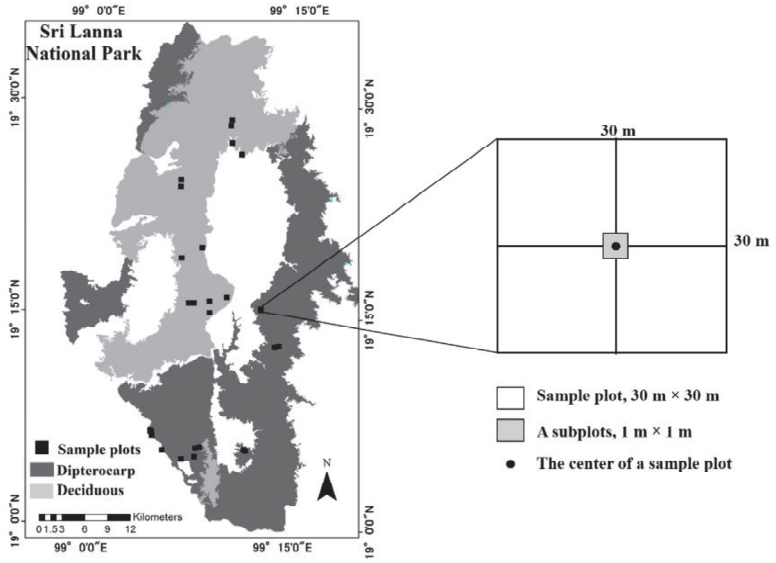

Figure 4.1 Sample plots in dipterocarp and deciduous forests

4.2.2 Standard leaf biomass calculation

A survey was performed in each of the 30 × 30 m^2 sampling areas. All live trees with a diameter of 4.5 cm or more (or a girth of 15 cm or more) and a height of more than 1.5 m were identified for each of the tree species. The identified trees were also measured for stem circumference at breast height (girth at breast height) (GBH) or 1.3 m height

from the ground surface using a tape, and the tree height was estimated using a clinometer. The values of GBH were then converted to diameter at breast height (DBH) in an Excel spreadsheet. Allometric equations based on the relationship between DBH and height were used to calculate the standard leaf biomass produced by the trees, which can be seen as green canopies. The leaf biomass of the dipterocarp forest was calculated using Equation 4.1, developed by Ogino et al. (1967). Equation 4.2, modified from Ogawa et al. (1965), was used for the calculation of the leaf biomass of the deciduous forest:

$$\frac{1}{W_{L-dip}} = \frac{11.4}{W_{S-dip}^{0.9}} + 0.172 \quad (4.1)$$

$$\frac{1}{W_{L-dec}} = \frac{22.5}{W_{S-dec}} + 0.025 \quad (4.2)$$

where $W_{L\text{-}dip}$ and $W_{L\text{-}dec}$ are the leaf biomass (kg) of the dipterocarp and deciduous samples, respectively, generally expressed in dry weight, which is proportional to fresh weight. The parameters $W_{S\text{-}dip}$ and $W_{S\text{-}dec}$ represent the stem biomass (kg) of the dipterocarp and deciduous samples, respectively, calculated from D (DBH in m) and H (height in m) using the following equations:

$$\log W_{S\text{-}dip} = 0.902\log(D^2H) + 2.2764 \quad (4.3)$$

$$\log W_{S\text{-}dec} = 0.9326\log((D(100))^2H) - 1.402 \quad (4.4)$$

4.2.3 Leaf fuel load calculation

During the sampling process, leaf litter mass was collected for leaf fuel load calculation, later used for model validation. Leaf fuel load was measured in a representative 1 × 1 m^2 subplot of the 30 × 30 m^2 sampling area. All leaf litter on the ground surface within each subplot was collected and weighed (kg) using a field scale. A small sample of the leaf litter from each subplot was selected at random and placed in a sealed envelope for later laboratory analysis to determine the fuel moisture content (FMC) for the leaf fuel load calculation.

Leaf fuel load is defined as the weight of the leaf fuel per unit area, often expressed in kg ha^{-1}, as described in Equation 4.5.

$$\text{Leaf fuel load} = \frac{W_{CL} \times 100 \times 10000}{(100 + \text{FMC}) \times \text{Plot size}} \quad (4.5)$$

where W_{CL} is the weight of all the leaf litter collected from the 1 × 1 m^2 subplot (kg) and FMC is the fuel moisture content (%).

The FMC was calculated following procedures described by Desbois et al. (1997). Leaf litter samples were weighed on the scale before drying in an oven (wet weight in g) at 80°C for 48 h. After drying, the samples were weighed again (dry weight in g) to calculate FMC, as follows:

$$\text{FMC} = \frac{\text{Wet weight} - \text{Dry weight}}{\text{Dry weight}} \times 100\% \quad (4.6)$$

4.2.4 Landsat 8 OLI data and preprocessing

Establishment of leaf fuel load model required two Landsat 8 images from different seasons; here, we used images acquired on October 14, 2014 (normal season) and February 19, 2015 (dry season). The Landsat 8 data sets used were the L1G-level products, which were geographically corrected and projected onto the UTM Zone 47N with a WGS84 datum, and clipped based on the study area. The Landsat 8 data were available in the form of digital numbers (DNs). We then followed the steps to transform these DNs using the reflectance values provided by the USGS (2013) for calculating the VIs. Finally, image preprocessing was performed, which included masking of clouds and cloud shadows.

4.2.5 Calculation of VIs

VIs are generally defined based on the calculation of surface reflectance from sensors mainly using visible (red) and NIR spectral bands. The seven VIs considered in this study have been commonly used for the detection and quantitative assessment of biomass. The NDVI represents the normalized reflectance difference between the red and NIR bands, as introduced by Rouse et al. (1973), which is used to evaluate the density of vegetation. The NDWI is calculated from NIR and shortwave infrared (SWIR) reflectance (Gao, 1996) and it is normally used for estimating the leaf water content at the canopy level. The CVI is proposed to estimate leaf chlorophyll concentration at the canopy scale (Vincini et al., 2007). This index is obtained from the NIR/green reflectance ratio by introducing the red/green ratio to minimize the sensitivity to differences within

the canopy. The DVI, suggested by Richardson and Wiegand (1977), is the simplest VI that reflects the amount of vegetation. The EVI2 is also calculated from the red and NIR reflectance to obtain the sensitivity of high canopies. This index can effectively reduce the noise caused by soil or the atmosphere (Jiang et al., 2008). Jordan (1969) developed the RVI for capturing, in the simplest form, the contrast in the NIR and red values of areas of healthy green vegetation. Finally, the SAVI was proposed by Huete (1988). This index is suitable for minimizing the effects of the soil background on the vegetation signal by incorporating a constant soil adjustment factor L into the denominator of the NDVI equation. Factor L varies with the reflectance characteristics of the soil (e.g., color and brightness). All the above VIs are calculated as per the following equations:

$$\mathrm{NDVI} = \frac{\mathrm{NIR} - \mathrm{RED}}{\mathrm{NIR} + \mathrm{RED}} \tag{4.7}$$

$$\mathrm{NDWI} = \frac{\mathrm{NIR} - \mathrm{SWIR}}{\mathrm{NIR} + \mathrm{SWIR}} \tag{4.8}$$

$$\mathrm{CVI} = \frac{\mathrm{NIR} \times \mathrm{RED}}{\mathrm{GREEN} \times \mathrm{GREEN}} \tag{4.9}$$

$$\mathrm{DVI} = \mathrm{NIR} - \mathrm{RED} \tag{4.10}$$

$$\mathrm{EVI2} = 2.5 \times \frac{\mathrm{NIR} - \mathrm{RED}}{\mathrm{NIR} + 2.4(\mathrm{RED}) + 1} \tag{4.11}$$

$$\mathrm{RVI} = \frac{\mathrm{NIR}}{\mathrm{RED}} \tag{4.12}$$

$$\mathrm{SAVI} = 1 + \mathrm{L}\frac{\mathrm{NIR} - \mathrm{RED}}{\mathrm{NIR} + \mathrm{RED} + \mathrm{L}} \tag{4.13}$$

where NIR, RED, and GREEN are the reflectances of the NIR, red, and green bands, respectively, and L is a constant soil adjustment factor (L = 0.5).

According to the outlined functions of these VIs, they are reasonable for the estimation of vegetation status and as surrogates of the amount of vegetation and green biomass. Therefore, these VIs were extracted from the Landsat 8 image of the normal season, because trees during the normal season are fully leaved and thus, more representative of the standard leaf biomass. The extraction of the VIs in the normal season were later analyzed in relation to the calculated standard leaf biomass in the sample plots to establish the leaf biomass estimation equation.

4.2.6 Leaf biomass estimation equation based on VI

In this study, biomass was defined as leaf biomass because leaves represent a core component of the surface fuel. Regression analysis, which is the most commonly used approach in estimations of aboveground biomass (Steininger, 2000; Zheng et al., 2004), was used to establish a linear equation for leaf biomass estimation. The equation was based on the relationship between the VIs and the calculated standard leaf biomass in the plots (Note: the VIs were extracted at the same locations as the calculated standard leaf biomass in the plots). Then, the equation with the highest R-squared (R^2) value and lowest root mean square error (RMSE) was selected as the leaf biomass estimation equation, which was used to estimate the leaf biomass in the normal and dry seasons. The estimated leaf biomass equation was expressed by the following linear equation:

$$LB = a + b(VI) \quad (4.14)$$

where LB is the estimated leaf biomass of the entire tree (kg ha^{-1}), which was generated separately for the dipterocarp and deciduous forests based on allometric equations, VI is the VI most highly correlated with the calculated standard leaf biomass extracted during the normal season, and a and b are the intercept and slope of the regression coefficient, respectively.

The equation of leaf biomass estimation was tested with assumptions to confirm it was the best-fitting equation for estimating leaf biomass. We used the following key assumptions in the statistical tests. (i) Linearity was checked using the F-test for testing both the overall significance of the equations and the linear relationship between both variables (the calculated standard leaf biomass as the dependent variable and VI as the independent variable). (ii) Normality was checked with a histogram and a fitted normal curve or a normal probability plot (P-P plot) to verify the normality of the distributed variables. (iii) Homoscedasticity (constant variance) was checked using a scatter plot of the residual and the Breusch-Pagan test to confirm that the errors of the leaf biomass estimation were the same across all values of the independent variable.

4.2.7 Leaf fuel load prediction model

An estimate of the leaf biomass could be achieved using VI as a predictor; therefore, the quantity of green leaf biomass in different seasons (normal and dry seasons) could be estimated using the seasonal variation of the VI values, and this could contribute to

the assessment of leaf fuel load. Thus, the seasonal variation of the VI values between normal and dry seasons was applied to estimate the different quantities of leaf biomass in both seasons based on the leaf biomass estimation equation (Equation 4.14). Subsequently, the difference between the leaf biomass values was calculated to determine the missing leaf biomass that was considered equivalent to the surface leaf fuel load during the dry season. The missing leaf biomass was considered to comprise the fallen leaves on the ground surface, which constituted dead leaves or the so-called "surface fuel." The leaf fuel load prediction model can therefore be defined as:

$$\text{Leaf fuel load} = LB_N - LB_D \tag{4.15}$$

where leaf fuel load is the missing leaf biomass (kg ha^{-1}), while LB_N and LB_D represent the estimated leaf biomass (Equation 4.14) extracted from a VI during the normal and dry seasons, respectively.

The predictive model was validated by ground and remote sensing data. We used the calculated leaf fuel load in the plots to evaluate the accuracy of the model by statistical inference: (i) Pearson's correlation coefficient, (ii) R^2, (iii) RMSE, (iv) the precision of the model, and (v) the paired t-test (p-value = 0.05). The paired t-test was used for testing the null hypothesis that there is no significant difference between the means in respect of the calculated and predicted leaf fuel loads. The precision (%) of the model was calculated as follows:

$$\text{Precision} = \left[1 - \sqrt{\frac{\sum[(Yi - Y'i)/Y'i]^2}{N}}\right] \times 100\% \tag{4.16}$$

where Y_i is the calculated leaf fuel load of the field samples, Y'_i is the predicted leaf fuel load using the developed regression model, and N is the sample size.

Finally, the validated model was applied to the seasonal Landsat 8 images acquired on October 14, 2014 (normal season) and February 19, 2015 (dry season), in relation to the dipterocarp and deciduous forests within the study area, to predict and map the leaf fuel load distribution

4.3 Results and Discussion

4.3.1 Relationship between calculated standard leaf biomass and VIs

This study focused on leaf biomass because dead leafage forms the largest component of fuel on the ground surface. Field data collection revealed that surface fuel consisted of dead leaves (83.34%), dead or downed branches (9.16%), and weeds (7.50%). The capabilities of seven VIs (NDVI, NDWI, CVI, DVI, EVI2, RVI, and SAVI) extracted from Landsat 8 OLI data were compared for estimating leaf biomass. The VI with the strongest correlation with leaf biomass was then used to establish a leaf fuel load model. Table 4.1 shows that the leaf biomass estimation equations generated from the NDVI, for both dipterocarp and deciduous forests, had a stronger relationship with the calculated standard leaf biomass (R^2 = 0.87 and 0.78, respectively; p-value <0.01) than with the other VIs. Using the NDVI as a predictor for estimating leaf biomass also resulted in a lower RMSE (dipterocarp: 211.41 kg ha^{-1} and deciduous: 315.54 kg ha^{-1}). The sequence of relationships between the VIs and leaf biomass for dipterocarp forest (ranked from high to low based on R^2) was as follows: NDVI, SAVI, EVI2, RVI, DVI, and NDWI. The CVI was weakly related to leaf biomass. Similar results were evident for deciduous forest, where the NDVI had the strongest correlation with leaf biomass (highest R^2). Although the RVI was also strongly correlated with leaf biomass, the RMSE indicated that the error of leaf biomass estimation was higher than with the NDVI, whereas, SAVI, EVI2, DVI, NDWI, and CVI performed with lower values of R^2. Notably, the relationships of NDWI and CVI with leaf biomass had the lowest significance.

The established statistical equations for leaf biomass estimation (Table 4.1) revealed the relationship between the VIs and the calculated standard leaf biomass. The sequence of their relationship in dipterocarp forest (ranked from high to low) was as follows: NDVI, SAVI, EVI2, RVI, DVI, NDWI, and CVI. Meanwhile, the sequence of their relationship in deciduous forest (ranked from high to low) was as follows: NDVI, RVI, SAVI, EVI2, RVI, DVI, NDWI, and CVI. The equations relating the NDVI to the calculated standard leaf biomass showed the best performance for both dipterocarp and deciduous forests, with the highest R^2 values and lowest RMSEs. This is because the principle of the NDVI formula, which is defined as the ratio of the differences of the NIR and red bands, normalized by the sum of those bands, can determine and quantify the density of biomass. Radiation in the visible red light part of the spectrum is strongly

Table 4.1 Summary of leaf biomass equations for dipterocarp and deciduous forests

Forest type	Variable	Linear leaf biomass equation (kg ha^{-1})	Statistical significance		
			R^2	RMSE	F value
Dipterocarp	NDVI	13,231.58(NDVI) – 6,093.07	0.87*	211.41	82.26*
	NDWI	9,270.37(NDWI) – 709.02	0.57	389.90	15.71
	CVI	61,405.06(CVI) + 1,282.17	0.04	580.11	0.52
	DVI	18,066.85(DVI) – 1,786.52	0.79*	270.84	45.43*
	EVI2	12,064.45(EVI2) – 2,416.56	0.84*	240.41	60.89*
	RVI	739.94(RVI) – 1,299.84	0.82*	250.07	55.37*
	SAVI	13,727.03(SAVI) – 3,137.06	0.85*	231.70	66.47*
Deciduous	NDVI	16,943.39(NDVI) – 8,350.30	0.78*	315.54	38.93*
	NDWI	5,496.61(NDWI) + 621.38	0.12	629.22	1.56
	CVI	85,954.07(CVI) + 1,039.88	0.11	635.00	1.33
	DVI	16,380.13(DVI) – 1,099.38	0.56	445.02	14.10
	EVI2	11,615.77(EVI2) – 1,957.75	0.62	415.26	17.83
	RVI	988.38(RVI) – 2,064.29	0.73*	352.49	29.01*
	SAVI	13,281.48(SAVI) – 2,677.71	0.63	407.85	18.89

[a] * is significant at the 0.01 level

absorbed (or poorly reflected) by the chlorophyll in green plants, while radiation in the NIR part of the spectrum is strongly reflected by the mesophyll cells of leaves. Therefore, the NDVI can serve for detecting green stands or biomass.

The results also showed that all VIs were correlated more strongly with leaf biomass in dipterocarp forest than in deciduous forest. A possible reason for this is the difference in leaf structure of trees between the two forest types. Typically, the leaf size of the dipterocarp species is large and ovular (5–7-cm wide and 10–16-cm long), whereas the leaves of deciduous species are typically smaller and rounder (3–6-cm wide and 4–8-cm long). Therefore, the leaves of dipterocarp trees tend to have greater area. This means the VI values based on dipterocarp species can be improved by leveraging information of reflectance; thus, showing better correlation with leaf biomass than for deciduous species.

The SAVI is calculated using a soil adjustment factor (L), which means it also is highly correlated with leaf biomass, although it is only appropriate for use with dipterocarp species. Possible reasons for this are related to the structural differences of the leaves of trees between the two forest types and the use of a constant value of the L factor (i.e., 0.5), which is appropriate for dipterocarp forest but might not be appropriate for deciduous forest. Similarly, the EVI2 was also better correlated with

the leaf biomass of dipterocarp forest than deciduous forest because of soil interference, which is dependent on vegetation coverage. The RVI had significant correlation with leaf biomass for both forest types because its mathematical formula is applied from the contrast in the NIR and red values. However, the RVI shows only a ratio calculation, which has low dynamic range; therefore, it is not as precise as the NDVI indicating the different proportions of vegetation or leaf biomass. The DVI is also the simplest VI, such that the dense canopy cover of the study area limited its potential for providing accurate information on leaf biomass. The NDWI and the CVI had the lowest correlations with leaf biomass in both forest types. As the NDWI varies according to the relative water content of leaves (Gao, 1996), the index is suited to indicate healthy leaves, although it is poorly correlated to quantities of vegetation biomass. The CVI results in this study presented the least significant correlation with leaf biomass. This is because the efficiency of the CVI depends on the type of vegetation. The CVI index can be used well as a leaf chlorophyll estimator for planophile/herbaceous crops such as wheat, corn, and soybean (Vincini et al. 2008), i.e., green structural crops (leaf, sheath, and stem are normally green), which can be considered for pigment content estimation by the CVI. However, this index was weakly correlated with the leaf biomass of trees in the forests in this study.

A comparison of the capabilities and limitations of each VI revealed that the relationships between the VIs and leaf biomass varied because of the different characteristics and structures of the forest types, e.g., canopy structure, leaf area index, and crown cover. Consequently, this reduced the reliability of the relationship between those VIs and leaf biomass in both forest types. The NDVI demonstrated a stable and reliable correlation with leaf biomass in both forest types. Therefore, the NDVI was selected as a predictor to estimate leaf biomass because it was strongly correlated with leaf biomass for both forest types (highest R^2) and it demonstrated greater ability in estimating leaf biomass (lowest RMSE values).

4.3.2 Leaf biomass estimation equation based on VI

We then tested the assumptions of linear regression to verify that the selected equation was appropriate for leaf biomass estimation. The results of the F-test showed there was linear correlation between the calculated standard leaf biomass and the NDVI (p-value <0.01; Table 4.1).

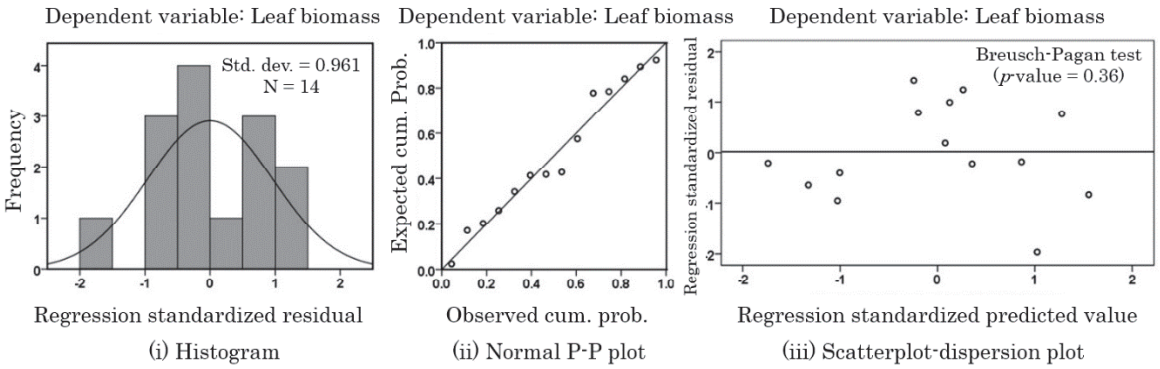

(a) Dipterocarp

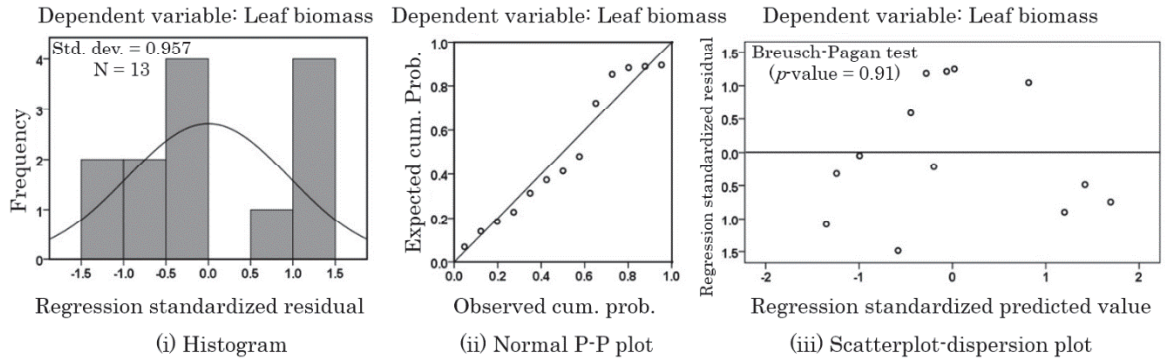

(b) Deciduous

Figure 4.2 Test results for assumptions of regression leaf biomass equations: (i) the histograms, (ii) probability plots, and (iii) scatter plots-dispersion plots: (a) dipterocarp and (b) deciduous forests

With regard to normality, a normal distribution was found, as shown in Figure 4.2a(i) and 4.2b(i), where the histograms are symmetric and bell-shaped within 0.96 (dipterocarp) and 0.96 (deciduous) of the standard deviations (SDs). The P-P plots also show normal distributions, because the points on both plots have a nearly linear pattern (Figure 4.2a(ii) and 4.2b(ii)). Finally, homoscedasticity was satisfied because the errors in the relationship between the calculated standard leaf biomass and the NDVI were constant, as shown by spread of the residuals without a pattern in Figure 4.2a(iii) and 4.2b(iii). In addition, the results of the Breusch-Pagan test were not significant at a p-value >0.05, which indicated that the errors of the leaf biomass estimation from the values of the NDVI were the same.

Based on the results of these tests, the equations were found reliable and accurate following statistical tests with three key assumptions of linear regression (i.e., linearity, normality, and homoscedasticity). The results of reliability from the statistical tests

demonstrated that the equations using the NDVI as a predictor were was satisfactory and reliable for the estimation of leaf biomass. The verified equations were later used to estimate the quantity of seasonal leaf biomass, using a seasonal NDVI, during the normal and dry seasons.

4.3.3 Leaf fuel load prediction model

The verified equations were applied to estimate leaf biomass in normal (LB_N) and dry (LB_D) seasons (Table 4.2), as predicted by a seasonal NDVI (normal and dry seasons). The quantities of LB_N and LB_D in both forest types were distinctly different; some plots had no leaf biomass in the dry season because the trees had shed all their leaves. The values of LB_N and LB_D were subtracted following the leaf fuel load prediction model to determine the missing leaf biomass, which became the predicted leaf fuel load on the ground surface. In dipterocarp forest, the average predicted leaf fuel load and the calculated leaf fuel load in the field showed a slight difference (1,966.94 and 2,118.06 kg ha^{-1}) with SDs of 517.75 and 635.27 kg ha^{-1}, respectively. In the deciduous forest, the average predicted and calculated leaf fuel loads were closer at 1,637.67 and 1,771.22 kg ha^{-1} with SDs of 534.34 and 509.16 kg ha^{-1}, respectively.

A seasonal NDVI can result in different estimations of leaf biomass. This is because during the normal season with full-cover green canopies, the NDVI mainly reflects healthy green canopies, which results in a high value of leaf biomass estimation. Conversely, during the dry season with canopy leaf-out, the NDVI mainly reflects other objects unrelated to greenness (e.g., stems, branches, soil, and fallen leaves on the ground surface). Consequently, these objects show low values of the NDVI that could be considered to represent unhealthy green canopies showing a decrease in estimated leaf biomass. Therefore, the estimated leaf biomass based on the seasonal variation of the NDVI values showed different quantities (as shown in Table 4.2). In some instances, some trees had shed all their leaves (i.e., there was no canopy cover) and thus, the NDVI value was very low. Consequently, the leaf biomass estimated by our model became negative and therefore, negative values of estimated leaf biomass were substituted by 0.00 (kg), expressing no leaf biomass, as shown in Table 4.2.

Table 4.2 Estimated leaf fuel biomass in normal and dry seasons, and a comparison between the missing leaf biomass or predicted leaf fuel loads and the calculated leaf fuel loads in the field

Dipterocarp (kg ha^{-1})					Deciduous (kg ha^{-1})				
Plot no.	LB_N*	LB_D**	Predicted leaf fuel load or missing leaf biomass	Calculated leaf fuel load in the field	Plot no.	LB_N*	LB_D**	Predicted leaf fuel load or missing leaf biomass	Calculated leaf fuel load in the field
1	1,869.03	377.84	1,491.19	1,449.80	1	2,157.68	1,032.21	1,125.47	1,288.36
2	1,446.94	0.00***	1,446.94	1,250.93	2	3,392.54	1,759.62	1,632.92	1,481.99
3	3,036.30	954.05	2,082.25	1,773.64	3	2,521.99	720.74	1,801.25	2,324.49
4	1,863.91	0.00***	1,863.91	1,820.96	4	2,348.97	1,426.04	922.93	1,194.51
5	2,311.39	0.00***	2,311.39	2,589.47	5	1,685.21	0.00***	1,685.21	1,606.42
6	2,651.96	197.06	2,454.90	2,827.87	6	2,389.38	0.00***	2,389.38	2,528.81
7	1,682.07	0.00***	1,682.07	2,250.20	7	2,241.85	227.67	2,014.18	1,992.28
8	2,602.11	819.66	1,782.45	2,514.15	8	2,472.76	709.79	1,762.97	1,507.27
9	3,179.39	0.00***	3,179.39	3,408.52	9	3,569.25	3,056.33	512.92	985.50
10	3,343.91	1,925.05	1,418.86	1,187.23	10	1,894.27	0.00***	1,894.27	1,773.75
11	2,940.96	1,438.99	1,501.97	1,671.71	11	3,023.80	864.53	2,159.27	2,407.94
12	2,496.42	903.92	1,592.50	2,087.33	12	1,751.32	0.00***	1,751.32	2,163.32
13	2,331.16	123.03	2,208.13	2,547.74					
14	2,521.22	0.00***	2,521.22	2,273.23					
Mean	2,448.34	481.40	1,966.94	2,118.06	Mean	2,454.09	816.41	1,637.67	1,771.22
SD	574.94	628.06	517.75	635.27	SD	603.05	922.48	534.34	509.16

[a] * is the estimated leaf biomass in normal season, [b] ** is the estimated leaf biomass in dry season

[c] *** shows no leaf biomass on trees, meaning all leaves were shed

The estimated leaf biomass between the normal and dry seasons for the dipterocarp and deciduous forests was clearly different. Leaf biomass was higher in the normal season than in the dry season, because trees in both types of forest shed their leaves cyclically in order to survive the changing weather conditions. Trees shed their leaves at the beginning of the dry season, resulting in a leaf biomass reduction. Consequently, the shed or fallen leaves become the primary fuel, which acts as an ignition source and cause of fire intensity. The estimated leaf biomass of the normal and dry seasons was subtracted to assess the quantity of missing leaf biomass in the dry season (Table 4.2), which reflects the leaf fuel load on the ground surface. Therefore, a seasonal NDVI between the normal and dry seasons can be applied to estimate the different quantities of leaf biomass, which establishes the missing leaf biomass that represents the quantity

of dead leaves on the ground surface. In other words, the fuel load, derived from changes in leaf biomass, can be estimated based on difference of a seasonal NDVI.

The calculated leaf fuel loads in the sample plots were essential to verify the findings, as well as to confirm whether the predicted leaf fuel loads of both forest types differed from the calculated leaf fuel loads. Based on the results from Table 7, the predicted leaf fuel load generated by the models and the calculated leaf fuel load in the field were then used to validate the model accuracy based on statistical metrics, as shown in Table 4.3. The models showed a strong relationship between the predicted and calculated leaf fuel loads. The values of the Pearson's correlation coefficient for both models were >0.80 and the models had RMSE values of dipterocarp and deciduous forests at 355.43 and 261.56 kg ha^{-1}, respectively. The paired t-test results for both models indicated there were no significant differences between the means of the predicted and calculated leaf fuel loads (p-value >0.05). This supports our hypothesis that the predicted leaf fuel load generated from models can be used as a substitute for the leaf fuel load in forest areas. Moreover, the model precisions based on statistical inference, which were evaluated from field and estimated data, achieved at 80.43% (dipterocarp) and 71.36%, (deciduous), respectively.

Table 4.3 Statistical validations of leaf fuel load prediction models for dipterocarp and deciduous forests

Forest type	Leaf fuel load prediction models (kg ha^{-1})	N	Pearson's correlation coefficient	R^2	RMSE	Paired t-test sig.	Precision (%)
Dipterocarp	$[13{,}231.58(NDVI_N) - 6{,}093.07] - [13{,}231.58(NDVI_D) - 6{,}093.07]$	14	0.85*	0.73*	355.43	0.11	80.43
Deciduous	$[16{,}943.39(NDVI_N) - 8{,}350.30] - [16{,}943.39(NDVI_D) - 8{,}350.30]$	12	0.88*	0.77*	261.56	0.10	71.36

[a] * is significant at the 0.01 level

Figure 4.3 shows the spatial distributions in the study area of the predicted leaf fuel load derived from the models. The predicted leaf fuel loads in the dry season of both forest types showed close values. The estimated leaf fuel load ranged from 17.48–4,474.39 kg ha^{-1} with a mean value of 2,228.46 kg ha^{-1} in the dipterocarp forest, and from 20.75–5,262.74 kg ha^{-1} with a mean value of 2,631.43 kg ha^{-1} in the deciduous forest.

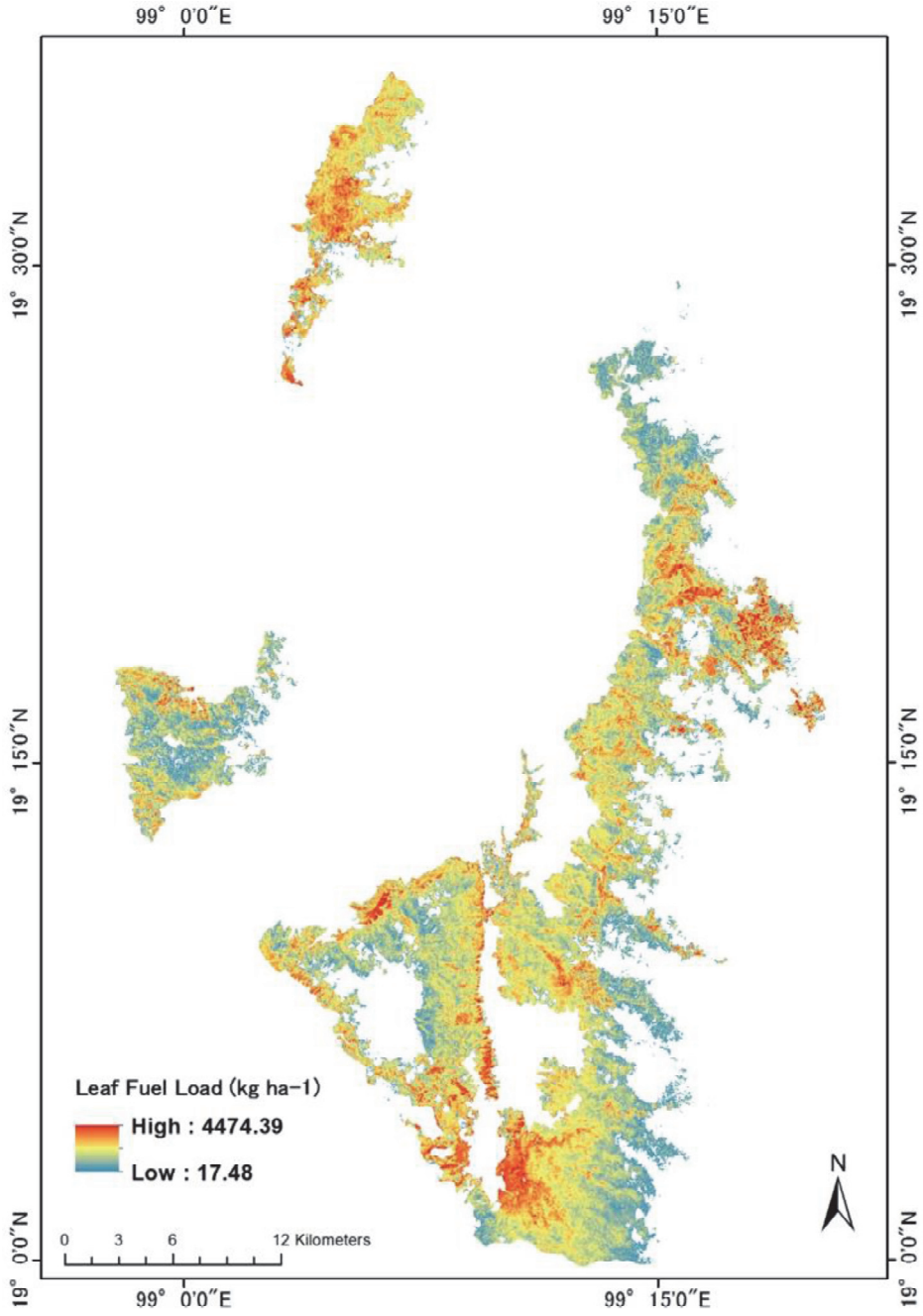

(a) Dipterocarp

Figure 4.3 Distribution of leaf fuel loads from statistical models of (a) dipterocarp and (b) deciduous forests in Sri Lanna National Park during the dry season

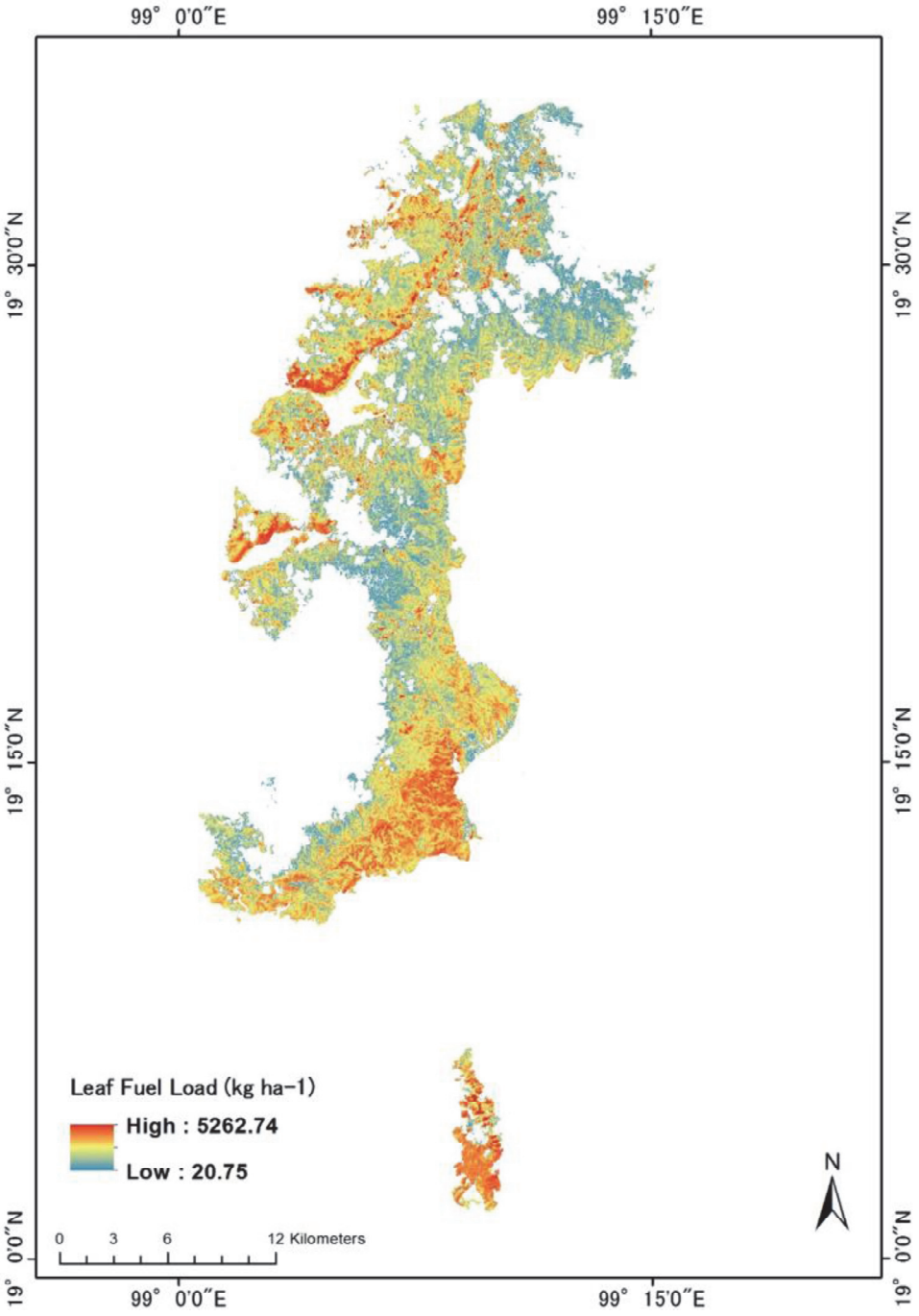

(b) Deciduous

Figure 4.3 Continued

Mapping the distribution of leaf fuel load generated from the models showed the average predicted leaf fuel loads were similar to those reported by Akaakara et al. (2004), who studied fuel characteristics of dry dipterocarp forest at Huai Kha Khaeng Wildlife Sanctuary in Thailand. Their results showed that the highest average loading of leaf fuel was 2,688.82 kg ha^{-1} in February, which is a value close to our average predicted leaf fuel load (2,228.46 kg ha^{-1}). Mapping fuel load distribution is a short-term estimation in the dry season, which can be used to investigate areas prone to wildfires. Areas with heavy fuel load are at higher risk of wildfire occurrence, which leads to negative fire behavior. Moreover, such distribution maps can be useful to fire managers as a guideline for reducing overloaded fuel by creating fuel breaks to reduce fire spread and intensity, as well as to local governments attempting to mitigate fire risk and making decisions on wildfire management. However, the application of predictive models derived from remotely sensed data for leaf fuel load estimation should be considered on optimally selected dates in both seasons.

4.4 Conclusions

In this study, we combined field data with remotely sensed Landsat 8 OLI data to generate models of leaf fuel load prediction for two forest types (dipterocarp and deciduous), based on VI and using regression analysis, and we mapped the spatial distribution of leaf fuel load. The capabilities of seven potential VIs were explored in terms of the relationship with the standard leaf biomass calculated in the field. The NDVI had the strongest correlation (R^2 of 0.87 and 0.78 for dipterocarp forest and deciduous forest, respectively; p-value < 0.01), and it was selected to estimate the seasonal leaf biomass to establish a fuel load prediction model. Using the NDVI as a predictor provided a statistically reliable linear equation for leaf biomass estimation. Our study advanced the work of previous studies that have estimated leaf biomass based on the NDVI. We exploited this strong relationship between leaf biomass and the NDVI further to determine the seasonal changes in leaf biomass, as measured by a seasonal NDVI (normal and dry seasons), for the purpose of establishing a fuel load prediction model. A seasonal NDVI can deliver different estimations of leaf biomass values in different seasons, which allows the missing leaf biomass or leaf fuel load on the ground surface to be assessed. The model validation supported the hypothesis and revealed that the leaf fuel load predicted by the remotely sensed model can be used as a substitute for the field-derived leaf fuel load (paired t-test results; p-value > 0.05). In

addition, the model precisions based on statistical inference, which were based on the measured field data and data predicted by the model, were greater than 80% and 71% for dipterocarp and deciduous forests, respectively. Therefore, it is because fuel load is associated with changes in total biomass, a seasonal NDVI can estimate the change in seasonal leaf biomass between the normal and dry seasons, contributing to the determination of the leaf fuel load on the ground surface. Mapping of leaf fuel load distribution can be used as complementary data when updating decisions on fire pre-suppression and suppression activities, as well as creating a guide for fuel load reduction.

CHAPTER 5

Mapping Soil Moisture as an Indicator of Wildfire Risk Using Landsat 8 Images in Sri Lanna National Park, Northern Thailand

5.1 Introduction

Severely dry climate plays an important role in the occurrence of wildfires. In Thailand, wildfires are particularly prevalent during the dry season and are especially damaging because of forest loss and degradation. During the dry season, the number of wildfires in Thai conserved forest areas were 4207, 4982, and 6685 in 2014, 2015, and 2016, respectively (Forest Fire Control Division, 2016). These numbers indicate that the number of wildfires appears to be increasing because Thailand has been experiencing longer dry seasons and under dry conditions, wildfires can ignite easily, as fuel sources are readily available. Fuel availability, which drives wildfire occurrences and directly affects wildfire behavior, depends on fuel characteristics, which are fuel load (influencing fire intensity) and fuel moisture content (influencing both fire ignition and spread). It appears that recurring dry seasons foster fuel availability and reduce fuel moisture content, resulting in potentially more damaging high-intensity fires, which may spread rapidly during extremely dry conditions.

Soil moisture, defined as the volumetric water content of soil (Eller and Denoth, 1996), is an important indicator of dry conditions and is linked to wildfire occurrence. The reduction of water in soil increases dry conditions (Kozlowski and Pallardy, 2002; Chmura et al., 2011), resulting in more intense and longer burning fires. Previous studies pointed out that soil moisture affects wildfire occurrence. For example, Krueger et al. (2015) showed that large growing-season wildfires occurred exclusively under conditions of low soil moisture. Yebra et al. (2013) suggested that improving wildfire assessments involves using soil moisture as a representative for fuel moisture, which is a key factor for ignition and spread of wildfires. Therefore, surface measurements of soil moisture may provide opportunities for improving estimates of fuel moisture (Qi, et al., 2012), because both are physically linked through soil-plant interactions (Hillel, 1998).

Remote sensing techniques have been extensively used for the analysis of soil moisture, and have provided alternative tools for obtaining rapid estimates of soil moisture on large spatial scales (Goward et al., 2002; Sandholt et al., 2002; Ishimura et al., 2011). VIs, which are mathematical combinations of different spectral bands from satellite remotely sensed data, have been utilized to estimate soil moisture (Z. Gao et al., 2011; Chen et al., 2015). The NDVI is the normalized reflectance difference between NIR and visible red bands, which measures changes in chlorophyll content. As a result, it is considered a function of vegetation strength, which changes as vegetation interacts with soil moisture. The NDWI is a more recent satellite-derived index from the NIR and SWIR channels that reflects changes in both water content and spongy mesophyll in vegetation canopies (Gao, 1996). This index has been employed for the determination of vegetation water content and stress (Ceccato et al., 2002), and is therefore expected to be linked to soil moisture due to its impact on vegetation water stress. Moreover, LST can rise rapidly with water stress (Goetz, 1997), which is directly related to soil moisture. Accordingly, LST is also widely used as a soil moisture indicator (Carlson, 2007).

The relationship between VI and LST has been investigated to evaluate evapotranspiration rates. The VI-LST relationship normally shows a negative correlation, resulting in triangular-shaped VI-LST plots at different spatial scales (Nemani et al., 1993; Goetz, 1997). Based on the VI-LST correlation, the TVDI, computed from the NDVI-LST relationship has become a widely used dryness index to estimate surface soil moisture (Sandholt et al., 2002; Mallick et al., 2009; Patel et al., 2009). For example, Wang et al. (2007) applied NDVI-LST produced from MODIS data to investigate the correlation with soil moisture determined by field measurements. The results revealed that NDVI-LST is strongly correlated with soil moisture and can be used to generate soil moisture estimates. Chen et al. (2015) used the TVDI (NDVI-LST) derived from Landsat-5 TM data to estimate soil moisture and found that the TVDI can reflect the soil moisture status under different tree species. In this study, we propose a new application of the NDWI-LST relationship, which could enhance the efficiency of the TVDI calculation. Additionally, the NDDI, which combines information about both greenness and water obtained from the NDVI and the NDWI (Gu et al., 2007), has been applied in numerous studies to evaluate drought and it was found that it is an appropriate indicator for the dryness of a particular area (Renza et al., 2010; Gouveia

et al., 2012). The NDDI appears to respond to soil moisture based on drought conditions, and was used in this study to determine soil moisture.

The objectives of this study are to estimate the spatial distribution of soil moisture using VIs based on Landsat 8 OLI/TIRS data and to evaluate the use of soil moisture data for wildfire risk assessment. Specifically, this paper includes: (1) soil moisture estimates for mapping the spatial distribution of soil moisture by combining TVDI and NDDI based on a regression approach. We propose a possible adaptation and application of NDWI and LST for constructing a TVDI based on the similar design of the triangular NDVI-LST space. We then compare the efficiencies of NDVI-LST and NDWI-LST for calculating the TVDI. (2) An investigation of the relationship between estimated soil moisture and fuel moisture measured in the field to assess the suitability of the simulated soil moisture data for wildfire prediction. (3) We hypothesize that (i) the NDWI-LST relationship performs as well as or better than the NDVI-LST relationship and can be applied for calculating TVDI, and (ii) that estimated soil moisture derived from our model is directly related to fuel moisture, influencing wildfire occurrence. In this study, we used the Landsat 8 TIRS and MODIS products for calculating LST and the Landsat 8 OLI product for determining TVDI and NDDI.

This study could also be used as an approach to enhance the efficiency of wildfire assessment using soil moisture as a surrogate for fuel moisture, identifying areas prone to wildfire across different landscapes. Until now, Thailand has not widely applied remote sensing to wildfire management. Using soil moisture measured by remote sensing as a complementary dataset for wildfire management may have the unique potential to predict wildfire danger for Thailand's forest areas and enhance the effectiveness of planning and decision-making in the area of wildfire management.

5.2 Materials and methods

5.2.1 Field data measurement

Thirty-four sample plots with heterogeneous landscape and ecological conditions were selected using a topographic map and Landsat 8 image provided radiometric and geometric corrections for different slopes, aspects, and forest types. The selected plots were evaluated during the dry season in March 2015. Larger 30 m × 30 m sample areas, corresponding to the spatial resolution of Landsat 8 images (30 m × 30 m pixel size) used for linear regression analysis, were divided into five subplots (1 m × 1 m) for collecting soil samples and fuel or litter from the ground surface (Figure 5.1).

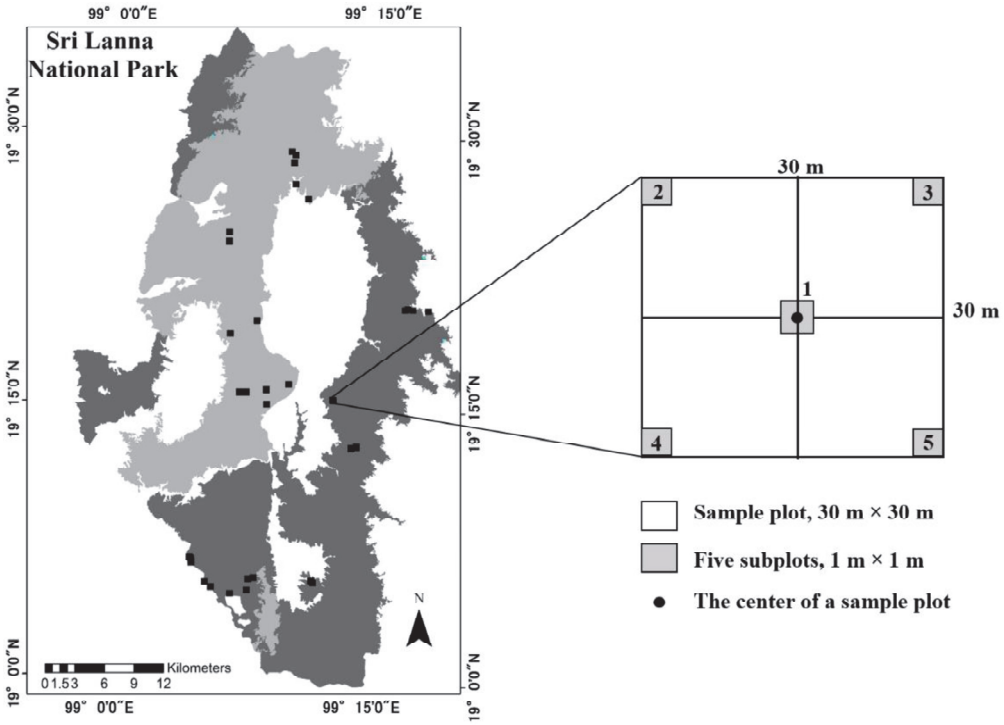

Figure 5.1 Sample plots in dipterocarp and deciduous forests

5.2.2 Gravimetric Soil Moisture Measurements

Soil samples were collected from each of the five 1-m² subplots, which are representative of the soil within each sample plot. The soil samples were taken at a standard depth of 10 cm, because previous studies have indicated that it is feasible to estimate surface (0 to 0.76 cm) soil moisture from visible and NIR reflectance (Kaleita et al., 2005). In addition, VIs show the highest correlation with surface soil moisture at 10 cm depth (Zhang et al., 2013). Each soil sample was placed in a plastic container and sealed tightly for further laboratory analysis. For the gravimetric analysis of soil moisture, we first weighed the soil samples (wet weight in grams) using a standard laboratory scale and then placed them in a drying oven at 105 °C for 48 hours (Gardner, 1986). After drying, we weighed the dried soil samples (dry weight in grams). The percentage of gravimetric soil moisture was calculated using Equation 5.1:

$$\text{Soil moisture} = \frac{\text{wet weight} - \text{dry weight}}{\text{dry weight}} \times 100\% \qquad (5.1)$$

Five soil moisture measurements from each of the five subplots within each sample plot were averaged to obtain representative soil moisture for each 30-m² site, corresponding

to the spatial resolution of the Landsat 8 images. The averaged soil moisture data from 34 sample plots were used for both training (80%) and validation (20%) data.

5.2.3 Leaf Fuel Moisture Measurements

Leaf fuel was collected for fuel moisture measurements, which were used for analyzing the relationship with simulated soil moisture. We specifically focused on dead leaves on the ground surface, because those represent the largest fuel component. A small sample of leaf litter was randomly collected from each 1-m^2 subplot and then placed into a sealed envelope for further laboratory analysis. In the laboratory, leaf litter samples were weighed and oven-dried at 80 °C for 48 h, then weighed again to calculate the FMC in percent following the procedure described by Desbois et al. (1997). The most common FMC calculation is the ratio of water to dry weight as expressed by Equation 5.2. The FMC values for the five subplots were averaged to obtain a representative FMC for each 30-m^2 sample plot.

$$\mathrm{FMC} = \frac{\text{wet weight - dry weight}}{\text{dry weight}} \times 100\% \tag{5.2}$$

5.2.4 Remotely Sensed Data and Preprocessing

We used cloud-free Landsat 8 OLI/TIRS and MODIS eight-day composite LST datasets at a spatial resolution of 30 m and 1000 m, respectively, as primary data (Table 5.1). The Landsat 8 data were converted from DNs to reflectance values before calculating the VI values. The DN conversion followed the steps of the USGS (2013). Estimates of soil moisture require: (i) Landsat 8 images to extract the TVDI and NDDI, and (ii) MODIS eight-day composite LST and Landsat 8 thermal infrared (TIR) data to produce the LST. Landsat 8 datasets used are the L1G level product and were geographically corrected and clipped based on the study area's boundary. The MODIS data were (i) projected to UTM Zone 47N with the WGS84 datum, (ii) clipped based on the study area's boundary, and (iii) co-registered to Landsat 8 images to reduce potential geometric errors.

Table 5.1 Selected Landsat 8 and MODIS images for dry season

Season	Parameter	Landsat 8		MODIS eight-day composite	
		Acquisition date	Spectral band	Acquisition date	Product
Dry	TVDI, NDDI	19 Feb 2015	Visible, NIR, SWIR	–	–
Dry	LST	19 Feb 2015	TIR (band 10)	18-25 Feb 2015	MOD11A2

5.2.5 Soil Moisture Estimates

5.2.5.1 Calculation of the TVDI

The LST is the temperature of the Earth's surface as derived from remotely sensed thermal infrared data (Weng, Fu, and Gao, 2014). It depends on the albedo, vegetation cover, and soil moisture. The Landsat 8 LST was computed by fusing images of MODIS LST and Landsat 8 brightness temperature (Tb), provided by Hazaymeh and Hassan (2015). Generating Landsat 8 LST was based on the linear relationship between MODIS LST and Landsat 8 Tb, which were obtained almost simultaneously and under similar atmospheric conditions.

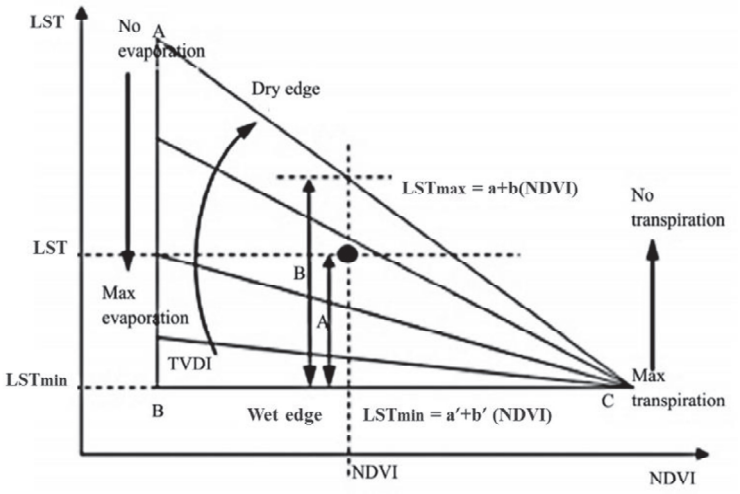

Figure 5.2 Simplified presentation of TVDI based on the triangular shape of the NDVI-LST relationship (adapted from Sandholt et al., 2002)

A scatter plot of remotely sensed LST and VI often results in a triangular shape (Price, 1990; Carlson et al., 1994) and the "dry" and "wet" edges of the triangle can be used to obtain information on soil moisture content. Figure 5.2 shows the conceptual TVDI based on the NDVI-LST triangle, where LST is plotted as a function of NDVI.

The linear combination of NDVI-LST typically shows a strongly negative relationship and the TVDI can be estimated from the dry and wet edges of the triangle.

In the feature space, TVDI is computed based on information about the wet edge representing the minimum LST (LST_{min}, maximum evapotranspiration and thereby, unlimited water access) as a straight line parallel to the NDVI axis. The dry edge, representing the maximum LST (LST_{max}, limited water availability) is linearly correlated with NDVI. Therefore, the TVDI is related to the soil moisture status in that high values indicate dry conditions and low values indicate moist conditions. In this study, the correlations of both NDVI and NDWI to the LST were observed. The TVDI for each pixel can be defined using Equation 5.3:

$$TVDI = \frac{LST - LST\min}{LST\max - LST\min} \tag{5.3}$$

Where, LST is the LST (°C) at a given NDVI and NDWI value, LST_{min} is the minimum LST (°C) based on the NDVI and NDWI values along the wet edge, and LST_{max} is the maximum LST (°C) based on the NDVI and NDWI values along the dry edge.

To calculate LST_{max} (dry edge) and LST_{min} (wet edge), we created scatter plots for each NDVI-LST and NDWI-LST pair. Linear regression was applied to scatter plots of the resulting LST_{max} and LST_{min} based on the upper and lower boundary lines of the scatter plots. Positive NDVI and NDWI values were ranked from 0 to 1 and divided into units of 0.01, 0.015, 0.02, 0.025, … 1. Then, each of the individual values of the scaled NDVI and NDWI were paired with a corresponding LST such as $NDVI_1$, LST_{max1} and $NDVI_1$, LST_{min1} or $NDWI_1$, LST_{max1} and $NDWI_1$, LST_{min1}. Finally, we employed a linear regression approach to fit the point pairs for generating LST_{max} and LST_{min}:

$$LST_{max} = a + b\,(VI) \tag{5.4}$$

$$LST_{min} = a' + b'\,(VI) \tag{5.5}$$

where, a and b are regression coefficients of LST_{max}, a' and b' are regression coefficients of LST_{min}, and VI represents the NDVI and NDWI values. The NDVI is a normalized ratio of the NIR and red reflectance (Tucker, 1979) as described in Equation 5.6. The NDWI is calculated from NIR and SWIR reflectance (Gao, 1996) as shown in Equation 5.7.

$$NDVI = \frac{NIR - RED}{NIR + RED} \quad (5.6)$$

$$NDWI = \frac{NIR - SWIR}{NIR + SWIR} \quad (5.7)$$

We investigated the NDVI and the NDWI performance and selected the index showing the strongest correlation with LST based on the adjusted R-squared (adj-R^2) of LST_{max} and LST_{min}. The best relationship of the index and LST was later used for TVDI calculation following Equation 5.3.

5.2.5.2 Calculation of the NDDI

The NDDI was computed from the NDVI and NDWI values according to the definition proposed by Gu et al. (2007). The combination of information about both vegetation (NDVI) and water (NDWI) conditions can be used to determine vegetation drought conditions, which reflect the effects of soil moisture. Due to the variation of the NDVI and NDWI within a range from -1 to +1, these values were converted to 8 bits (0-255) for the calculation of the NDDI, which ranges between -1 and +1. Higher NDDI values indicate more severe drought and lower soil moisture. The NDDI is computed as:

$$NDDI = \frac{NDVI - NDWI}{NDVI + NDWI} \quad (5.8)$$

5.2.5.3 Soil Moisture Model and Validation

We established a soil moisture estimation model based on a collection of field sampling and remote sensing data. A stepwise multiple regression approach was used to assess the relationship between field soil moisture data and remote sensing data, i.e., TVDI and NDDI were used as independent variables. The model can be computed by a regression formula as follows:

$$\text{Estimated soil moisture} = a + b(TVDI) + b'(NDDI) \quad (5.9)$$

where, the estimated soil moisture is given as a percentage (%), and a, b, and b' are the coefficients of the regression lines of the TVDI and NDDI.

The model was validated by ground and remote sensing data. We used the actual soil moisture from the field measurements to evaluate the accuracy of the predictive model by statistical inference: (i) the adjusted R-squared (adj-R^2), (ii) root mean squared

error (RMSE), (iii) absolute average difference (AAD), and (iv) the precision of the model. The precision (%) of the model is calculated as follows:

$$\text{Precision} = \left[1 - \sqrt{\frac{\sum[(Yi - Y'i)/Y'i]^2}{N}}\right] \times 100\% \quad (5.10)$$

where, Yi is the actual soil moisture of the field samples (%), Y'i is the estimated soil moisture from remotely sensed data (%), and N is the sample size.

Finally, the validated model was applied to a Landsat 8 image acquired on 19 February 2015 in Sri Lanna National Park (dipterocarp and deciduous forests) in order to estimate and map the spatial soil moisture distribution during the dry season.

5.2.6 Analysis of the Relationship Between Estimated Soil Moisture and Leaf Fuel Moisture

To investigate the relationship between soil moisture estimated from our model and FMC, we performed a correlation analysis using the Pearson correlation and linear regression methods. Estimated soil moisture was extracted from the model at the same locations as were used to measure leaf fuel moisture in the field to determine correlation. We then explored the possibility of applying estimated soil moisture from our model to the prediction of wildfire occurrences.

5.3 Results and Discussion

Scatter plots of the relationships between NDVI-LST and NDWI-LST are shown in Figure 5.3. Compared to the NDVI-LST plot, the NDWI-LST relationship shows a clearer triangular shape, following the theoretical triangle of the TVDI. We determined LST_{max} (dry edge) and LST_{min} (wet edge) to highlight linear trends. A comparison of pixels representing LST_{max} and LST_{min} extracted from the NDVI-LST and the NDWI-LST plots indicates a stronger relationship between these pixels in the NDWI-LST space. Based on Figure 5.3, the LST_{max}, representing the dry edge, shows a strong negative correlation between the NDWI and LST (adj-R^2 = 0.84, p-value < 0.01), and the LST_{min}, representing the wet edge, shows a negative correlation between the NDWI and LST with adj-R^2 = 0.63 at a significant level for $p < 0.01$. In contrast, NDVI has a lower correlation with LST, with LST_{max} at adj-R^2 = 0.62 (p-value > 0.05) and LST_{min} at adj-R^2 = 0.47 (p-value < 0.01). The results of the collinearity requirement indicate that

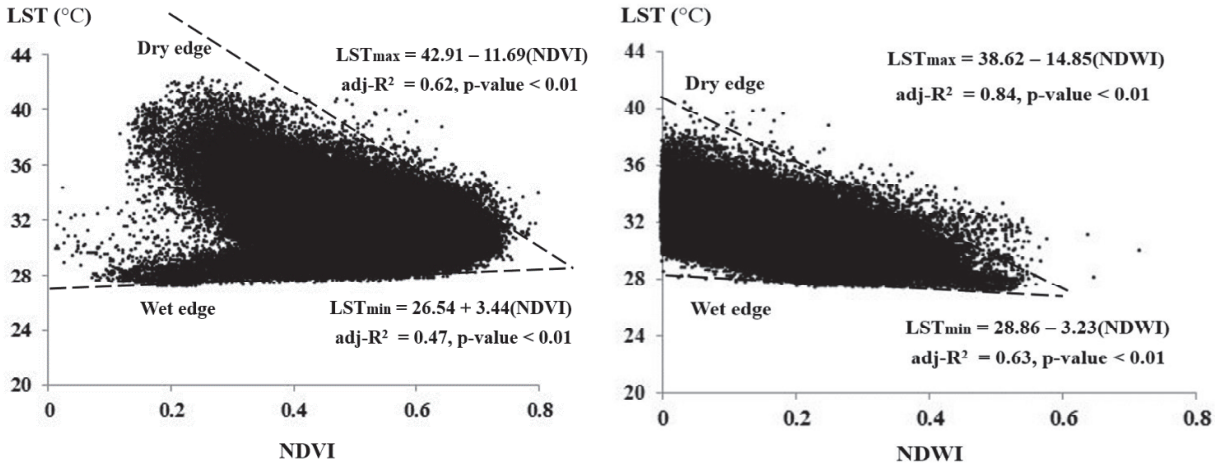

Figure 5.3 Observed relationships for NDVI-LST and NDWI-LST, based on the conceptual TVDI model

the NDWI has a stronger negative correlation with the LST than the NDVI, which is why the NDWI was used to calculate TVDI.

The reason for the better correlation between the NDWI and LST might be that LST is more strongly related to the water content of vegetation (captured by NDWI) than to the chlorophyll content (captured by NDVI). The NDVI measures changes in chlorophyll content (absorption of visible red radiation) and in the leaf spongy mesophyll (reflection of NIR radiation) within the vegetation canopy. Consequently, the NDVI has a limited capability for retrieving vegetation water content information, as it provides information on vegetation greenness (chlorophyll), which is not directly and uniformly related to the quantity of water in the vegetation (Ceccato et al., 2002). A change in chlorophyll content detected using the NDVI does not imply a direct change in leaf water content. Conversely, the NDWI is sensitive to changes in leaf water content because the green vegetation spectra in the SWIR region are dominated by water absorption.

The water content in leaves is directly affected by temperature conditions, especially high temperatures. As temperature increases, evaporation from leaves is higher, which affects the water content of the leaves. Evaporation within leaves also causes an increase in heat, and the leaf temperature rises relative to the air temperature or LST. Therefore, NDWI is more sensitive to LST, resulting in a stronger negative correlation with LST. Gu et al. (2007) found that NDWI values exhibited a quicker response to drought conditions when compared to NDVI values. This is because the NDWI is constructed from the SWIR, which is more sensitive to moisture than other spectra. As

a result, the NDWI shows a better correlation with LST and follows more closely the conceptual TVDI model. This result supports our hypothesis that the relationship between the NDWI and LST can be used to improve the calculation of the TVDI.

A TVDI map of the study area extracted from LST_{max} and LST_{min} based on the strong NDWI-LST relationship is shown in Figure 5.4a, while a NDDI map computed from the NDVI and the NDWI is shown in Figure 5.4b. Both maps, which show drought conditions during the dry season, can reflect the degree of soil moisture because drought influences the soil moisture status. Extreme drought results in lower soil moisture content. Therefore, both VIs can be used as predictor variables to estimate soil moisture.

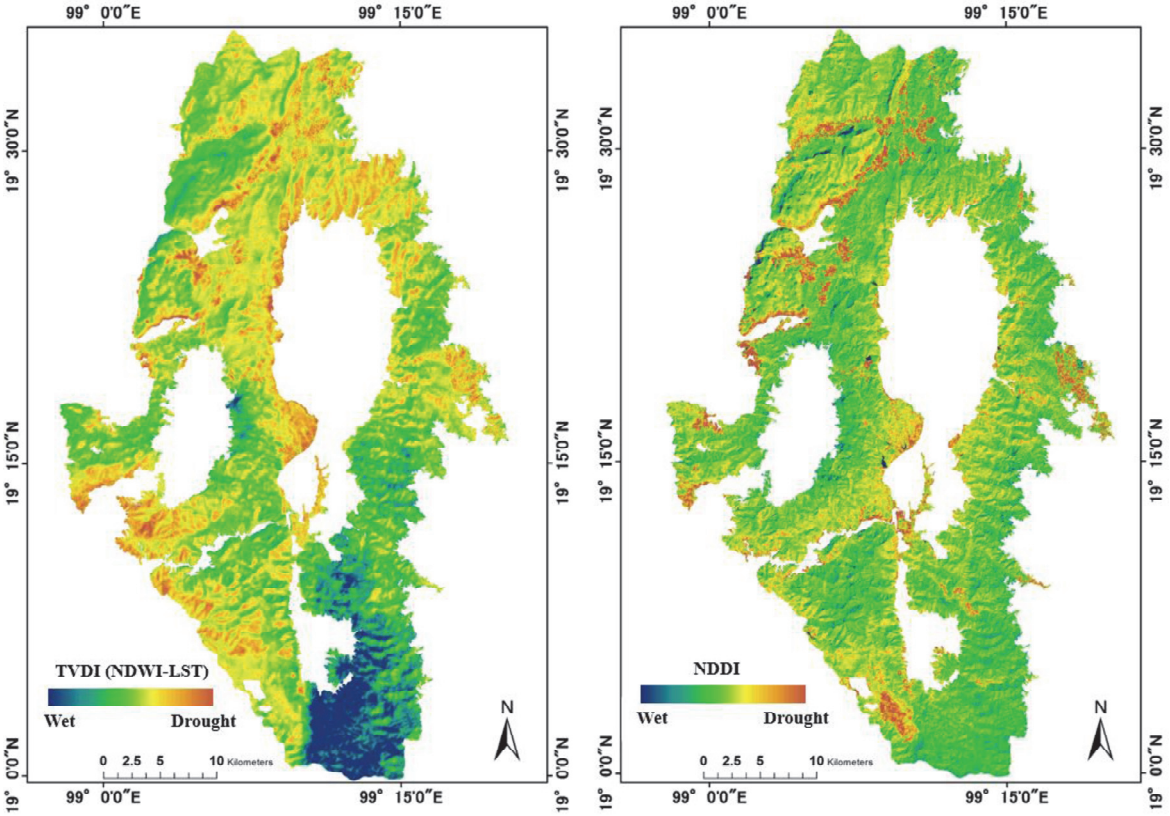

(a) $TVDI_{NDWI-LST}$ (b) NDDI

Figure 5.4 Extraction of a Landsat 8 image from 19 February 2015 for (a) $TVDI_{NDWI-LST}$ and (b) NDDI

Linear regression models for soil moisture estimation shown in Table 5.2 were calculated using the modified $TVDI_{NDWI-LST}$ and the NDDI as independent variables, and field-measured soil moisture content as the independent variable. The model constructed from both indices has the strongest response to the actual soil moisture and

likely has a greater ability to accurately estimate soil moisture, based on its high adj-R^2 (0.89, p-value < 0.01) and low RMSE (0.87%) for actual versus estimated soil moisture. In contrast, the model that only uses $TVDI_{NDWI\text{-}LST}$ has a lower adj-R^2 (0.72, p-value < 0.01) and a higher RMSE value of 1.39 %. Similarly, the model that only uses the NDDI shows the weakest correlation with an adj-R^2 of 0.52 (p-value < 0.01) and the highest RMSE of 1.82%. Thus, the soil moisture model using both the $TVDI_{NDWI\text{-}LST}$ and the NDDI fulfills the collinearity requirements with an increase in the adj-R^2 and a reduced RMSE, which can enhance the efficiency of soil moisture estimation.

Table 5.2 Comparison of statistical soil moisture models

Predictor variable	Soil moisture model (%)	N	adj-R^2	RMSE (%)
$TVDI_{NDWI\text{-}LST}$	10.67 – 12.24(TVDI NDWI-LST)	27	0.72*	1.39
NDDI	13.93 – 35.44(NDDI)	27	0.52*	1.82
$TVDI_{NDWI\text{-}LST}$, NDDI	14.32 – 9.45(TVDI NDWI-LST) – 21.78(NDDI)	27	0.89*	0.87

[a] * is significant at the 0.01 level.

The best model, developed from the combination of the modified $TVDI_{NDWI\text{-}LST}$ and the NDDI, was tested for accuracy with regard to field-measured soil moisture, resulting in the statistical parameters shown in Table 5.3. The model fulfills the statistical requirements. We found a high adj-R^2 of 0.75 with a p-value of < 0.01. We obtained low RMSE and AAD values of 1.22% and 1.06% between the actual and estimated soil moisture, respectively. In addition, the model precision was found it to be 76.65% consistent with the actual and estimated soil moisture. These statistical tests demonstrate that the model generated from the modified $TVDI_{NDWI\text{-}LST}$ and the NDDI can provide reliable estimates of soil moisture.

Table 5.3 Statistical validation between the actual and soil moisture estimated from the model

Soil moisture model (%)	N	adj-R^2	RMSE (%)	AAD (%)	Precision (%)
14.32 – 9.45(TVDI NDWI-LST) – 21.78(NDDI)	7	0.75*	1.22	1.06	76.65

[a] * is significant at the 0.01 level.

These results demonstrate that the efficacy of soil moisture estimation can be greatly enhanced using TVDI (modified from NDWI-LST) and NDDI as dependent variables, because both VIs show a strong correlation with soil moisture measured in the field. The reason for this strong correlation is the causal relationship between variations in

soil moisture and changes in vegetation; consequently, soil moisture deficits are ultimately tied to drought stress in plants (Gu et al., 2008), which is captured by both the TVDI and NDDI. Based on these results, we applied the model to a Landsat 8 image taken during the dry season to estimate soil moisture (Figure 5.5). The spatial distribution map shows that the percentage of soil moisture in Sri Lanna National Park is quite low during the dry season at around 0.001% to 31.1%, with a mean value of 15.49%. The degree of estimated soil moisture can indicate drought conditions, which in turn influence the occurrence of wildfires. Areas with

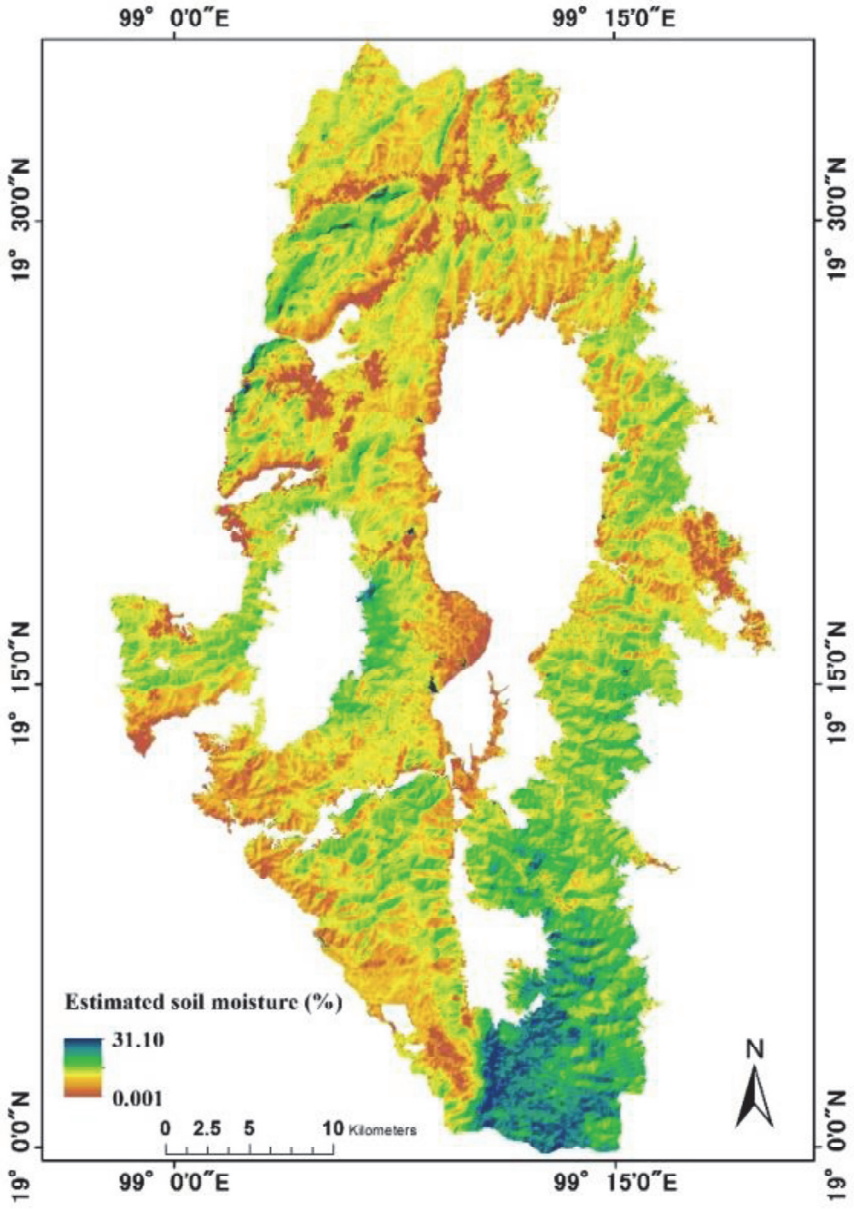

Figure 5.5 Spatial distribution of soil moisture derived from the model generated by the modified $TVDI_{NDWI-LST}$ and the NDDI in Sri Lanna National Park during the dry season on 19 February 2015

lower soil moisture and resulting lower fuel moisture, which influences fire ignition and spread, are more prone to wildfire occurrence.

We also investigated the correlation between the estimated soil moisture and leaf fuel moisture determined in the field (Figure 5.6). Pearson's correlation reveals that leaf fuel moisture shows a statistically significant positive correlation to the estimated soil moisture (Pearson's correlation coefficient = 0.67, p-value < 0.01). Larger values of estimated soil moisture tend to be associated with larger values of leaf fuel moisture. This implies that leaf fuel moisture has a tendency to increase when estimated soil moisture increases and vice versa. The statistical tests also support our hypothesis that the estimated soil moisture is directly related to FMC.

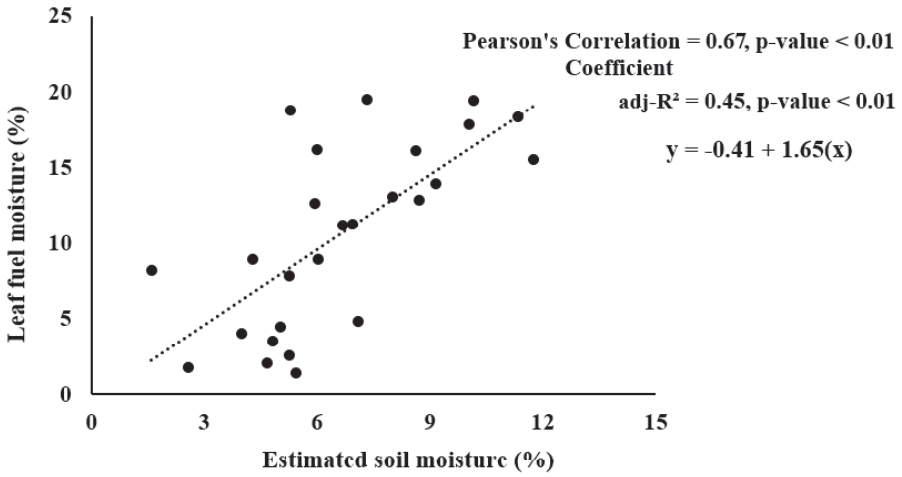

Figure 5.6 Scatter plot of leaf fuel moisture measured in the field and estimated soil moisture

Moreover, a median adj-R^2 of 0.45 with a p-value of < 0.01 as shown in Figure 24 indicates that estimated soil moisture is a significant variable for predicting leaf fuel moisture. This suggests that soil moisture is a factor that influences FMC since soil moisture condition affects fuel moisture levels which are directly related to wildfire occurrence. At high temperatures during the dry season, soil moisture and FMC are positively correlated, because high temperatures result in low soil moisture, which in turn leads to low FMC. As a result, we can use soil moisture to assess wildfire risks by exploiting the relationship between soil moisture and FMC. When FMC is high, fires do not readily ignite, because heat energy has to be used to evaporate water from plant material before it can burn. During the combustion of the above ground plant material and surface organic layers, the heat energy created is then transferred in the soil

(DeBano et al., 1998). Thus, fuel load with low moisture can transfer more heat into the soil during the combustion of fuel. Soils with higher moisture content tend to absorb more heat energy (DeBano et al., 1998; 2005); as a result, the intensity of the fire is reduced. In cases where both the FMC and soil moisture are low, wildfires will start much easily and spread rapidly resulting in uncontrollable fire condition.

Based on the result, mapping of estimated soil moisture can be used to investigate wildfire risk in large areas. Additionally, soil moisture can give an insight on the dryness of the fuel, which is a crucial parameter for wildfire risk. Therefore, to reduce wildfire risk and intensity, soil moisture should be considered as another indicator for monitoring wildfire prone areas. An analysis of soil moisture could considerable enhance wildfire management, thus in our study we highly recommend estimating soil moisture by remotely sensed data to be used as a complementary dataset for wildlife management in terms of risks and danger assessment.

5.4 Conclusions

The main goal of this study was to estimate the spatial distribution of soil moisture using TVDI and NDDI derived from Landsat 8 OLI/TIRS data for wildfire risk assessment. Results reveal that an accurate estimate of TVDI can be obtained from the relationship between NDWI, which is more significantly correlated to LST than the NDVI, and LST. This modified $TVDI_{NDWI\text{-}LST}$ can be used together with the NDDI to enhance the efficacy of soil moisture estimation. A scatter plot of NDWI-LST shows a linear relationship and is a good match with the theoretical concept of the TVDI, which is characterized by the triangular shape of the NDVI-LST relationship. The good correlation between NDWI and LST fulfills the collinearity requirements for extracting LST_{max} and LST_{min}; consequently, the NDWI-LST relationship provides a better estimate of the TVDI than the NDVI-LST relationship.

The soil moisture model generated from a combination of the modified $TVDI_{NDWI\text{-}LST}$ and NDDI can improve the accuracy of soil moisture estimates. The accuracy of the model was tested using statistical metrics, and was found to be more than 76% consistent with actual soil moisture and estimated soil moisture derived from our model. We further explored the relationship between estimated soil moisture and wildfire risk by investigating the correlation between estimated soil moisture and leaf fuel moisture measured in the field. Results show that estimated soil moisture is positively correlated to leaf fuel moisture with a Pearson's correlation coefficient of 0.67

(p-value < 0.01). This relationship demonstrates that wildfire-prone areas, which are characterized by low FMC, can be identified through soil moisture estimates, because both soil moisture and FMC show the same or similar behavior under conditions of high temperatures during the dry season.

The model allows to remotely determine the spatial distribution of soil moisture as a complementary dataset for identifying wildfire-prone areas, which is a fundamental step toward involving soil moisture in the assessment of wildfire risk. We therefore recommend soil moisture estimation by remotely sensed model as another indicator for monitoring wildfire risks and intensity. Furthermore, the demonstrated NDWI-LST relationship provides another option for researchers studying soil moisture when the established TVDI based on the NDVI-LST relationship is insufficient.

CHAPTER 6

Assessment of Wildfire Risk at Recreational Sites in Sri Lanna National Park, Chiang Mai, Northern Thailand, using Remote Sensing and GIS Techniques

6.1 Introduction

National parks in Thailand are protected forest areas that contain natural resources, biodiversity, and appealing scenery and landscape that attracts tourism. Recreation and tourism play an important role in the life of the national park because most visitors cite scenery and landscape as their main reasons for visiting a national park. Recreation areas in the national park have a wide variety of natural places and landscapes that enable activities for tourism such as camping, boating, walking and climbing trails, and wildlife viewing. Such recreational areas are increasingly threatened and damaged by wildfires, resulting in a decline in tourism activities. Wildfires are complicated events that occur as a result of natural processes and human activities (Vasilakos et al., 2009). Statistical evidence demonstrates increasing trends in fire frequency and area burned within Thai protected forest areas from 2014 to 2016, with 4,207, 4,982, and 6,685 wildfires, accounting for 50,723, 60,453 and 125,896 ha of burned area in 2014, 2015, and 2016, respectively (Forest Fire Control Division, 2016). These numbers imply that the wildfires are occurring more frequently and are burning larger areas, expanding into recreational zones. Most wildfires in Thailand occur in national parks, especially in the north, and are mainly attributed to human activities.

Wildfires occur when three requirements needed for ignition and combustion are met, the so-called fire triangle: fuel to burn, air to supply oxygen, and a heat source to ignite the fire. After a fire starts, a wide range of factors determines the fire duration and intensity. These factors include the quantity and type of fuel, topographic characteristics (slope, aspect, and elevation), favorable environmental conditions (e.g., extreme drought and low soil moisture), which can accelerate fire combustion and result in uncontrollable spread of fire over large areas. Hence, factors influencing fire behavior need to be analyzed when mapping wildfire risk zones (Chuvieco and Congalton, 1989).

Satellite remote sensing and GIS techniques have been widely used in wildfire assessment, such as predicting wildfire severity based on VI, establishing wildfire risk

models, and analyzing factors responsible for wildfire. Topography, anthropogenic data, and the characteristics of vegetation or fuel have been used as the most important factors influencing wildfire occurrence. Many studies have integrated these factors to establish wildfire risk models. Jaiswal et al., (2002) undertook a wildfire risk assessment for areas in India. They used the vegetation type, slope, aspect, and distance from roads and settlements to establish a wildfire risk model that showed strong agreement with actual fire-affected sites. Adab et al., (2013) applied vegetation moisture, slope, aspect, elevation, distance from roads, and vicinity to settlements as factors influencing accidental fires. Moreover, the quality, size, and shape of vegetation or fuel were used with other wildfire potential factors (slope, elevation, aspect, weather, land cover/use map, etc.) to establish a wildfire risk and hazard model (Yakubu et al., 2013). In addition to fuel type and moisture input, the quantity of fuel should also be analyzed, since large amounts of fuel result in higher intensity fires. Additionally, soil moisture should be considered as a wildfire factor because it is positively correlated with fuel moisture content (Burapapol and Nagasawa, 2016a). The present study integrated remote sensing and GIS techniques for modeling and mapping wildfire risk and evaluating recreation sites at risk from wildfires. To achieve these goals, data were obtained from Landsat 8 OLI/TIRS, and MODIS images, and were integrated with GIS data to establish a wildfire risk model for mapping wildfire-prone areas in Sri Lanna national park. This study introduces soil moisture as a new factor for establishing a wildfire risk model, and proposes a differenced normalized burn ratio (dNBR) to rate wildfire sensitivity for subclasses of each risk factor. A wildfire risk map produced from our model was used to assess potential wildfire risk at recreation sites. We propose that a wildfire risk map produced our model can be used as a complementary data for local officials and other decision makers dealing with wildfires, in developing appropriate plans for preventing wildfires in national parks and recreational areas.

6.2 Materials and methods

6.2.1 Dataset

The datasets and overall methodology used in the present study are presented in Figure 6.1, where the corresponding data sources are shown in Table 6.1. The parameters involved in wildfire occurrence and those influencing wildfire behavior were selected as described in the following sub-sections:

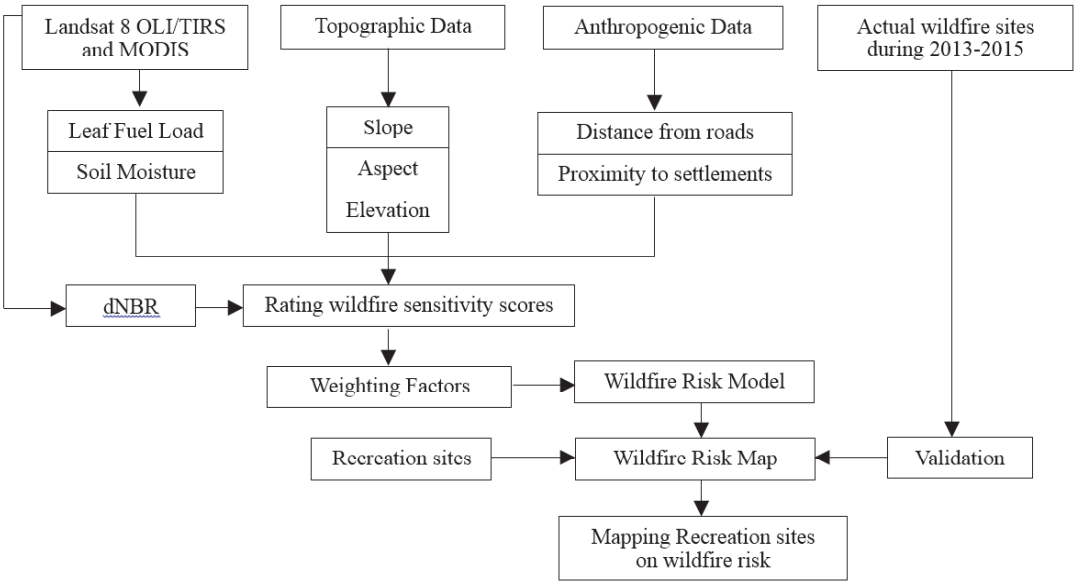

Figure 6.1 Overall methodology

1) Leaf Fuel Load

The fuel plays a major role in the initial stage of wildfires (fire ignition), and the fuel load also contributes to fire intensity. Higher fuel loads create longer flames and more intense fires for a given rate of spread. The largest component of surface fuel is dead leaves, which provide an efficient fuel for surface wildfires. In this study, we therefore focused on analyzing leaf fuel load. Leaf fuel load can be assessed using the greenness index, especially the NDVI which has been tested to predict leaf fuel load (Burapapol and Nagasawa, 2016b) as analyzed in chapter 4. Their predictions were applied here to estimate the spatial distribution of leaf fuel load. Seasonal NDVI values were calculated from the Landsat 8 OLI.

2) Soil Moisture

A low degree of soil moisture can indicate drought conditions, which influence the likelihood of wildfires. Soil moisture is positively correlated with fuel moisture. Under dry conditions, areas with low soil moisture and resulting low fuel moisture are more prone to wildfires and fires spread quickly. Therefore, soil moisture should be considered as a factor in wildfire models. A soil moisture model established by Burapapol and Nagasawa (2016a) was used to estimate the spatial distribution of soil moisture in the study area as analyzed in chapter 5.

Table 6.1 Data sources of parameters used for modeling and mapping wildfire risk and evaluating wildfire risk to recreational sites

Data/Parameters	Source of data	Creation of data	Acquisition date	Purpose
Leaf fuel load	Landsat 8 OLI (30m)	NDVI in normal season NDVI in dry season	14 Oct 2014 19 Feb 2015	Modeling wildfire risk
Soil moisture	Landsat 8 OLI/TIRS (30m)	NDDI and TVDI	19 Feb 2015	Modeling wildfire risk
	MODIS (1km)/ MOD11A2	LST	18–25 Feb 2015	
Slope	DEM (30 m)	Slope map	–	Modeling wildfire risk
Aspect	DEM (30 m)	Aspect map	–	Modeling wildfire risk
Elevation	DEM (30 m)	Elevation map	–	Modeling wildfire risk
Distance from roads	Shapefile	Lines	–	Modeling wildfire risk
Proximity to settlements	Shapefile	Points	–	Modeling wildfire risk
dNBR	Landsat 8 OLI (30m)	NBR pre fire NBR post fire	14 Oct 2014 19 Feb 2015	Rating wildfire sensitivity scores
Actual wildfire sites	Shapefile	Points	2013–2015	Validating wildfire risk map
Recreation sites	Shapefile	Points	–	Evaluating risk of wildfire

3) Topographic data

The topography is the most stable variable in fire behavior. The slope can be a primary influence on wildfire behavior (Weise and Biging, 1997) and affects both the rate and direction of fire spread. Fires generally tend to move faster up, rather than down, a slope (Adab et al., 2011). Steeper slopes result in faster fires due to more aggressive wind action. The aspect (slope direction) determines how much radiated heat a slope will receive from the sun. South to southwest aspects receive the most solar radiation, with comparatively higher temperature and lower humidity. Therefore, fuels tend to dry out sooner, ignite more thoroughly, and burn longer on south-facing slopes (Noonan, 2003 and Iwan et al., 2004). The elevation influences the amount of precipitation, wind exposure, temperature, and moisture that an area receives. Thus, elevation plays a large role in determining the condition of the fuel (Castro and Chuvieco, 1998). At lower elevations, fuels tend to dry out fast because of higher temperatures and lower precipitation. In this study, the slope, aspect, and elevation

data were extracted from a digital elevation model (DEM), provided by the Royal Thai Survey Department.

4) Anthropogenic data

Wildfires can be caused by the movements of humans and vehicles. Human activities are often linked to the occurrence of fires (Dong et al., 2005). Forests that are near centers of human activity, such as roads and settlements, can be more prone to fires, especially accidental man-made fires and hence, the distance from roads and settlements are important variables. For the proposed model, distances from roads and settlements were obtained from the DNP and were available in the GIS database in vector format (Shapefile).

5) dNBR

The dNBR is calculated from the normalized burn ratio (NBR) of pre-fire and post-fire events. Initially, the dNBR and NBR estimated from remotely sensed data were developed to identify burned from unburned areas (Lopez-Garcia and Caselles, 1991). Both indices were accepted for their ability to distinguish levels of burn severity within a fire-affected region (Bisson et al., 2008 and Key and Benson, 2006). We therefore applied the dNBR to evaluate the wildfire sensitivity rating scores for subclasses of each factor. An NBR dataset was generated from the reflectances of the NIR and SWIR bands of Landsat 8 OLI images, as expressed by Equation 6.1. A final dNBR dataset was derived from NBR values of pre-fire and post-fire images, as described by Equation 6.2.

$$\mathrm{NBR} = \frac{\mathrm{NIR} - \mathrm{SWIR}}{\mathrm{NIR} + \mathrm{SWIR}} \tag{6.1}$$

$$\mathrm{dNBR} = \mathrm{NBR}_{pre\ fire} - \mathrm{NBR}_{post\ fire} \tag{6.2}$$

6.2.2 Methodology

The study methodology comprised two main parts: modeling and mapping wildfire risk, and evaluating recreational sites for wildfire risk. These are presented in the following sections in more detail.

6.2.2.1 Preprocessing Remotely Sensed Data

Landsat 8 and MODIS images acquired for the study area are shown in Table 12. The Landsat 8 data were converted from DNs to reflectance values before calculating the

VI values. The DN conversion followed the steps of the USGS (2013). The Landsat 8 dataset used were L1G-level products, which were geographically corrected and projected into the UTM (Zone 47N, WGS 84 datum) coordinate system. Then, MODIS imagery was co-registered to Landsat 8 imagery to reduce potential geometric errors. Finally, both Landsat 8 and MODIS data were clipped within the boundary of the study area, and clouds and cloud shadows were removed.

6.2.2.2 Preparing GIS Data

Leaf fuel load and soil moisture were classified into three intervals on thematic maps. Slope, aspect, and elevation computed from the DEM (30 m resolution) were clipped based on the corresponding study area, and then categorized into different intervals on thematic maps. Settlement and road locations were buffered at specified distances. Buffer zones of 2,000 m and 4,000 m were created around the settlement locations, and 1,000 m and 2,000 m were used around roads. The stratification of each factor is presented in Table 6.2.

Table 6.2 Subclasses of each factor

Factors	Subclasses
Leaf fuel load (kg ha^{-1})	<1000, 1000–2500, >2500
Soil moisture (%)	<5 , 5–10 , >10
Slope(degrees)	<15 , 15–35 , >35
Aspect	north, east, south, west
Elevation (m)	<700, 7000–1400, >1400
Distance from roads (m)	< 1000, 1000 – 2000, > 2000
Proximity to settlements (m)	< 2000, 2000 – 4000, > 4000

6.2.2.3 Rating Wildfire Sensitivity Scores

The dNBR of the thematic map was assigned a value of 1 for burned areas and 0 for non-burned. The stratified subclasses of each factor were overlaid with the dNBR. The frequency of burned areas was used to assign different wildfire sensitivity scores to subclasses. For each class, the total number of burned pixels was calculated as a percentage of the total class area. The percentage was ordered to evaluate its susceptibility to wildfire (3 = high, 2 = moderate, and 1 = low). The subclass with the highest percentage of burned area was labelled as high wildfire risk and was given the

highest ranking of 3. Next, the class with a smaller percentage was assigned a moderate risk of score 2, and the class with lowest percentage was rated as low risk with a score of 1.

6.2.2.4 Weighting Factors on Wildfire

A pairwise comparison method developed by Saaty (1980) in the context of the analytic hierarchy process (AHP) decision making process, was applied to prioritize the factors for wildfire risk in the study area. The pairwise comparison was weighted by decision makers to make comparative judgments. This method has been tested theoretically and empirically for a variety of decision situations and multi-criteria decision making problems, including spatial decision making (Malczewski, 1999). It has been effectively adopted into GIS-based decision making on wildfires (Vasilakos et al., 2007, Vadrevu et al., 2010 and Yakubu et al., 2013). Each factor was compared pairwise and weighted on a scale of 1 to 9. According to Saaty's ranking scale, a scale of 1 indicates equal importance for wildfire risk between two factors, whereas a scale of 9 indicates that one factor is 9 times more important for wildfire risk than the other (Table 6.3). Three wildfire experts and stakeholders from the DNP (a fire specialist, a fire planner, and a wildfire fighter), who are involved in wildfire management in Thailand, were asked to weight the importance and priority of these pairwise comparisons. Then, a decision matrix (comparison table) was constructed using a ratio matrix. The relative weights were normalized to sum to 1, and finally averaged among the three experts.

Table 6.3 Numerical rating of the fundamental scale

Verbal importance	Numerical rating
Extremely important	9
Very strongly to extremely	8
Very strongly	7
Strongly to very strongly	6
Strongly	5
Moderately to strongly	4
Moderately	3
Equally to moderately	2
Equally	1

6.2.2.5 Establishing and Validating Wildfire Risk Model and Map

The weighted factors (layers), which were rated in different subclasses, were integrated using the GIS union process to establish a wildfire risk model. The model used to determine wildlife risk areas is shown in Equation 6.3:

$$WFR = W_1(F_{i=1\text{-}3}) + W_2(SM_{i=1\text{-}3}) + W_3(S_{i=1\text{-}3}) + W_4(A_{i=1\text{-}4}) + W_5(E_{i=1\text{-}3}) + W_6(R_{i=1\text{-}3}) + W_7(ST_{i=1\text{-}3}) \quad (6.3)$$

where WFR is the numerical index of wildfire risk; $W_{1–7}$ are the weighting values of each factors based on the pairwise comparison; F, SM, S, A, E, R and ST are the factors influencing wildfire, namely: leaf fuel load, soil moisture, slope, aspect, elevation, distance from roads, and proximity to settlements, respectively. The superscript i indicates subclasses based on rating the wildfire sensitivity scores using the dNBR. We then defined the interval size of the WFR value to classify wildfire risks into three risk categories; low, medium, and high. Finally, we obtained a map showing the wildfire risk zones in different categories.

The accuracy of the wildfire risk map was tested against actual wildfire occurrences during 2013–2015. A confusion matrix, showing the correspondence between predicted and actual classifications (Congalton, 1991), was adopted to verify the map. The actual wildfire points were used as ground-truth data for the high risk class only. Both the actual and predicted wildfire points were evaluated in the matrix (Table 6.4) and the accuracy was calculated from the percentage of correctly classified instances, as described by Equation 6.4:

$$\%\ \text{of correctly classified instances} = \frac{A + D}{(A+B+C+D)} \times 100 \quad (6.4)$$

Table 6.4 Confusion matrix modified from Congalton (1991)

Actual wildfire points	Predicted wildfire points		
		H	M or L
	H	A	B
	M or L	C	D

[a] H = High risk, M = Moderate risk and L = Low risk

6.2.2.6 Assessment of Wildfire Risk at Recreational Sites

The verified wildfire risk map was further used to evaluate the risk of wildfire to recreational sites within Sri Lanna national park. Buffers of 500 m were created around recreational sites and overlaid with the wildfire risk map. From the buffered areas, the fraction of each area prone to wildfire was assessed based on the wildfire risk categories. Finally, a map was produced showing wildfire risk within the buffered areas, which can help in wildfire prevention at these locations.

6.3 Results and Discussion

The burned areas in 2015 (Figure 6.2a) detected by dNBR covered 4,489.38 ha (5.40% of total area). The dNBR in the thematic map was overlaid with each factor assigned to different subclasses. The relative frequencies of burned areas in each subclass were calculated to evaluate the wildfire sensitivity of each subclass, as illustrated in Table 6.5.

Areas with leaf fuel load >2,500 kg ha^{-1} showed the highest percentage of burned area, indicating greatest sensitivity to wildfire (score of 3). In comparison, leaf fuel loads of 1,000–2,500 kg ha^{-1} and <1,000 kg ha^{-1} had lower percentages of burned areas, and were ranked as having moderate (score of 2) and low (score of 1) wildfire sensitivity, respectively (Figure 6.2b). Hence, the risk of wildfire is a function of the amount of leaf fuels. The results showed that soil moisture levels were inversely related to the number of burned areas. Areas with soil moisture <5% showed a high percentage of burned area, and therefore categorized as having high wildfire sensitivity (score of 3). Areas with soil moisture of 5–10% and >10% had lower percentages of burned areas and were classified as having moderate (score of 2) and low (score of 1) wildfire sensitivity, respectively (Figure 6.2c). This implies that lower soil moisture is associated with increased wildfire risk, and vice versa. This supports the findings of previous research, which showed that low soil moisture was associated with large wildfires during the vegetation growing season (Krueger et al., 2015).

Table 6.5 Rating wildfire sensitivity scores assigned to subclasses for wildfire risk modeling

Factor	Subclass	Burned area (ha)	Total area (ha)	Percentage of burned area	Rating	Wildfire sensitivity
Leaf fuel load (kg ha^{-1})	<1000	171.99	25,532.37	3.84%	1	Low
	1000–2500	1,034.55	45,253.98	23.04%	2	Moderate
	>2500	3,282.84	12,407.94	73.12%	3	High
Soil moisture (%)	<5	4,188.06	36,952.02	93.29%	3	High
	5–10	299.43	38,757.60	6.67%	2	Moderate
	>10	1.89	7,484.67	0.04%	1	Low
Slope (degrees)	<15	2,641.05	35,957.97	58.83%	3	High
	15–35	1,579.41	44,394.30	35.18%	2	Moderate
	>35	268.92	28,42.02	5.99%	1	Low
Aspect	North	678.06	19,524.15	17.79%	1	Low
	East	1,028.92	19,827.63	27.00%	2	Moderate
	South	1,834.20	22,371.84	48.13%	3	High
	West	948.24	21,470.67	24.88%	2	Moderate
Elevation (m)	<700	3,355.29	46,425.24	74.74%	3	High
	700–1400	1,133.10	36,749.61	25.24%	2	Moderate
	>1400	0.99	19.44	0.02%	1	Low
Distance from roads (m)	<1000	1,796.76	28,714.86	40.02%	3	High
	1000–2000	982.08	22,721.31	21.88%	1	Low
	>2000	1,710.54	31,758.12	38.10%	2	Moderate
Proximity to settlements (m)	<2000	1,749.60	26,458.38	38.97%	3	High
	2000–4000	1,623.06	40,861.71	36.16%	2	Moderate
	>4000	1,116.72	15,874.2	24.87%	1	Low

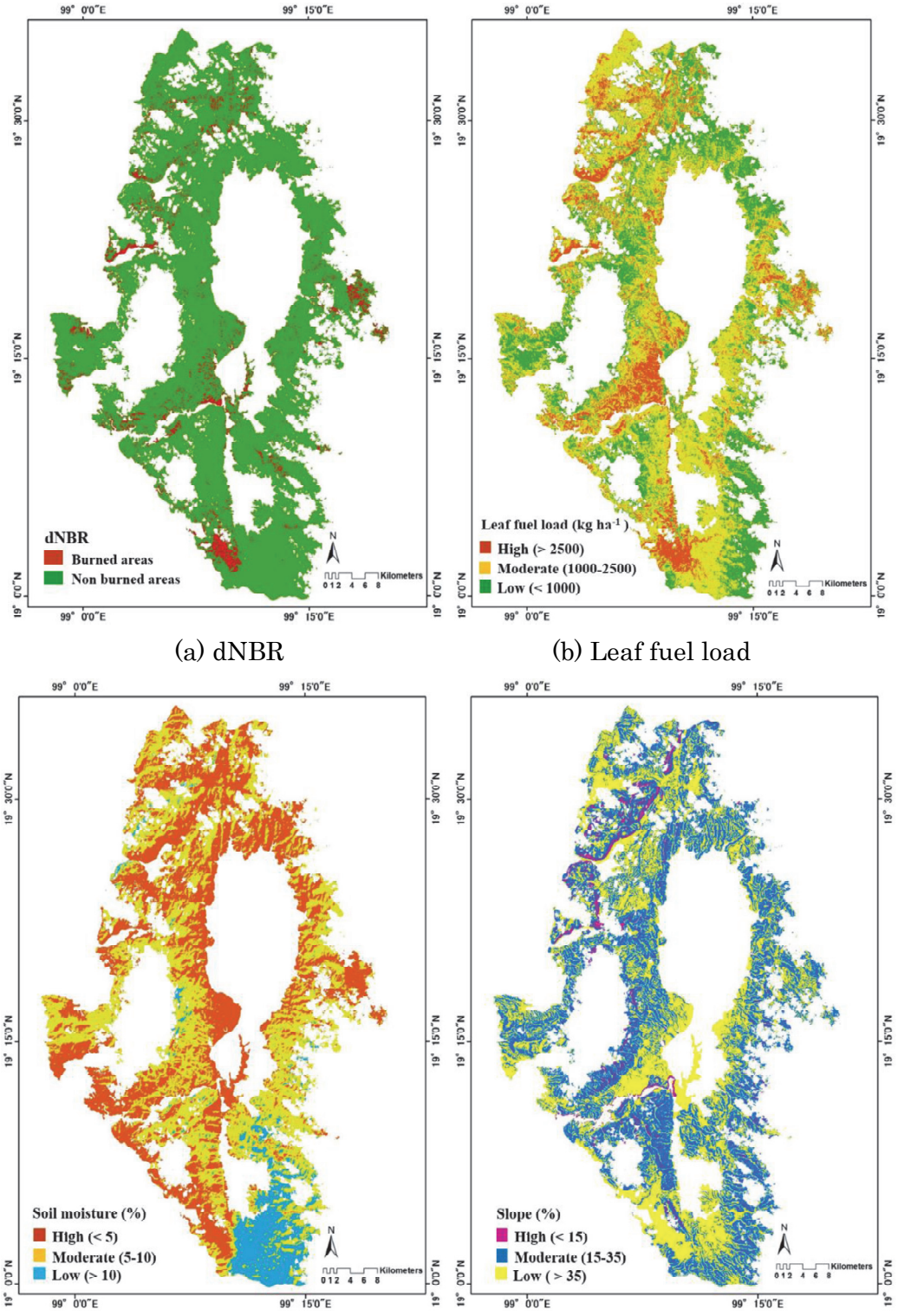

(a) dNBR (b) Leaf fuel load

c) Soil moisture (d) Slope

Figure 6.2 (a) The dNBR in Sri Lanna National Park obtained from Landsat 8 images; (b) leaf fuel load with rated subclasses; (c) soil moisture with rated subclasses; (d) slope with rated subclasses; (e) aspect with rated subclasses; (f) elevation with rated subclasses; (g) road buffer with rated subclasses, and (h) settlement buffer with rated subclasses

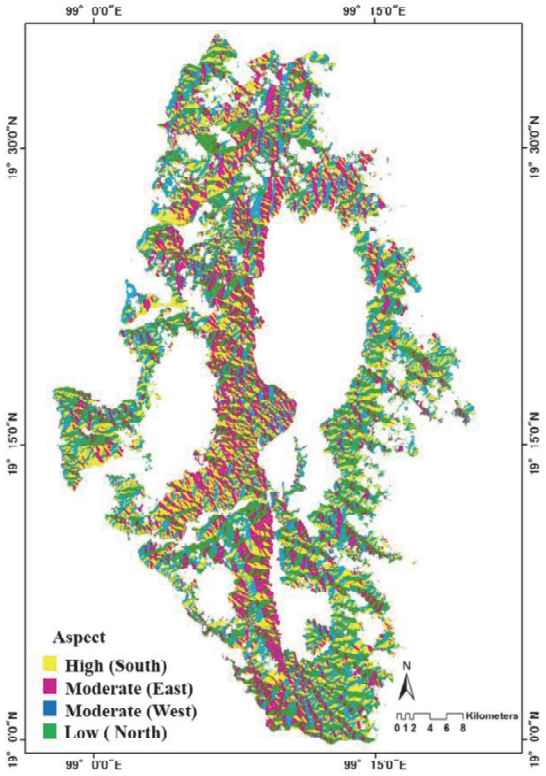

(e) Aspect

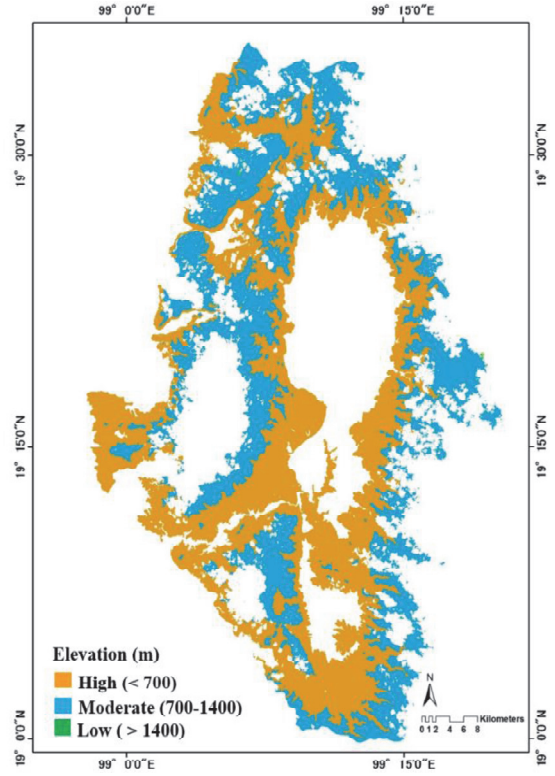

(f) Elevation

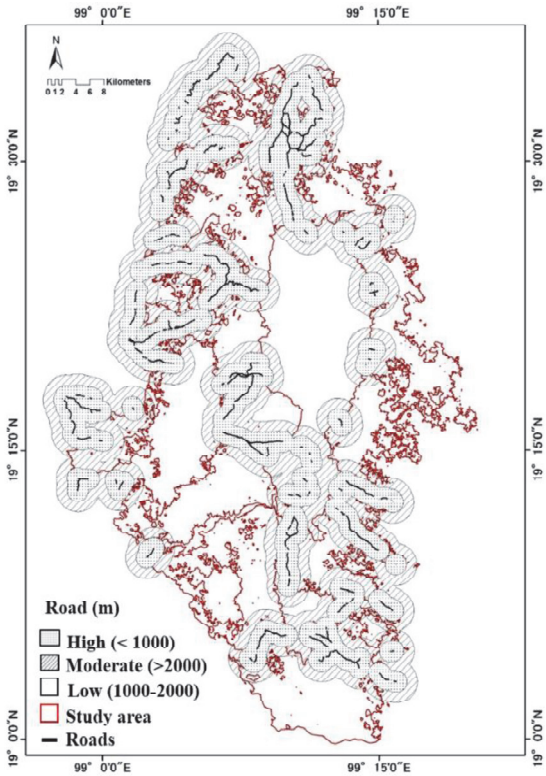

(g) Distance from roads

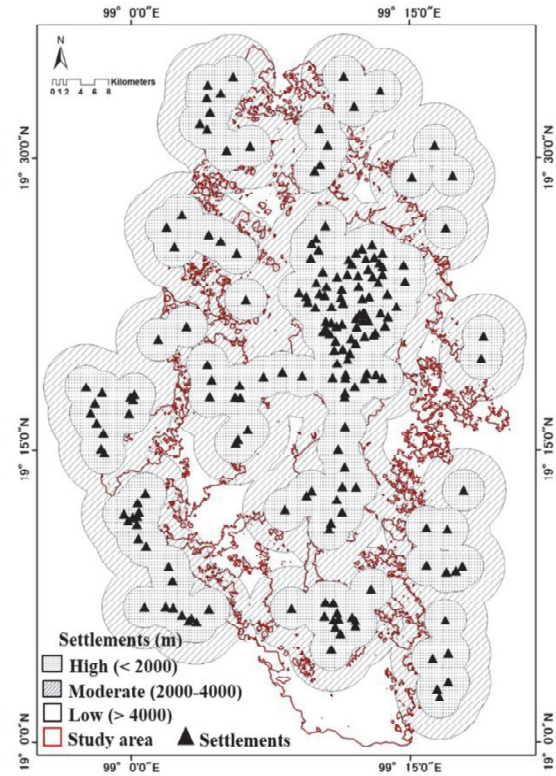

(h) Proximity to settlements

Figure 6.2 Continued

In Figure 6.2d, a large percentage of burned areas occurred in areas with slopes less than 15 degrees, which was therefore classified as having high wildfire sensitivity (score of 3). It was found that most of the areas with slopes less than 15 degrees were close to settlements and agricultural areas, which might account for their high sensitivity to wildfire. Areas with the slopes of 15–35 degrees and slopes steeper than 35 degrees were evaluated as having moderate (score of 2) and low (score of 1) wildfire sensitivity, respectively. It was found in Figure 6.2e that south-facing areas showed the highest percentage of burned areas (approximately 48%), and were therefore rated as having high wildfire sensitivity (a score of 3). This is because south-facing areas usually receive more sunlight resulting in higher temperatures and fuel with a lower moisture content. Therefore, wildfires can more easily ignite and spread more rapidly. Hence, south-facing areas are the most critical in terms of the initiation and spread of wildfires. East- and west-facing areas were assigned moderate wildfire sensitivity (score of 2). Lastly, north-facing areas had lower percentage of burned area (approximately 17%), and were therefore evaluated as having low wildfire sensitivity (a score of 1). According to the percentage of burned area, high elevation areas were less susceptible to wildfires (Figure 6.2f). Most of the burned area occurred at elevations below 700 m which was assigned a score of 3. This is probably because there is much more moisture in the air and less oxygen at higher elevations, so wildfires are less likely to occur. Meanwhile, areas at 700–1,400 m elevation had the second-highest percentage of burned area, and were assigned moderate wildfire sensitivity (a score of 2). The smallest percentage of burned area was found at elevations higher than 1,400 m, which were evaluated as having low wildfire sensitivity with a score of 1.

Areas <1,000 m from road networks had the highest percentage of burned area and were assigned a high wildfire sensitivity of 3, while areas 1,000–2,000 m and >2,000 m from roads were classified as having low and moderate wildfire sensitivity, respectively (Figure 6.2g). The largest percentage of burned areas was found at distances <2,000 m from settlements (highly sensitive to wildfire). Those areas at distances of 2,000–4,000 m and >4,000 m from settlements were classified as having moderate and low wildfire sensitivity, respectively (Figure 6.2h). Hence, forest areas located close to roads and settlements are at highest risk from wildfires. According to the results of rating scores, dNBR can be appropriately applied to all factors to evaluate the levels of wildfire sensitivity. This is because factors assigned a wildfire sensitivity by the dNBR followed

the same trends as the physical theory of wildfire behavior and interactions in the fire environment.

All factors with subclasses rated the scores were weighted according to their corresponding risk for wildfire, based on the judgments of wildfire experts and stakeholders. Calculation of the weighting scores of factors using pairwise the comparison matrix of each person is presented in Table 6.6. Then, the calculated weighted scores of three experts were averaged to finalize the weighted scores as shown in Table 6.7.

Table 6.6 Calculation of factor weightings based on pairwise comparison matrix of three experts in wildfires. Weightings based on opinions and judgments of:

1) Wildfire specialist

Factor	Leaf fuel load	Soil moisture	Slope	Aspect	Elevation	Roads	Settlements	Normalized weight (1)
Leaf fuel load	0.365	0.209	0.276	0.267	0.232	0.368	0.387	0.301
Soil moisture	0.041	0.023	0.006	0.008	0.007	0.011	0.043	0.020
Slope	0.052	0.163	0.039	0.038	0.166	0.011	0.043	0.073
Aspect	0.052	0.116	0.039	0.038	0.033	0.011	0.043	0.048
Elevation	0.052	0.116	0.008	0.038	0.033	0.011	0.043	0.043
Roads	0.073	0.163	0.276	0.267	0.232	0.074	0.055	0.163
Settlements	0.365	0.209	0.355	0.344	0.298	0.516	0.387	0.353
Sum	1.000	1.000	1.000	1.000	1.000	1.000	1.000	1.000

2) Wildfire planner

Factor	Leaf fuel load	Soil moisture	Slope	Aspect	Elevation	Roads	Settlements	Normalized weight (1)
Leaf fuel load	0.431	0.366	0.600	0.333	0.217	0.446	0.446	0.406
Soil moisture	0.086	0.073	0.086	0.111	0.130	0.050	0.050	0.084
Slope	0.062	0.073	0.086	0.111	0.130	0.149	0.149	0.108
Aspect	0.048	0.024	0.029	0.037	0.043	0.030	0.030	0.034
Elevation	0.086	0.024	0.029	0.037	0.043	0.030	0.030	0.040
Roads	0.144	0.220	0.086	0.185	0.217	0.149	0.149	0.164
Settlements	0.144	0.220	0.086	0.185	0.217	0.149	0.149	0.164
Sum	1.000	1.000	1.000	1.000	1.000	1.000	1.000	1.000

Table 6.6 Continued

3) Wildfire-fighter

Factor	Leaf fuel load	Soil moisture	Slope	Aspect	Elevation	Roads	Settlements	Normalized weight (1)
Leaf fuel load	0.039	0.232	0.061	0.010	0.010	0.023	0.200	0.082
Soil moisture	0.006	0.033	0.078	0.010	0.007	0.339	0.067	0.077
Slope	0.353	0.232	0.548	0.483	0.362	0.475	0.467	0.417
Aspect	0.275	0.232	0.078	0.069	0.258	0.014	0.067	0.142
Elevation	0.196	0.232	0.078	0.014	0.052	0.014	0.067	0.093
Roads	0.118	0.007	0.078	0.345	0.258	0.068	0.067	0.134
Settlements	0.013	0.033	0.078	0.069	0.052	0.068	0.067	0.054
Sum	1.000	1.000	1.000	1.000	1.000	1.000	1.000	1.000

Table 6.7 Weightings assigned to factors influencing wildfire, based on the judgments of wildfire experts and stakeholders using a pairwise comparison method

Factors	Weighting scores			
	Wildfire specialist	Wildfire planner	Wildfire-fighter	Average
Leaf fuel load	0.301	0.406	0.082	0.263
Soil moisture	0.020	0.084	0.077	0.060
Slope	0.073	0.108	0.417	0.200
Aspect	0.048	0.034	0.142	0.075
Elevation	0.043	0.040	0.093	0.059
Distance from roads	0.163	0.164	0.134	0.154
Proximity to settlements	0.353	0.164	0.054	0.191
Sum	1.000	1.000	1.000	1.000

Leaf fuel load had the highest weighting (therefore contributing greatly to wildfire), followed by slope, proximity to settlements, distance from roads, aspect, and soil moisture, whereas elevation was the least important. It can be concluded that, among these factors, fuel load is highly influential for wildfire and is considered the most important factor because it contributes both stages of wildfire occurrence (ignition and spread/intensity). The averaged weighting of each factor was substituted in the wildfire risk model using Equation 6.3. The wildfire risk map produced from the model shows the estimated possibility of wildfires in the study area (Figure 6.3a)

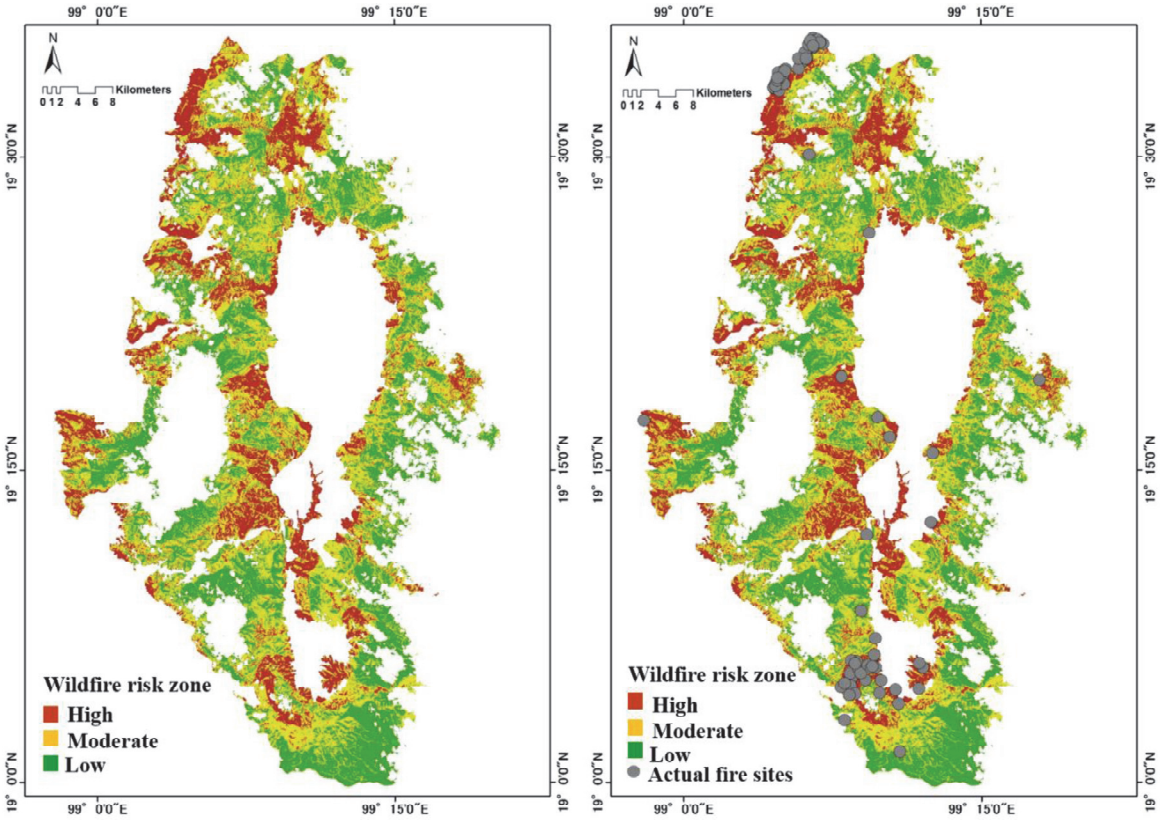

Figure 6.3 (a) Spatial map of estimated wildfire risk and (b) estimated wildfire risk compared with actual wildfire sites

Model validation is an essential part in any natural hazards assessment, where the predictions are compared to a real-world dataset (Begueria, 2006). Therefore, in this study, we used wildfire site data to validate our wildfire risk maps. The number of wildfire sites in each risk class was determined and the fraction of correctly classified instances. The results shown in Figure 6.3b demonstrate that the actual wildfire sites are mostly found in the high risk zone (56) as classified by the model. In addition, the confusion matrix showed that the map achieved 74.67% classification accuracy (Table 6.8). Hence, the proposed model can reliably estimate wildfire risk. The use of the seven factors generated from remotely sensed and GIS data was effective for predicting wildfire-prone areas.

Table 6.8 Accuracy assessment of wildfire risk map based on the confusion matrix

Actual wildfire points	Predicted wildfire points		% of correctly classified instances
	H	M or L	
H	56	0	74.67%
M or L	19	0	

Table 6.9 shows the verified wildfire risk zones corresponding to levels of wildfire risk. The map identified low, moderate, and high risk levels. An area of 18,868 ha (22.15%) was estimated as having high wildfire risk, followed by 42.25% moderate and 35.60% low risk. The high-risk zones were mostly located around the boundary of the national park, adjacent to roads and settlements, and generally had large amounts of leaf fuel.

Table 6.9 Results of the wildfire risk map

WFR value	Description of the value	Number of pixels	Total area prone to wildfire	
			ha	%
0.5 – 1.9	Low-risk wildfire area	209,640	30,330	35.60
2.0 – 2.4	Moderate-risk wildfire area	399,889	35,990	42.25
2.5 – 3.0	High-risk wildfire area	336,998	18,868	22.15
	Total	946,527	85,188	100

Finally, the verified map was overlaid with the 500 m buffer zones created around recreational sites, producing a map of sites susceptible to wildfire risk (Figure 6.4), where the potential effects of wildfires on these sites was evaluated (Table 6.10). The majority of recreational sites had a moderate to high risk of wildfire. Six recreational sites had high risk of being affected by wildfire, especially sites 5, 17, and 22, which had >70% risk. A further seven sites showed moderate risk and only one recreational site was in the low-risk category. Eight recreation sites had negligible probability of wildfire risk. The resulting map contributes to minimizing wildfire impacts at recreational sites and can help in planning and decision making regarding the prevention and control of wildfires. Moreover, the findings of this study can help develop appropriate method for accessing areas prone to wildfires.

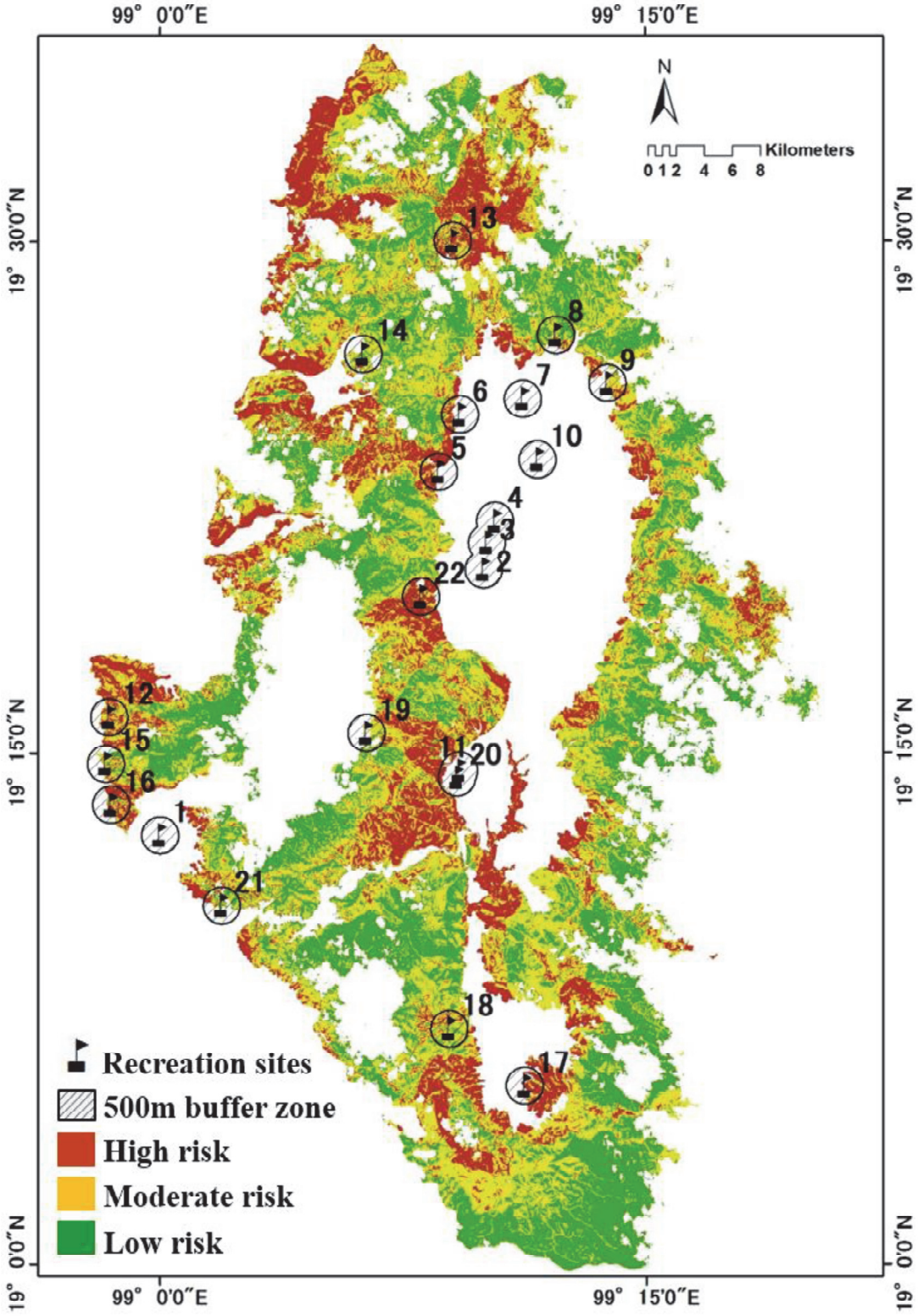

Figure 6.4 Recreational sites overlaid onto zones of estimated wildfire risk

Table 6.10 Evaluation of wildfire potential at recreational sites based on the wildfire risk map

ID (Figure 28b)	Name of recreational site	Type of recreation	Areas prone to wildfire		
			Risk level	%	ha
1	Wat Mae Pang	Temple site	None	0.00	0.00
2	Wat Tham Doi Kham	Temple site	None	0.00	0.00
3	Nam Ru Conservation Forest	Natural learning site	None	0.00	0.00
4	Wat Phra Chao Lan Thong	Temple site	None	0.00	0.00
5	Mae Wa Reservoir	Rest viewpoint	High	77.68	24.75
6	Ban Nong Krok Hot Spring	Hot spring	High	65.63	5.67
7	Wat Phrathat Doi Nang Lae	Temple site	None	0.00	0.00
8	Huai Pa Phlu Waterfall	Waterfall	Low	50.39	35.10
9	Mae Kon Reservoir	Rest viewpoint	Moderate	74.44	29.88
10	Wat Phrathat Jai Klang Muang	Temple site	None	0.00	0.00
11	Mae Pang Reservoir	Rest viewpoint	None	0.00	0.00
12	Huay Kum Nature Trail and Camping site	Nature trail and campsite	Moderate	54.12	40.77
13	Pha Daeng Cave	Cave	High	51.89	40.77
14	Pla Prung Reservoir	Rest viewpoint	Moderate	63.41	37.44
15	The Elephant Training Center, Chiang Dao	The Elephant Training Center	Moderate	72.71	39.33
16	The Elephant Training Center, Mae Ping	The Elephant Training Center	High	53.38	29.88
17	Wat Phrathat Muang Noeng	Temple site	High	76.76	22.59
18	Nang Lae Waterfall	Waterfall	Moderate	60.71	47.7
19	Mon Hin Lai Waterfall	Waterfall	Moderate	65.37	18.18
20	Mon Hin Lai Viewpoint	Rest viewpoint	None	0.00	0.00
21	Sri Lanna office area, Mae Ngad Reservoir	Rest viewpoint and campsite	Moderate	46.92	17.82
22	Doi Jom Hod	Rest viewpoint	High	72.36	56.07

6.4 Conclusions

The present study proposes integrating remote sensing and GIS techniques to identify areas prone to wildfires in forest areas of Sri Lanna National Park, northern Thailand. GIS and remotely sensed data were combined to model wildfire risk based on leaf fuel load, soil moisture, slope, aspect, elevation, distance from roads, and proximity to settlements. The findings revealed that using dNBR as an evaluator was appropriate for rating the wildfire sensitivity of factor subclasses. The selected factors produced a reliable model for mapping wildfire-prone areas, with the resulting risk map showing strong agreement with actual wildfire sites. The leaf fuel load showed the greatest

influence on wildfires, and we proposed soil moisture as a new factor for predicting wildfires. The resulting map of wildfire risk can be used for evaluating recreational sites under threat of potential fires, which is helpful for preventing fire damage at such sites. The findings of this study could improve wildfire risk assessment in Thai national parks and other similar locations. Moreover, the map can be used to develop basic guidelines for relevant local officials and decision makers, to enable appropriate fire management for high-risk areas in order to protect recreational areas from wildfire damage and support the sustainable operation of national parks.

CHAPTER 7

General Discussions and Conclusions

7.1 Discussion and Conclusions

The goals of the study were to assess wildfire risk in Sri Lanna national park using remote sensing and GIS techniques based on several factors associated with wildfire, and then to exploit the assessed wildfire risk to evaluate the wildfire risk at recreational sites. The research sought to combine the factors influencing risk in relation to wildfire in order to model and map wildfire risk at recreational sites. This new approach to establishing a wildfire risk model based on the utilization of remote sensing and GIS data was subsequently used for mapping and assessment of recreational sites with respect to wildfire risk. The factors selected for the proposed wildfire risk model are widely recognized as factors in wildfire occurrence, namely, leaf fuel loads, soil moisture, slope, aspect, elevation, distance from roads and proximity to settlements. Data on some of these factors were obtained from Landsat 8 OLI/TIRS and MODIS images (leaf fuel loads and soil moisture), and these data were integrated with GIS data (slope, aspect, elevation, distance from roads and proximity to settlements) to establish a wildfire risk model for mapping wildfire-prone areas in Sri Lanna national park. This study introduces soil moisture as a factor in a wildfire risk model, and proposes the dNBR to rate wildfire sensitivity for subclasses of each factor. This chapter therefore provides a summary of the main research findings and provides overall conclusions.

The goals of the research were formulated into five objectives as follows:

(6) To estimate the spatial distribution of the leaf fuel load, as one of the selected factors influencing wildfire, by generating a predictive model of leaf fuel load using remotely sensed data based on VIs derived from a Landsat 8 OLI.

(7) To predict the spatial distribution of soil moisture, as one of the selected factors responsible for wildfire occurrence, by establishing a predictive model of soil moisture using remote sensing based on VIs computed from Landsat 8 OLI/TIRS and MODIS data.

(8) To evaluate the use of soil moisture data for wildfire risk assessment.

(9) To map wildfire risk zones based on the integration of several factors contributing to wildfire, including leaf fuel loads, soil moisture, slope, aspect, elevation, distance from roads and proximity to settlements.

(10) To assess wildfire risk at recreational sites using GIS.

In addressing these objectives, the research concentrated particularly on the following hypotheses:

Regarding the first objective, to study the leaf fuel load estimation based on VIs, we hypothesized that:

(ii) The difference in estimated leaf biomass between normal and dry seasons (estimated by a seasonal VI) can express the quantity of the missing leaf biomass, (i.e., the surface leaf fuel load), and that this can be used as a substitute for the actual leaf fuel load in the forest.

Regarding the second objective, to estimate the soil moisture based on VIs, we hypothesized that:

(ii) The relationship between the NDWI and the LST performs as well as, or better than, the relationship between the NDVI and the LST, and can be applied for calculating the TVDI.

(iii) The estimated soil moisture derived from the developed model is directly related to the fuel moisture influencing wildfire occurrence.

In the first objective (chapter 4), we combined field data with remote sensing data from the Landsat 8 OLI to generate an empirical model of leaf fuel load based on a regression approach for mapping the spatial distribution of the leaf fuel load. Firstly, the capabilities of seven VIs extracted from Landsat 8 OLI data were compared with regard to estimating leaf biomass, which is a parameter used in the leaf fuel load prediction model. The model contributes to the assessment of wildfire risk by identifying the spatial distribution of the leaf fuel load to assess wildfire-prone areas across different landscapes. Significant relationships between the calculated standard leaf biomass in the field and the seven VIs showed that the NDVI had the strongest relationship with leaf biomass and could be used to estimate amount of leaf biomass. This is because the NDVI is a greenness index, mainly used to evaluate the density of vegetation. Hence, it can determine and quantify the density of biomass. The NDVI images for normal and dry seasons, (i.e., the seasonal NDVIs) were used to estimate the quantities of seasonal leaf biomass and to detect the missing leaf biomass or the leaf fuel load on the ground surface. Significant correlations were found between the

predicted and calculated leaf fuel loads of the dipterocarp and deciduous forests (Pearson's correlation coefficients > 0.80). This result supports our hypothesis *(i)*, that the predicted leaf fuel load generated from models can be used as a substitute for the leaf fuel load in forest areas. Moreover, the model for leaf fuel load prediction, based on the seasonal NDVI images, achieved accuracies of 80.43% (dipterocarp) and 71.36% (deciduous), using statistical inferences between the predicted and field-derived data. Therefore, the predicted leaf fuel load derived from the developed model could be used as a substitute for estimating the actual leaf fuel load in forested areas, especially in dipterocarp and deciduous forests. It can be stated that a seasonal NDVI can show the changes in the quantity of leaf biomass in different seasons, and that this is associated with the leaf fuel load prediction. Therefore, in chapter 4, a major finding is that the different amounts of leaf biomass in the normal and dry seasons (estimated by a seasonal NDVI) can be used to assess leaf fuel load in the dry season. A seasonal NDVI for both seasons can be appropriately used to estimate the different quantities of leaf biomass, thus establishing the missing leaf biomass that represents the quantity of dead leaves on the ground surface. In other words, the fuel load, derived from changes in leaf biomass, can be estimated based on differences between seasonal NDVIs.

In the second and third objectives (chapter 5), we analyzed remote sensing data from Landsat 8 OLI/TIRS and MODIS to establish an empirical model for soil moisture estimation based on field data with remote sensing data, using a regression approach. This research proposed a possible adaptation and application of NDWI and LST for constructing a TVDI based on the similar design of the triangular NDVI-LST space. The efficiencies of NDVI-LST and NDWI-LST were compared with regard to calculating the TVDI. The results revealed that scatter plots of NDWI-LST exhibit the typical triangular shape of the theoretical TVDI, and offer a more accurate measure of TVDI than NDVI-LST. A relationship between NDWI and LST values is shown under the same theoretical TDVI line as the relationship between NDVI and LST. In addition, values predicted by NDWI-LST are more accurately aligned with the TVDI line (with a strong adjusted $R^2 = 0.84$ at p-value < 0.01). Linear regression analysis, carried out to extract the maximum and minimum LSTs (LST_{max} and LST_{min}), indicate that LST_{max} and LST_{min} defined by the NDWI better fulfill the collinearity requirement than those defined by the NDVI. The reason for the better correlation between the NDWI and LST is that the NDWI values exhibited a quicker response to drought conditions compared to the NDVI values. This is because the NDWI is constructed from the SWIR, which is

more sensitive to moisture than other spectra. As a result, the NDWI shows a better correlation with LST and follows more closely the conceptual TVDI model. This result supports our hypothesis *(ii)*, that the relationship between the NDWI and LST can be used to improve the calculation of the TVDI. This modified index, called $TVDI_{NDWI\text{-}LST}$, was applied together with the NDDI to establish a regression model for soil moisture estimates. The soil moisture model fulfills statistical requirements by achieving 76.65% consistency between the actual soil moisture and estimated soil moisture generated by our model. The soil moisture estimated from the model shows a significant positive correlation with the estimated soil moisture (Pearson's correlation coefficient = 0.67, p-value < 0.01). The statistical tests also support our hypothesis *(iii)*, that the estimated soil moisture is directly related to FMC, and hence, soil moisture should be considered as another indicator for monitoring wildfire-prone areas. Therefore, in chapter 5, the main finding is that the NDWI-LST relationship is better suited to calculating the TVDI, and that the NDWI-LST can be used instead of NDVI–LST when the NDVI–LST relationship is insufficient. Another finding is that the combination of the modified $TVDI_{NDWI–LST}$ and the NDDI has an improved ability to accurately estimate soil moisture. Moreover, the study suggests that including soil moisture as a wildfire factor can improve wildfire risk assessment by acting as a proxy for fuel moisture.

In the fourth and fifth objectives (chapter 6), we clearly brought out the spatial distribution of wildfire risk by integrating remote sensing and GIS techniques for modeling and mapping wildfire risks, to evaluate the potential for fires at recreational sites. The factors selected for a wildfire risk model were computed from both remote sensing and GIS data, and were utilized to generate a GIS wildfire risk model. Firstly, the dNBR was used to rate wildfire sensitivity for subclasses of each factor, and it was found that each subclass rated by the dNBR could be given a score for wildfire sensitivity. This is because those factors assigned a wildfire-sensitivity score by the dNBR followed the same trends as those in the physical theory of wildfire behavior and interactions in the fire environment. All factors with differently rated subclasses were then weighted using pairwise comparison to prioritize their importance with respect to wildfire occurrence. The results revealed that leaf fuel load was the most important factor for wildfires because it contributes to both stages of a wildfire occurrence (ignition and spread/intensity). All weighted factors were later integrated to establish a GIS wildfire risk model. The model correctly classified 74.67% of wildfire instances, confirming that these factors provide a reliable wildfire risk model for mapping wildfire-

prone areas. The mapping showed three different categories of wildfire risk: 35.60% of the study area was predicted to be a high wildfire risk zone, and 42.25% and 22.15% were categorized as moderate and low risk respectively. A map of wildfire risk zones was overlaid with recreation sites in Sri Lanna national park, revealing that six of 22 recreational sites were at high risk from wildfires. Therefore, in chapter 6 the major findings are that a dNBR can be applied to factors to evaluate the levels of wildfire sensitivity, and that seven selected factors can be reliably used to assess the spatial distribution of wildfire risk. Finally, the results of this study can provide a valuable contribution towards reducing wildfire in recreational areas. The application of both remote sensing and GIS techniques in tandem could enhance the effectiveness of wildfire risk assessment and may offer the possibility of short-term estimations, which could be useful in updating decisions on fire pre-suppression and suppression activities.

7.2 Recommendations

In establishing a leaf fuel load model, analysis of a seasonal NDVI can be useful in the short term, for predicting the annual leaf fuel load during the fire season. Therefore, because fuel load is associated with changes in total biomass, a seasonal NDVI can estimate the change in seasonal leaf biomass between the normal and dry seasons, contributing to the determination of the leaf fuel load on the ground surface. However, fire behavior analysis not only estimates fuel load but also uses fuel moisture simulations to minimize the hazards of fire. Therefore, any further study should analyze potential VIs for fuel moisture. Future studies should also address soil moisture as one of the factors used for enhancing estimates of FMC, since soil moisture is shown to be correlated with FMC.

However, the results of this study show that remote sensing and GIS techniques that make use of spatial data integrated with an appropriate algorithm or model can provide information sets that can be used to produce wildfire risk maps. The subjective weight of each factor was developed only for dipterocarp and deciduous forests. Hence, we cannot use the same weighting values for other regions, because the forest types and wildfire characteristics are different in each region. Therefore, to apply this method more generally, the factors affecting the wildfire must be weighted appropriately for each region. Finally, future studies on wildfire risk could be assessed using higher-resolution remote sensing data, and other significant factors driving wildfire occurrence, such as fuel moisture, could be added in order to increase the precision of the wildfire risk assessment.

References

Adab, H., Kanniah, K. and Solaimani, K., 2011. GIS-based probability assessment of fire risk in grassland and forested landscapes of Golestan province, Iran. *IPCBEE*, 19

Adab, H., Kanniah, K. D. and Solaimani, K., 2013. Modeling forest fire risk in the Northeast of Iran using remote sensing and GIS techniques. *Nat Hazards*, 65, 1723–1743. DOI: 10.1007/s11069-012-0450-8

Akaakara, S., Wiriya, K., Tongton. T. and Nuechaiya, P., 2004. Report of fuel characteristics in dry dipterocarp forest at Huai Kha Khaeng wildlife sanctuary. From; http://www.dnp.go.th/forestfire/reserch/allfuel.pdf

Albertz, J., 2007. Einführung in die Fernerkundung Grundlagen der Interpretation von Luftund Satellitenbildern, 3rd edition. Darmstadt: Wissenschaftliche Buchgesellschaft

Ambrosi. V. G., Buechel, S. W., Brass, J. A., Peterson, J. R., Davies, R. H., Kane, R. J. and Spain, S., 1998. An Integration of remote sensing, GIS, and information distribution for wildfire detection and management. *Photogrammetric Engineering & Remote Sensing*, 64(10), 977–985

Anderson, G. L. and Hanson, J. D., 1992. Evaluating hand-held radiometer derived vegetation indices for estimating above ground biomass. *Geocarto International*, 1, 71–78

Anderson, H. E., 1982. Aids to determining fuel models for estimating fire behavior. USDA Forest Service, Intermountain Forest and Range Experiment Station Ogden, UT

Avila-Flores, D., Pompa-Garcia, M., Antonio-Nemiga, X., Rodriguez-Trejo, D., Vargas-Perez, E. and Santillan-Perez, J., 2010. Driving factors for forest fire occurrence in Durango State of Mexico: a geospatial perspective. *Chin Geograph Sci.*, 20(6), 491–497. DOI: 10.1007/s11769-010-0437-x

Bachmann, A. and Allgower, B., 2000. The need for a consistent wildfire risk terminology. In *Neuenschwander*. L., Ryan, K., Golberg, G. (eds.), Crossing the millennium: Integrating spatial technologies and ecological principles for a new age in fire management. The University of Idaho and the International Association of Wildland Fire, Moscow, ID, 67–77

Baimai, V., 2010. Biodiversity in Thailand. *The Journal of the Royal Institute of Thailand (JRIT)*, 2, 107–118

Balling, Jr. R. C., Meyer, G. A. and Wells, S. G., 1992. Relation of surface climate and burned area in Yellowstone National Park. *Agricultural and Forest Meteorology*, 60(3-4), 285–293

Bannari, A., Morin, D., Bonn, F. and Huete, A., 1995. A review of vegetation indices, *Remote Sens. Rev.*, 13, 95–120

Barrett, E. C. and Curtis, L. F., 1992. Introduction to Environmental Remote Sensing, (3rd edition). Chapman & Hall, London

Begueria, S., 2006. Validation and evaluation of predictive models in hazard assessment and risk management. *Nat Hazards*, 37(3), 315–329. DOI: 10.1007/s11069-005-5182-6

Bennett, M., Fitzgerald, S. and Parker B., 2010. Reducing fire risk on your forest property. From; http://knowyourforest.org/sites/default/files/documents/ Reducing_Fire_Risk_full.pdf

Bisson, M., Fornaciai, A., Coli, A., Mazzarini, F. and Pareschi, M., 2008. The vegetation resilience after fire (VRAF) index: development, implementation and an illustration from central Italy. *International Journal of Applied Earth Observation and Geoinformation*, 10, 312–329. DOI: 10.1016/j.jag.2007.12.003

Blaschke, T., 2010. Object based image analysis for remote sensing. *ISPRS Journal of Photogrammetry and Remote Sensing*, 65, 2–16. DOI:10.1016/j.isprsjprs. 2009.06.004

Bond, W. J. and Keeley, J. E., 2005. Fire as global "herbivore": The ecology and evolution of flameble ecosystems. *TREND in Ecology and Evolution*, 20, 387–394

Boyd, S. W., 2006. The TALC model and its application to national parks. In *The Tourism Area Life Cycle: Applications and modifications*, R. W. Butler (ed.), 119–138. Channel View Publications, Clevedon, ISBN: 1845410254

Bracmort, K., 2013. Wildfire fuels and fuel reduction. Congressional Research Service

Brillinger, D. R., 2010. Some examples of the communication of risk and uncertainty. *Environmetrics*, 21, 719–727. DOI: 10.1002/env.1040

Brown, A. A. and Davis, K. P., 1973. Forest fire: Control and use, (2nd edition). McGraw-Hill Book Co, Inc, New York, USA

Brown, J. K., Kapler, S. J. (eds.), 2000. Wildland fire in ecosystems: effects of fire on flora. Gen. Tech. Rep. RMRS-GTR-42-vol. 2. Ogden, UT: U.S. Department of Agriculture, Forest Service, Rocky Mountain Research Station

Brown, J. K., Oberheu, R. D. and Johnston, C. M., 1982. Handbook for inventorying surface fuels and biomass in the interior west. Gen. Tech. Rep. INT-129. Ogden, UT: U.S. Department of Agriculture, Forest Service, Intermountain Forest and Range Experiment Station

Burapapol, K. and Nagasawa R., 2016a. Mapping soil moisture as an indicator of wildfire risk using Landsat 8 images in Sri Lanna national park, Northern

Thailand. *Journal of Agricultural Science*, 8(10), 107–119. DOI: 10.5539/jas.v8n10p107

Burapapol, K. and Nagasawa, R., 2016b. Mapping wildfire fuel load distribution using Landsat 8 Operational Land Imager (OLI) data in Sri Lanna national park, Northern Thailand, *The Japanese Agricultural Systems Society (J.A.S.S)*, 32(4), 133–145

Burgan, R. E., Klaver, R. W. and Klaver, J. M., 1998. Fuel models and fire potential from satellite and surface observations. *Int. J. Wildland Fire*, 8(3), 159–170

Burrough, P. A., 1986. Principles of Geographic Information Systems for land resource assessment. Monographs on Soil and Resources Survey, 12. Oxford Science Publications, New York, USA

Carlson, T. N., 2007. An overview of the triangle method for estimating surface evapotranspiration and soil moisture from satellite imagery. *Sensors*, 7, 1612–1629. DOI: 10.3390/s7081612

Carlson, T. N., Gillies, R. R. and Perry, E. M., 1994. A method to make use of thermal infrared temperature and NDVI measurements to infer surface soil water content and fractional vegetation cover. *Remote Sensing Reviews*, 9, 161–173

Castro, R. and Chuvieco, E., 1998. Modeling forest fire danger from geographic information systems. *Geocarto Int*, 13(1), 15–23

Ceccato, P., Gobron, N., Flasse, S., Pinty, B. and Tarantola, S., 2002. Designing a spectral index to estimate vegetation water content from remote sensing data: Part 1 Theoretical approach. *Remote Sensing of Environment*, 82, 188-197. DOI: 10.1016/S0034-4257(02)00037-8

Chafer, C. J., Noonan, M. and Macnaught, E., 2004. The post-fire measurement of fire severity and intensity in the Christmas 2001 Sydney wildfires. *International Joural of Wildland Fire*, 13, 227–240

Chang, K., 2014. Introduction to Geographic Information Systems, 7th edition. McGraw-Hill, New York, USA

Chen, S., Wen, Z., Jiang, H., Zhao, Q., Zhang, X. and Chen, Y., 2015. Temperature vegetation dryness index estimation of soil Moisture under different tree species. *Sustainability*, 7, 11401–11417. DOI: 10.3390/su70911401

Chmura, D. J., Anderson, P. D., Howe, G. T., Harrington, C. A., Halofsky, J. E., Peterson, D. L., et al., 2011. Forest responses to climate change in the northwestern United States: Ecophysiological foundations for adaptive management. *Forest Ecology and Management*, 261, 1121–1142. DOI: 10.1016/j.foreco.2010.12.040

Chuvieco, E. and Congalton, R. C., 1989. Application of remote sensing and geographic information systems to forest fire hazard mapping. *Remote Sens. Environ*, 29, 147–159

Chuvieco, E., Coceroa, D., Rian, D., Martinc, P., Martı´nez-Vegac, J., Rivad, J. D. and Pe´rez, F., 2004. Combining NDVI and surface temperature for the estimation of live fuel moisture content in forest fire danger rating. *Remote Sensing of Environment*, 92, 322–331. DOI: 10.1016/j.rse.2004.01.019

Colwell, R. N., 1983. Manual of remote sensing volume I: Theory, instruments and techniques. American Society of Photogrammetry

Congalton, R. G., 1991. A review of assessing the accuracy of classification of remotely sensed data. *Remote Sensing of Environment*, 37, 35–46

Cracknell, A. P. and Hayes, L., 2007. ntroduction to Remote Sensing, 2nd edition. Taylor & Francis Group, Boca Raton, Florida

Curran, P. J., Dungan, J. L. and Gholz, H, L., 1992. Seasonal LAI in slash pine estimated with landsat TM. *Remote Sensing of Environment*, (1), 3–13

Curry, J. R. and Fons, W. L., 1938. Rate of spread of surface fires in the ponderosa pine type of California. *J. Agr. Res.* 57, 239–267.

Curry, J. R. and Fons, W. L., 1940. Forest fire behavior studies. 219–225. Mech. Engng, New York, USA

Darmaran, M., Aniya, M. and Tsuyuki, S., 2001. Forest fire hazard model using remote sensing geographic information system: Toward understanding of land and forest degradation in lowland areas of East Kalimantan, Indonesia. In *Paper presented at the 22nd Asian Conference on remote sensing*, Singapore, on 5-9 November 2001

DeBano, L. F., Neary, D. G. and Ffolliott, P. F., 1998. Fire's effects on ecosystems. John Wiley & Sons Inc., New York, USA

DeBano, L. F., Neary, D. G. and Ffolliott, P. F., 2005. Soil physical properties. D. G. Neary, K. C. Ryan and L. F. DeBano (eds.), Wildland fire in ecosystems effects of fire on soil and water, 21–55. USDA Forest Service Gen. Tech. Rep, USA

Deeming, J. E. and Brown, J. K., 1975. Fuel models in the national fire-danger rating system. J*ournal of Forestry*, 73(6), 347–350(4)

Deeming, J. E., Burgan, R. E. and Cohen, J. D., 1977. The national fire danger rating system. USDA Forest Service, Intermountain Forest and Range Experiment Station Ogden, UT

Desbois, N., Deshayes, M. and Beudoin, A., 1997. Protocol for fuel moisture content measurements. In *a review of remote sensing methods for the study of large*

wildland fires, E. Chuvieco (ed.), Departamento de Geografía, Universidad de Alcalá: Alcalá de Henares, Spain, 61–72

Dimitrakopoulos, A. P., Bemmerzouk, A. M. and Mitsopoulos, I. D., 2011. Evaluation of the canadian fire weather index system in an eastern mediterranean environment. *Meteorol. Appl.*, 18, 83–93. DOI: 10.1002/met.214

DNP (Department of National Parks, Wildlife and Plant Conservation), 2003, Sri Lanna National Park's area management master plan. Ministry of Natural Resources and Environment, Bangkok, Thailand

DNP (Department of National Parks, Wildlife and Plant Conservation), 2014. Statistical data 2014. Bangkok, Thailand. From; http://www.dnp.go.th/ statistics/2557/stat2557.asp, Thailand.

Dong, X., Li-Min, D., Guo-Fan, S., Lei, T. and Hui, W., 2005. Forest fire risk zone mapping from satellite images and GIS for Baihe forestry bureau, Jilin, China. *J For Res*, 16(3), 169–174

Eagles, P. F. J., McCool, S. F. and Haynes, C., 2002. Sustainable tourism in protected areas: Guidelines for planning and management. Best practice protected area guidelines services No. 8. World Commission on Protected Areas, IUCN (The World Conservation Union), Cambridge

Eller, H. and Denoth, A. A., 1996. Capacitive soil moisture sensor. *Journal of Hydrology*, 185, 137–146

Escuin, S., Navarro, R. and Fernández, P., 2008. Fire severity assessment by using NBR (Normalized Burn Ratio) and NDVI (Normalized Difference Vegetation Index) derived from LANDSAT TM/ETM images. *International Journal of Remote Sensing*, 29(4), 1053–1073. DOI: 10.1080/01431160701281072

ESRI, 1990. Understanding GIS: The ARC/INFO method. Redlands, CA: Environmental Systems Research Institute (ESRI)

FAO, 2006. Fire management: voluntary guidelines. Principles and strategic actions. Food and Agriculture Organization of the United Nations. From; http://www.fao.org/docrep/009/j9255e/j9255e00.htm/

Fennell, D., and Smale, B., 1992. Ecotourism and natural resource protection. *Tourism Recreation Research*, 17 (1), 21–32. DOI: 10.1080/02508281.1992.11014638

Finney, M. A., 2005. The challenge of quantitative risk analysis for wildland fire. Forest ecology and management, 211, 97–108. DOI: 10.1016/j.foreco.2005.02.010

Finney, M. A., 2005. The challenge of quantitative risk analysis for wildland fire. *Ecol Manag.*, 211, 97–108. DOI:10.1016/j.foreco.2005.02.010

Flannigan, M. D., Stocks, B. J. and Wotton, B. M., 2000. Climate change and forest fires. *Science of the Total Environment*, 262(3), 221–229

Forest Fire Control Division, 2011. Fire fighting using MODIS hotspots in Thailand. DNP, Thailand. In *Asian Forum on Carbon Update 2011*, Bandung, Indonesia

Forest Fire Control Division, 2015, Statistics of fire 2015. DNP, Thailand. From; http://www.dnp.go.th/forestfire/2546/firestatistic%20Th.htm

Forest Fire Control Division, 2016. Statistics of fire. DNP, Thailand

Franklin, S. E., 2001. Remote sensing for sustainable forest management. Boca Raton, Florida: CRC Press

Fried, J. S. , Gilless, J. K., Riley, W. J., Moody, T. J., Blas de, C. S., Hayhoe, K., Moritz, M., Stephens, S., Torn. M., 2008. Predicting the effect of climate change on wildfire behavior and initial attack success. *Climatic Change*, vol. 87(1), 251-264. DOI 10.1007/s10584-007-9360-2

Fried, J. S., Torn, M. S. and Mills, E., 2004. The impact of climate change on wildfire severity: a regional forecast for northern California. *Climatic Change*, 64(1–2), 169–191

Gao, B. C., 1996. NDWI-A normalized difference water index for remote sensing of vegetation liquid water from space, *Remote Sensing of Environment*, 58, 257–266

Gao, Z., Gao, W. and Chang, N. B., 2011. Integrating temperature vegetation dryness index (TVDI) and regional water stress index (RWSI) for drought assessment with the aid of LANDSAT TM/ETM+ images. *International Journal of Applied Earth Observation and Geoinformation*, 13, 495–503. DOI: 10.1016/j.jag.2010.10.005

Gardner, W. H., 1986. Water content. In *Methods of soil analysis Part 1. Physical and Mineralogical Methods*, (2nd edition), A. Klute (ed.). Soil Science Society of America, Inc., Madison, Wisconsin, USA

Gibson, P. J. and Power, C. H., 2000. Introductory Remote Sensing: Principles and Concepts. Andoyer: Routledge, London

Gissibl, B., Höhler, S. and Kupper, P., 2012, Civilizing nature, national Parks in global historical perspective, Berghahn, Oxford

Goetz, S. J., 1997. Multisensor analysis of NDVI, surface temperature and biophysical variables at a mixed grassland site. *International Journal of Remote Sensing*, 18(1), 71–94. DOI: 10.1080/014311697219286

Gouveia, C. M., Bastos, A., Trigo, R. M. and Daamara1, C. C., 2012. Drought impacts on vegetation in the pre- and post-fire events over Iberian Peninsula. *Natural Hazards and Earth System Sciences*, 12, 3123–3137

Goward, S. N., Xue, Y. K. and Czajkowski, K. P., 2002. Evaluating land surface moisture conditions from the remotely sensed temperature/vegetation index measurements: An exploration with the simplified simple biosphere model. *Remote Sensing of Environment*, 79(2-3), 225–242. DOI: 10.1016/S00344257 (01)00275-9

Gu, Y., Brown, J. F., Verdin, J. P. and Wardlow, B., 2007. A five year analysis of MODIS NDVI and NDWI for grassland drought assessment over the central great plains of United States. *Geophysical Research Letters*, 34(6). DOI: 10.1029/2006GL029127

Gu, Y., Hunt, E., Wardlow, B., Basara, J. B., Brown, J. F. and Verdin J. P., 2008. Evaluation of MODIS NDVI and NDWI for vegetation drought monitoring using Oklahoma Mesonet soil moisture data. *Geophysical Research Letters*, 35, 1–5. DOI: 10.1029/2008GL035772

Harmon, M., 1982. Fire history of the westernmost portion of Great Smoky Mountains National Park. Bull Torrey Bot Club, 74–79

Haynes, R. and Cleaves, D., 1999. Uncertainty, risk, and ecosystem management. In *Ecological Stewardship, Volume III*. W.T. Sexton, A.J. Malk, R.C. Szaro, N.C. Johnson (eds.), 413–429. Elsevier Science Ltd: Oxford, UK

Hazaymeh, K. and Hassan, Q. K., 2015. Fusion of MODIS and Landsat-8 Surface Temperature Images: A New Approach. *PloS One*, 10(3), e0117755. DOI: 10.1371/journal.pone.0117755

Hillel, D., 1998. Environmental soil physics, 1st edition. Academic Press, San Diego, California, USA

Huete, A. R., 1988. A soil adjusted vegetation index (SAVI). *Remote Sensing of Environment*, 25(3), 295–309

Ishimura, A., Shimizu, Y., Rahimzadeh, B. P. and Omasa, K., 2011. Remote sensing of Japanese beech forest decline using an improved Temperature Vegetation Dryness Index (iTVDI). *iForest-Biogeosciences and Forestry*, 4, 195–199. DOI: 10.3832/ifor0592-004

IUCN, 1994. Guidelines for Protected Area Management Categories. International Union for Conservation of Nature and Natural Resources. Cambridge

Iwan, S., Mahmud, A. R., Mansor, S., Shariff, A. R. M. and Nuruddin, A. A., 2004. GIS-grid-based and multi-criteria analysis for identifying and mapping peat swamp forest fire hazard in Pahang, Malaysia. *Disaster Prev Manag*, 13(5), 379–386. DOI: 10.1108/09653560410568507

Jackson, R. D. and Huete, A. R., 1991. Interpreting vegetation indices. *Preventive Veterinary Medicine*, 11, 185–200

Jaiswal, R. K., Krishnamurthy, J. and Mukherjee, S., 2005. Regional study for mapping the natural resources prospect & problem zones using remote sensing and GIS. *Geocarto Int.*, 20(3), 21-31. DOI: 10.1080/10106040508542352

Jaiswal, R. K., Mukherjee, S., Raju, K. D. and Saxena, R., 2002. Forest fire risk zone mapping from satellite imageryand GIS. *Int J Appl Earth Obs Geoinf*, 4(1),1–10

Jaiswal, R. K., Mukherjee, S., Raju, K. D. and Saxena. R., 2002. Forest fire risk zone mapping from satellite imagery and GIS. *Int J Appl Earth Obs Geoinf*, 4(1), 1–10

Jiang, Z., Huete, A.R., Didan, K., and Miura, T., 2008. Development of a two-band enhanced vegetation index without a blue band. *Remote Sensing of Environment*, 112, 3833–3845. DOI: 10.1016/j.rse.2008.06.006

Jordan, C. F., 1969. Derivation of leaf-area index from quality of light on the forest floor. *Ecology*, 50(4), 663–666

Kaleita, A. L., Tian, L. F. and Hirschi, M. C., 2005. Relationship between soil moisture content and soil surface reflectance. *American Society of Agricultural Engineers*, 48(5), 1979–1986. DOI: 10.13031/2013.19990

Key, C. H. and Benson, N. C., 2006, Landscape assessment (LA). In *FIREMON: Fire effects monitoring and inventory system*. D. C. Lutes, R. E. Keane, J. F. Carati, C. H. Key, N. C. Benson and L. J. Gangi (eds). USDA Forest Service, Rocky Mountains Research Station General Technical Report

Kozlowski, T. T. and Pallardy, S. G., 2002. Acclimation and adaptive responses of woody plants to environmental stresses. *The Botanical Review*, 68(2), 270–334

Krawchuk, M. A., Moritz, M. A., 2011. Constraints on global fire activity vary across a resource gradient. *Ecology,* 92, 121–132

Krueger, E. S., Ochsner, T. E., Engle, D. M., Carlson, J. D., Twidwell, D., and Fuhlendorf, S. D., 2015. Soil moisture affects growing-season wildfire size in the Southern Great Plains. *Soil Science Society of America Journal*, 79, 1567–1576. DOI: 10.2136/sssaj2015.01.0041

Krueger, E. S., Ochsner, T. E., Engle, D. M., Carlson, J. D., Twidwell, D. and Fuhlendorf, S. D., 2015. Soil moisture affects growing-season wildfire size in the Southern Great Plains. *Soil Science Society of America Journal*, 79, 1567–1576. DOI: 10.2136/sssaj2015.01.0041

Kummer, D. M. and Turner, B. L., 1994. The human causes of deforestation in Southeast Asia. BioSci., 44, 323–323. DOI: 10.2307/1312382

Kuntz, S. and Karteris, M., 1995. Fire risk modelling based on satellite remote sensing and GIS. *EARSeL ADVANCES IN REMOTE SENSING*, 4(3), 39–46

Landsberg, T. D., 1997. Fire and forests: fire-a good servant or a bad master. In *Proceedings of XI World Forestry Congress*, Antalya, Turkey on 13–22 October 1997, 1, 209–214

Laurance, W. F., Goosem, M. and Laurance, S. G. W., 2009. Impacts of roads and linear clearings on tropical forests. *Trends Ecol Evol.*, 24(12), 659–669. DOI: 10.1016/j.tree.2009.06.009

Lein, J. K. and Stump, N. I., 2009. Assessing wildfire potential within the wildland–urban interface: a southeastern Ohio example. *Appl Geogr*, 29(1), 21–34. DOI: 10.1016/j.apgeog.2008.06.002

Lloyd, C., 2010. Spatial data analysis: An introduction for GIS users. Oxford University Inc., New York, USA

Lopez-Garcia, M. J. and Caselles, V., 1991. Mapping burns and natural Reforestation using thematic mapper data. *Geocarto International*, 1, 31–37

Malczewski, J., 1999. GIS and Multi criteria decision analysis, 137–269. John Wiley and Sons Inc., New York, USA

Mallarach, J. M. (ed.), 2008. Protected landscapes and cultural and spiritual values. Vol 2, In *the series values of protected landscapes and seascapes*, IUCN, GTZ and Obra Social de Caixa Catalunya. Kasparek Verlag, Heidelberg

Mallick, K., Bhattacharya, B. K. and Patel, N. K., 2009. Estimating volumetric surface moisture content for cropped soils using a soil wetness index based on surface temperature and NDVI. *Agricultural and Forest Meteorology*, 149, 1327–1342. DOI: 10.1016/j.agrformet.2009.03.004

Mark, A. C. and Kevin, C. R., 2009. Fire and fire ecology: Concepts and principles. In *Tropical fire ecology climate change, land use and ecosystem dynamics*. Springer Berlin Heidelberg, New York, USA

McArthur, A. G., 1968. Fire Behaviour in Eucalypt Forests. Leaflet No. 107, 9th Commonwealth Forestry Conference, India

Mouillot, F., Rambal, S. and Joffre, R., 2002. Simulating climate change impacts on fire frequency and vegetation dynamics in a mediterranean-type ecosystem. *Global Change Biology*, 8(5), 423–437

Myneni, R. B., Hall, F. G., Sellers, P., and Marshak, A. L., 1995. The interpretation of spectral vegetation indexes. *IEEE Transactions on Geoscience and Remote Sensing*, 33(2), 481–486

Neary, D. G., Ryan, K. C. and DeBano, L. F. (eds.), 2005. Wildland fire in ecosystems: effects of fire on soils and water. Gen. Tech. Rep. RMRS-GTR-42-vol.4. Ogden, UT: U.S. Department of Agriculture, Forest Service, Rocky Mountain Research Station

Nemani, R., Pierce, L., Running, S. and Goward, S., 1993. Developing satellite-derived estimates of surface moisture status. *Journal of Applied Meteorology*, 32, 548–557

Nepstad, D., Carvalho, G., Cristina, B. A., Alencar, A., Paulo, C. J., Bishop, J., et al., 2001. Road paving, fire regime feedbacks, and the future of Amazon forests. *For Ecol Manage.*, 154(3), 395–407

Newsome, D., Moore, S. A. and Dowling, R. K., 2002. Natural area tourism: Ecology, impacts and management. Channel View Publications, Sydney

Noonan, E. K., 2003. A coupled model approach for assessing fire hazard at Point Reyes national Seashore: FlamMap and GIS. In *Second international wildland fire ecology and fire management congress and fifth symposium on fire and forest meteorology*. Orlando, FL. American Meteorological Society, 127–128

Noonan-Wright, E. K., Vaillant, N. M. and Reiner, A. L., 2013. The effectiveness and limitations of fuel modeling using the fire and fuels extension to the forest vegetation simulator. *Forest Science*, 60(2), 231–240. DOI: 10.5849/forsci.12-062

Office of National Park, 2017. Thai natioal park database. DNP, Thailand

Ogawa, H., Yoda, K., Ogino, K. and Kira, T., 1965. Comparative ecological studies on three main type of forest vegetation in Thailand II. Plant biomass, Nature and Life in Southeast Asia, 4, 49–80

Ogino, K., Ratanawang, D., Tsustumi, T. and Shidei, T., 1967. The primary product of tropical forest in Thailand. The Southeast Asia studies, 5, 121–154

Parisien, M. A. and Moritz, M. A., 2009. Environmental controls on the distribution of wildfire at multiple spatial scales. *Ecological Monographs*, 79, 127–154

Patel, N. R., Anapashsha, R., Kumar, S., Saha, S. K. and Dadhwal, V. K., 2009. Assessing potential of MODIS derived temperature/vegetation condition index (TVDI) to infer soil moisture status. *International Journal of Remote Sensing*, 30, 23–39. DOI: 10.1080/01431160802108497

Pfeifer, M., Gonsamo, A., Disney, M., Pellikka, P. and Marchant, R., 2012. Leaf area index for biomes of the Eastern Arc MINountains: Landsat and SPOT observations along precipitation and altitude gradients. *Remote Sensing of Environment*, 118, 103–115. DOI: 10.1016/j.rse.2011.11.009

Price, J. C., 1990. Using spatial context in satellite data to infer regional scale evapotranspiration. *IEEE Transactions on Geoscience and Remote Sensing*, 28, 940–948

Pyne, S. J., Andrews, P. L. and Laven R. D., 1996. Introduction to wildland fire: Fire behavior. John Wiley & Sons, Inc., New York, USA

Pyne, S., Andrews, P. and Laven, R., 1996. Introduction to wildland fire. Wiley, New York, USA

Qi, Y., Dennison, P. E., Spencer, J. and Riaño, D., 2012. Monitoring live fuel moisture using soil moisture and remote sensing proxies. *Fire Ecology*, 8, 71–87. DOI: 10.4996/fireecology.0803071

Rego, F. C., 1992. Land use changes and wildfires. In *Responses of Forest Ecosystems to Environmental Changes*, A. Teller, P. Mathy, and J. N. Jeffers (eds.), 367–373. Elsevier, London, UK

Renza, D., Martinez, E., Arquero, A. and Sanchez, J., 2010. Drought estimation maps by means of multidate Landsat fused images. *Remote Sensing for Science, Education, and Natural and Cultural Heritage*, 775–782

Richardson, A. J., and Wiegand, C. L., 1977. Distinguishing vegetation from soil background information. *Photogramnetric Engineering and Remote Sensing*, 43(12), 1541–1552

Richardson, J. and Everitt, J. H., 1992. Using spectral vegetation indices to estimate rangeland productivity. *Geocarto International*, 1, 63–69

Rothermel, R. C., 1972. A mathematical model for predicting fire spread in wildland fuels. Research paper, INT-115. USDA Forest Service, Intermountain Research Station, Ogden, Utah, USA

Rothermel, R. C., 1972. A mathematical model for predicting fire spread in wildland fuels. In USDA Forest Service Research Paper. Ogden, Utah, USA

Rothermel, R. C., 1983. How to predict the spread and intensity of forest and range fires, USDA Forest Service, Intermountain Forest and Range Experiment Station Ogden, Utah, USA

Rothermel, R. C., 1991. Predicting behavior and size of crown fires in the Northern Rocky Mountains. Research Paper INT-438, USDA Forest Service, Intermountain Research Station

Rouse, J. W., Haas, R. H., Deering, D. W. and Schell, J. A., 1973. Monitoring the vernal advancement and retrogradation (green wave effect) of natural vegetation, In *NASA/GSFC Type III Final Report*, Greenbelt, Maryland, USA

Saaty, T. L., 1980. The analytic hierarchy process. Planning, piority setting Resource alllocation. McGraw-Hill, New York, USA

Sandholt, I., Rasmussen, K. and Andersen, J., 2002. A simple interpretation of the surface temperature/vegetation index space for assessment of surface moisture status. *Remote Sensing of Environment*, 79, 213–224. DOI: 10.1016/S0034-4257(01)00274-7

Santi, P., Cannon, S. and DeGraff, J., 2013. Wildfire and landscape change. *Treatise on Geomorphology*, 13, 262–287

Schoenberg, F. P., Peng, R., Huang, Z. and Rundel, P., 2003. Detection of non-linearities in the dependence of burn area on fuel age and climatic variables. *International Journal of Wildland Fire*, 12(1), 1–6

Scott, J. H. and Burgan, R. E., 2005. Standard fire behavior fuel models: A comprehensive set for use with Rothermel's surface fire spread model. USDA Forest Service, Rocky Mountain Research Station

Scott, J. H. and Reinhardt, E. D., 2001. Assessing crown fire potential by linking models of surface and crown fire behavior. Department of Agriculture, Forest Service, Rocky Mountain Research Station

Shugart, H. H., Caylor, K. K., Hely, C., Swap, R. J. and Dowty, P. R., 2006. Dynamic climate and land-use change in woodland and savana ecosystems of subtropical Africa. In *Emerging Threats to Tropical Forests*, 53–66. The University of Chicaco, USA

Siachalou, S., Doxani, G. and Tsakiri-Strati, M., 2009. Integrating remote sensing processing and GIS to fire risk zone mapping: a case study for the Seih-Sou forest of Thessaloniki. In *Proceeding of ICC 2009*, Santiago de Chile.

Sikder, I. U., Mal-Sarkar, S. and Mal, T. K., 2006. Knowledge-based risk assessment under uncertainty for species invasion. Risk Analysis, 26(1), 239–252. DOI: 10.1111/j.1539-6924.2006.00714.x

Sikder, I. U., Mal-Sarkar, S. and Mal, T. K., 2006. Knowledge-based risk assessment under uncertainty for species invasion. *Risk Analysis*, 26(1), 239–252. DOI: 10.1111/j.1539-6924.2006.00714.x

Star, J., and Estes, J., 1990. Geographic Information Systems: An introduction. Englewood Cliffs, NJ, Prentice Hall

Steininger, M. K., 2000. Satellite estimation of tropical secondary forest aboveground biomass data from Brazil and Bolivia. *International Journal of Remote Sensing*, 21, 1139–1157. DOI: 10.1080/014311600210119

Swain, P. H. and Davis, S. M., 1979. Remote sensing; The quantitative approach. McGraw-Hill International Book Company, New York

Thakur, A. K. and Singh, D., 2014. Forest fire risk zonation using geospatial techniques and analytic hierarchy process in Dehradun district. *Universal Journal of Environmental Research and Technology*, 4(2), 82–89

The Seub Nakhasathien foundation, 2017. Report of forest situation in Thailand. From; http://seub.or.th/

Timothy, R. N., 2014. Fire ecology and insect ecology: Insects, fire and conservation. Springer Cham Heidelberg New York Dordrecht London

Tribe, J., 2011. The economics of recreation, leisure, and tourism, 4th edition. Elsevier, Oxford, England

Tucker, C. J., 1979. Red and photographic infrared linear combinations for monitoring vegetation, *Remote Sensing of Environment*, 8, 127–150

USGS, 2013. Using the USGS Landsat 8 product. United States Geological Survey, USA. From; http://landsat.usgs.gov/ Landsat8_Using_Product.php

Vadrevu, K. P., Eaturu, A. and Badarinath, K. V. S., 2010. Fire risk evaluation using multicriteria analysis–a Case Study. *Environ Monit Assess*, 166(1). 223–239. DOI: 10.1007/s10661-009-0997-3

Vasilakos, C., Kalabokidis, K., Hatzopoulos, J. and Matsinos, I., 2009. Identifying wildland fire ignition factors through sensitivitya of a neural network. *Nat Hazards*, 50(1), 125–143. DOI: 10.1007/s11069-008-9326-3

Vasilakos, C., Kalabokidis, K., Hatzopoulos, J., Kallos, G. and Matsinos, Y., 2007. Integrating new methods and tools in fire danger rating. *International Journal of Wildland Fire*, 16, 306–316. DOI: 10.1016/j.jag.2007.12.003

Veblen, T. T., Kitzberger, T. and Donnegan. J., 2000. Climatic and human influences on fire regimes in ponderosa pine forests in the Colorado Front Range. *Ecol Appl.*, 10(4), 1178–1195

Velez, R., 1993. High intensity forest fires in the Mediterranean Basin: natural and socioeconomic causes. *Disaster Manage*, 5, 16–20

Vincini, M., Frazzi, E. and D'Alessio, P., 2007. Comparison of narrow-band and broad-band vegetation indices for canopy chlorophyll density estimation in sugar beet. In *Precision Agriculture '07 : Proceedings of the 6th European Conference on Precision Agriculture*, J. V. Stafford (ed.), Wageningen Academic Publishers, The Netherlands, 189–196

Vincini, M., Frazzi, E. and D'Alessio, P., 2008, A broad-band leaf chlorophyll vegetation index at the canopy scale. *Precision Agriculture*, 9, 303–319. DOI: 10.1007/s11119-008-9075-z

Wagle, R. F. and Eakle, T. W., 1979. A controlled burn reduces the impact of a subsequent wild fire in a ponderosa pine vegetation type. *Forest Science*, 25, 123–129

Wagtendonk, J. W. V. and Root, R. R., 2003. The use of multi-temporal Landsat normalized difference vegetation index (NDVI) data for mapping fuel models in Yosemite National Park, USA. *International Journal of Remote Sensing*, 24(8), 1639–1651. DOI: 10.1080/01431160210144679

Wang, L., Qu, J. J., Zhang, S., Hao, X. and Dasgupta, S., 2007. Soil moisture estimation using MODIS and ground measurements in eastern China. *International Journal of Remote Sensing*, 28(6), 1413–1418. DOI: 10.1080/01431160601075525

Weaver, D., 2001. Ecotourism. John Wiley and Sons, Sydney

Weise, D. R. and Biging, G. S., 1997. A qualitative comparison of fires models incorporating wind and slope effects. *For Sci*, 43(2), 170–180

Weng, Q., Fu, P. and Gao, F., 2014. Generating daily land surface temperature at Landsat resolution by fusing Landsat and MODIS data. *Remote Sensing of Environment*, 145, 55–67. DOI: 10.1016/j.rse. 2014.02.003

Worboys, G. L., Lockwood, M. and De Lacy, T., 2001. Protected area management: Principles and practice. Oxford University Press, London

Yakubu, I., Mireku-Gyimah, D. and Duker, A. A., 2013. Multi-spatial criteria modelling of fire risk and hazard in the West Gonja Area of Ghana. *Research Journal of Environmental and Earth Sciences*, 5(5), 267–277

Yebra, M., Dennison, P. E., Chuvieco, E., Riano, D., Zylstra, P., Hunt Jr., E. R., et al., 2013. A global review of remote sensing of live fuel moisture content for fire danger assessment: Moving towards operational products. *Remote Sensing of Environment*, 136, 455–469. DOI: 10.1016/j.rse.2013.05.029

Yongqiang, L., John, S. and Scott, G., 2010. Wildfire potential evaluation during a drought event with a regional climate model and NDVI. *Ecological Informatics*, 5, 418–428. DOI: 10.1016/j.ecoinf.2010.04.001

Young, J. A. T., 1986. A U.K Geographic information system for environmental mornitoring: Resource planning & management capable of integrating & using satellite remotely sensed data. The remote sensing society, Department of Geography, University of Nottingham, UK

Yunis, E., 2003. Sustainable tourism and poverty alleviation, World tourism organization, Spain. From; http://www.world-toursim.org

Zhang, N., Hong, Y., Qin, Q. and Zhu, L., 2013. Evaluation of the visible and shortwave infrared drought index in China. *International Journal of Disaster Risk Science*, 4(2), 68–76. DOI: 10.1007/s13753- 013-0008-8

Zheng, D., Rademacher J., Chen J., Crow T. and Bresee M., 2004. aboveground biomass using Landsat 7 ETM+ data across a managed landscape in northern Wisconsin, USA. *Remote Sensing of Environment*, 93, 402–411. DOI: 10.1016/j.rse.2004.08.008

List of Publications

CHAPTER 4

Author : Burapapol Kansuma, Ryota Nagasawa

Title : Mapping Wildfire Fuel Load Distribution using Landsat 8 Operational Land Imager (OLI) Data in Sri Lanna National Park, Northern Thailand

Journal : Journal of The Japanese Agricultural Systems Society (J.A.S.S), 2016, Vol.32, No.4, pp. 133–145.

CHAPTER 5

Author : Burapapol Kansuma, Ryota Nagasawa

Title : Mapping Soil Moisture as an Indicator of Wildfire Risk Using Landsat 8 Images in Sri Lanna National Park, Northern Thailand

Journal : Journal of Agricultural Science, 2016, Vol.8, No.10, pp. 107–119. DOI: 10.5539/jas.v8n10p107

CHAPTER 6

Author : Burapapol Kansuma, Ryota Nagasawa

Title : Assessment of Wildfire Risk at Recreational Sites in Sri Lanna National Park, Chiang Mai, Northern Thailand, using Remote Sensing and GIS Techniques

Journal : International Journal of Geoinformatics, 2017, Vol.13, No.3, pp.13-24.

Appendix

Appendix 1 Characteristic of the study area in dry season

Appendix 2 Examples of sample plots (a) dipterocarp and (b) deciduous plots.

(a) Dipterocarp plots

(b) Deciduous plots

Appendix 3 Equipments for field survey

Equipments for field survey included;

- Handheld GPS (Oregon550TC, GARMIN, USA)
- Haga altimeter
- Clinometer
- Diameter tape
- Compass

Appendix 4 Leaf biomass measured from the study area

Measurement of tree stem circumference at 1.3 m height from ground surface or at breast height

Measurement of tree height using haga altimeter and clinometer

Appendix 5 Leaf fuel loads collected from the study area

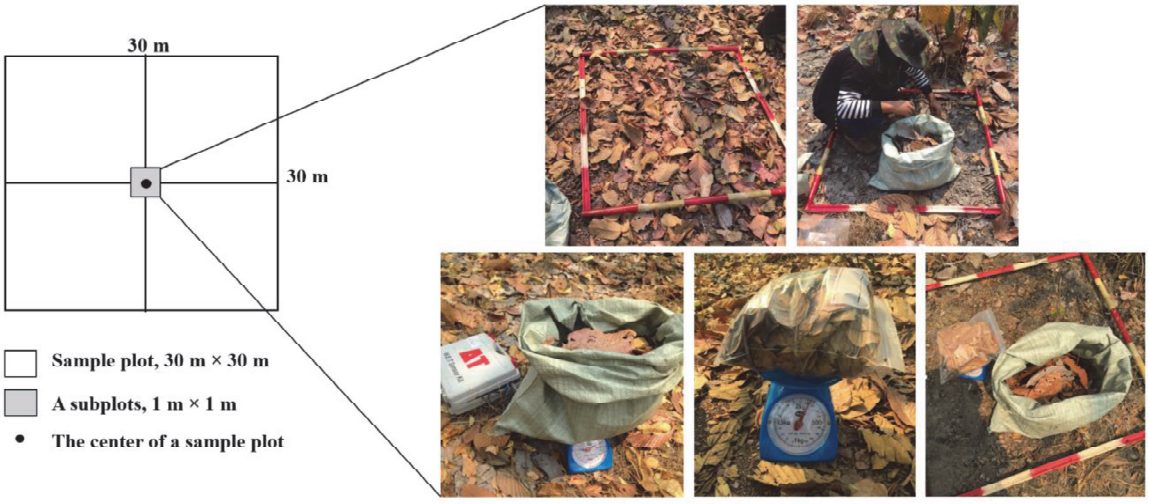

All of leaf litter in 1-m^2 subplot were collected and weighted. Then, some of leaf litter were put into a sealed envelope for laboratory analysis (dried-oven) to calculate leaf fuel moisture, which was later used to calculate leaf fuel load.

Appendix 6 Laboratory analysis for field leaf fuel calculation

A small sample of the leaf litter from each subplot was weighted on the scale before drying in an oven to determine FMC used for the leaf fuel load calculation

These samples of leaf litter were dried at 80°C for 48 h. After drying, the samples were weighed again to calculate FMC used for the leaf fuel load calculation

Appendix 7 Characteristic of soil in the study area during dry season

Examples of soil in sampling plots. The soil samples were taken at a standard depth of 10 cm. Each soil sample was placed in a plastic container and sealed tightly for further laboratory analysis.

Appendix 7 Laboratory analysis for soil moisture calculation

The soil samples were weighted using a standard laboratory scale and then placed them in a drying oven at 105 °C for 48 hours. After drying, the dried soil samples were weighed again to calculate the percentage of gravimetric soil moisture

Summary

Forest areas are often seen as recreational assets. Therefore, many countries, including Thailand, have made considerable efforts to protect forests, using several forms of conservation and protection such as national parks. National parks in Thailand are protected forest areas that contain natural resources, biodiversity and appealing scenery and landscapes, thus attracting tourism. Recreation and tourism clearly play an important role in the life of the national park, since most visitors cite scenery and landscape as their main reasons for visiting a national park. Recreational areas in the national park represent a wide variety of natural places and landscapes that enable activities such as camping, boating, walking, climbing and wildlife viewing. Recently, such recreational areas have been increasingly threatened and damaged by wildfires, resulting in a decline in tourism-related activities. Therefore, assessment of potential wildfire risk can prevent and minimize fire damage at recreational sites, contributing to the sustainability of national parks. The purpose of this study is firstly to assess wildfire risk and its corresponding risk levels by integrating the techniques of remote sensing and GIS, based on several factors associated with wildfire, and then to exploit the assessed wildfire risk to evaluate the wildfire risk at recreational sites. Data on various factors were analyzed from Landsat 8 OLI/TIRS and MODIS images (leaf fuel load and soil moisture), and were integrated with GIS data (slope, aspect, elevation, distance from roads and proximity to settlements) by using a GIS algorithm to establish a wildfire risk model for mapping wildfire-prone areas in Sri Lanna national park.

The study was conducted in Sri Lanna national park during the dry season of 2015, and focused on the dipterocarp and deciduous forests in which wildfire mostly occurs. The studies combined quantitative and qualitative methods, including remote sensing and GIS techniques, statistical analysis and field survey data to achieve the objectives of the study. The focus of *the first chapter* is on providing the background, objectives and outline of the dissertation.

Chapter 2 focuses on the theoretical and conceptual framework used throughout the whole dissertation. Suitable definitions of national parks and recreational areas, characteristics of wildfire, assessment of wildfire risk and general concepts of remote sensing and GIS are given. With regard to the characteristics of wildfire, seven factors selected in the study for modeling and mapping wildfire risks are described. These factors are widely recognized as influencing wildfire occurrence, especially the leaf fuel load, slope,

aspect, elevation, distance from roads and proximity to settlements. Leaf fuel loads and soil moisture factors were analyzed from remote sensing data and other five factors were obtained from GIS data. Finally, we present the structured methodology and overall conceptual framework of the research.

In *chapter 3*, the background of the study area of Sri Lanna national park is described, including physical conditions (such as geographical location, topographical characteristics and geological and soil characteristics), meteorological conditions, resources base and tourism/recreation in the park. The study reveals that some of the recreational areas in Sri Lanna national park have been damaged by wildfires, as their sites are mainly covered by the dipterocarp and deciduous forests in which wildfire mostly occurs.

The aim of *chapter 4* is to map the spatial distribution of the leaf fuel load which is one of selected factors in the study. Field data were combined with remote sensing data from Landsat 8 OLI to generate an empirical model of leaf fuel load based on a regression approach for mapping the spatial distribution of leaf fuel load. Firstly, the capabilities of seven VIs extracted from Landsat 8 OLI data were compared with regard to estimating leaf biomass, which is a parameter used in the leaf fuel load prediction model. The model contributes to the assessment of wildfire risk by identifying the spatial distribution of leaf fuel load for later use in the assessment of wildfire-prone areas. This study found that the NDVI had the strongest relationship with field leaf biomass and was appropriate for use in estimating the amount of leaf biomass. This relationship leads to the major finding that a seasonal NDVI for the normal and dry seasons can estimate the difference in the quantities of leaf biomass, thus establishing the missing leaf biomass that represents the quantity of dead leaves on the ground surface. In other words, the fuel load, derived from changes in leaf biomass, can be estimated based on differences between seasonal NDVIs.

In *chapter 5*, the spatial distribution of soil moisture, which is one of wildfire risk factors in the study, was estimated, and the relationship between the estimated soil moisture and leaf fuel moisture in the field investigated, in order to examine the use of soil moisture data for wildfire risk assessment. Firstly, TVDI and NDDI were derived from Landsat 8 OLI/TIRS and MODIS data to establish an empirical model for soil moisture estimation based on field data and remote sensing data, using a regression approach. A possible adaptation and application of NDWI and LST was proposed for constructing a TVDI based on the similar design of the triangular NDVI-LST space. The findings were that a relationship defined by the NDWI-LST better fulfills the collinearity requirement of the theoretical TVDI than a relationship defined by the NDVI-LST. TVDI values predicted by

the NDWI-LST are more accurate than those predicted by the NDVI-LST. A modified index, called $TVDI_{NDWI\text{-}LST}$, was applied with the NDDI to establish a regression model for soil moisture estimates. The major finding was that using both $TVDI_{NDWI\text{-}LST}$ and NDDI together can improve the accuracy of soil moisture estimates. Lastly, the estimated soil moisture was found to have a positive correlation with leaf fuel moisture, suggesting that including soil moisture as a wildfire factor could improve wildfire risk assessment, since it acts as a proxy for fuel moisture.

In *chapter 6*, the spatial distribution of wildfire risk is mapped by integrating remote sensing and GIS techniques for modeling and mapping wildfire risks, and the potential for fires at recreational sites is evaluated. At first, leaf fuel load and soil moisture as analyzed from chapter 4 and 5, respectively were rated with other factors (slope, aspect, elevation, distance from roads and proximity to settlements) to classify levels of wildfire sensitivity. A dNBR was used to rate wildfire sensitivity for subclasses of seven factors. Subsequently, all factors with differently rated subclasses were weighted using pairwise comparison to prioritize their importance with respect to wildfire occurrence. All weighted factors were later integrated to establish a GIS wildfire risk model. The main findings were that each subclass rated by the dNBR could be given a score for wildfire sensitivity. Leaf fuel load, weighted using a pairwise comparison matrix, is considered to be the most important factor for wildfires. In addition, the seven selected factors can be reliably used to assess the spatial distribution of wildfire risk because the model derived from these factors correctly classified 74.67% of wildfire instances. Finally, a map of wildfire risk zones produced from the model was overlaid with recreation sites in Sri Lanna national park, revealing that six of 22 recreational sites were at high risk from wildfires.

In the final chapter, the conclusions and main research findings of each chapter as described above are summarized. The implication of this research is that the developed approach can detect wildfire risk in large-scale areas and assess the corresponding risk levels of different areas. The informative and visual analytical techniques of remote sensing and GIS can be applied to enhance assessment of wildfire risk and to evaluate risk at recreational sites in national parks. The approach forms an effective method which can be used to develop decision-support systems for local officials, planners or decision-makers concerned with wildfire.

Key words: Wildfire Risk Assessment, Vegetation Index, Remote Sensing, GIS, National Park, Recreation Area, Northern Thailand

Japanese Summary

多くの国や地域において，森林はリクリエーション・ツーリズムの場として利用されている。タイ国においても例外ではなく，森林エリアの多くが国立公園として保全・保護され、さまざまな環境配慮がなされている。そこには多くの自然資源，生物多様性，美しい景観が随所に存在し，魅力的な自然環境資源を存在ており、キャンプ，登山・トレッキング，野生生物観察など野外活動が可能な恰好のリクリエーションの場が提供されている。しかしながら、近年こうしたリクリエーションエリアにおいて森林火災が多発するようになり，人々の野外活動に少なからず脅威をもたらしている。火災発生の頻度と規模の拡大は，短・中長期的に森林資源・景観の劣化に影響を及ぼすと考えられる。森林消失・荒廃による生態系の影響は，野生生物やリクリエーション・ツーリズムに対する地域の脆弱性を増大させることが危惧される。こうしたことから，森林火災に対する潜在的リスクを事前に評価することは，リクリエーションエリアにおける被害を最小限に抑え，国立公園の持続可能な自然管理に大きく貢献するものと考えられる。本研究の目的は，森林火災に関与する複数の外的要因を用いて衛星リモートセンシングと GIS の統合的利用によってその潜在的危険度を評価するモデルを構築し，実際のリクリエーションエリアに適用して危険度のランキングを図化する手法を確立することにある。対象地域は，タイ北部に位置するスリランナ国立公園であり，衛星画像データとして Landsat 8 OLI/TIRS と MODIS 画像を用い，外的要因に関わる GIS データ（地形傾斜，斜面方位，標高，主要道路や集落からの距離）と統合して解析し，対象地域の森林火災頻発エリアを地図化するためのリスクモデルを構築することを目指す。

解析は、2015 年乾季のスリランナ国立公園において森林火災が頻発するフタバガキ林・落葉広葉樹林内で行われた。調査は定量的・定性的な双方の手法を活用し、リモートセンシング・GIS、統計的な解析および野外観測・観察を並列して行った。本論の第 1 章では本研究の背景、目的とともに調査手法について詳述している。

第 2 章は、研究全体の理論的・概念的なフレームワークについて、特に国立公園・リクレーションエリアの定義、森林火災の特徴、火災リスクの評価に加えて主たる解析手法であるリモートセンシング・GIS の内容について解説している。このなかでは、火災リスクのモデリングやマッピングのために用いられた 7 つの外的要因の特徴についても詳述している。外的要因については、従来の森林火災研究の中でも議論されてきたが、ここでは特に林床可燃葉量、地形傾斜、斜面方位、標高、主要道からの距離および集落の近接性に注目した。

第 3 章では、調査対象地域であるスリランナ国立公園の地理的・気象的な特徴が記述されている。特に、公園内に分布するリクリエーションエリアのなかで実際に発生している森林火災の多くはフタバガキ林・落葉広葉樹林の範囲であることに注目し、その詳細について既往報告や現地調査に基づいて解説している。

第 4 章は、火災発生に関わるキーファクターである林床可燃葉量の空間的分布について論じている。ここでは、Landsat 8 OLI データの画像解析と現地観測調査の結果から経験モデルを構築した。Landsat データから計算される 7 つの Vis（植生指標）と現地観測で得た葉バイオマス量との関係を吟味し、林床葉量の空間的分布を図化するパラメータを求めた。このモデルは、火災頻発エリアの評価に際し林床可燃葉量の存在を同定し火災リスクを推定するためのものである。結果として、7 つの Vis のなかで NDVI 値が葉バイオマス量と最も大きい相関関係を示し、林床葉量の分布を推定するのに有効な指標であることがわかった。これにより、NDVI 値の季節変化から雨季と乾季における林床葉総量を求め、その差分から森林火災に関与する乾季の林床可燃葉量を推量された。言い換えると、NDVI 値の季節変動によって表される葉バイオマス量の変動より可燃葉量を得ることができた。

第 5 章は、森林火災リスクの重要な要因である土壌水分量の空間分布に関する議論である。まず、Landsat 8 OLI/TIRS と MODIS データから TVDI と NDDI を算出し、野外観測で得た土壌水分量との間で回帰モデルの構築を試みた。検討の結果は、NDWI-LST との関係で定義される TDVI 値が NDVI-LST によるそれよりも観測値に近似することが明らかになった。そこで、新たな指標値 $TVDI_{NDWI-LST,}$ を定義し、NDDI とともに土壌水分量を推算する経験モデルが構築した。これにより算出された土壌水分量と実際の可燃葉量の土壌水分量との間には明瞭な相関関係が見い出され、森林火災リスクを評価する要因としての土壌水分量マップが作成された。

第 6 章では、森林火災リスクの空間的分布をリモートセンシングと GIS の統合的利用によってモデリングして図化し、その結果からリクリエーションエリアの潜在的な火災リスクを評価している。4, 5 章で解説された林床可燃葉量と土壌水分量、およびその他の外的要因の値が GIS を用いて統合化され、森林火災に対する危険度がランキングされた。ここでは、dNBR 値が 7 つの外的要因のサブクラスに対する火災危険度をランキングするために用いられ、ペアワイズ比較の手法によってその重要度を判定した。結果は林床可燃葉量の存否が森林火災に対する最も重要な要因と抽出され、ここで選定された 7 つの外的要因によって 74.67%の森林火災が説明できることが明らかになった。最終的な結果として、このモデルにもとづいて森林火災リスクマップが作成され、スリランナ国立公園のリクリエーションエリアを示す地図とオーバレイされ、22 か所のサイトでその危険度が評価された。

最終章では、これまでの各章で得られた結論について再整理され解説されている。本研究で提示された手法によって比較的広範な地域における森林火災リスクをマッピングすることが可能になり、リモートセンシングと GIS の統合的利用に対する有効性が明らかに示された。これらの結果は、今後の国立公園における森林火災に対する対処法において、公園管理者、為政者に対して有効な手法・情報を提供するものと信じている。

キーワード：森林火災リスク評価、植生指標、リモートセンシング、GIS、故黒津公園、リクリエーションエリア、タイ北部